Okpara, Enyioma C, Quadri, Taiwo W, Ebenso, Eno E, Rowley-Neale, Samuel J and Banks, Craig E (2025) Advancing water purification: The role of copper-carbon nanostructured hetero-junctions in pollutant removal. Coordination Chemistry Reviews, 542. 216837 ISSN 0010-8545

DOI: https://doi.org/10.1016/j.ccr.2025.216837

Publisher: Elsevier

Version: Published Version

Coordination Chemistry Reviews 542 (2025) 216837

Contents lists available at ScienceDirect

Coordination Chemistry Reviews

journal homepage: www.elsevier.com/locate/ccr

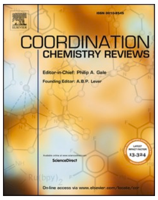

Review

Advancing water purification: The role of copper-carbon nanostructured heterojunctions in pollutant removal

Enyioma C. Okpara [a,*], Taiwo W. Quadri [b], Eno E. Ebenso [b], Samuel J. Rowley-Neale [a], Craig E. Banks [a,*]

[a] Faculty of Science and Engineering, Manchester Metropolitan University, Dalton Building, Chester Street, Manchester M1 5GD, Great Britain
[b] Centre for Materials Science, College of Science, Engineering and Technology, University of South Africa, Johannesburg 1710, South Africa

ARTICLE INFO

Keywords:
Organic pollutants
Copper materials
Carbonaceous materials
Water purification
Nanostructure-heterojunction
Catalysis
Adsorption
Metal leaching control

ABSTRACT

Water pollution remains a pressing global challenge, driven by the unchecked release of industrial effluents and agricultural runoff that introduce a broad spectrum of organic and inorganic contaminants into aquatic systems. Among various remediation approaches, such as adsorption, filtration, catalytic oxidation, ion exchange, Fenton-like processes, and photocatalysis, the choice and composition of catalysts critically influence treatment efficiency and sustainability. In this context, copper–carbon nanohybrid heterojunctions (CCNHs) have emerged as promising materials, combining the redox activity of copper-based nanostructures with the high conductivity and surface area of carbonaceous materials. These hybrids enhance charge separation, reduce electron–hole recombination, and exhibit superior adsorption and catalytic properties. This review comprehensively examines recent progress in CCNH-based systems for water purification, focusing on synthesis techniques, heterojunction engineering, defect and surface modification, stabilization strategies, and underlying removal mechanisms. We also highlight advances in pilot-scale applications, discuss challenges such as metal leaching and long-term stability, and propose future directions towards practical deployment of CCNHs in sustainable wastewater treatment technologies.

1. Introduction

Water pollution has become a universal problem, and constant appraisals of water resource policies and treatments are required to counter this challenge. Diseases and deaths are inflicted globally because of water pollution, and the mortality rate due to water pollution is approximately 14,000 per day [1–3]. Both developing and developed economies are confronted with the problem of water pollution [4]. Water is polluted by several factors, of which industrial waste is the most significant. In addition to industrial waste, other sources include atmospheric pollutants, pesticides, herbicides, pharmaceuticals and personal care products. Pathogenic exposure also causes critical diseases in humans [4]. Some of these pollutants are non-biodegradable and can persist in the environment. Please see Table 1, which summarizes organic pollutants, their chemical structure, and their reported adverse health effects.

In recent years, the rising demand for water across various sectors has led to significant shifts in the management of water resources, underscoring the urgent need for sustainable practices in water usage and conservation [99]. The treatment and recycling of water have become pressing environmental issues, with considerable implications for carbon emissions and energy consumption [100–102]. Treated wastewater can be categorized into various types, ranging from potable drinking water to non-potable reclaimed water, depending on its safety levels and intended applications. There is also an increasing concern regarding the potability of recycled water [103]. To improve the safety and suitability of reclaimed water for consumption, it is crucial to effectively remove trace pollutants using materials and techniques that present minimal environmental risks. These micropollutants, which include potential hazards associated with prolonged human exposure and environmental damage, underscore the urgency of the issue.

1.1. *Low-cost metal nanomaterials in environmental remediations*

In recent years, the feasible and economic development of nanomaterial catalysts for state-of-the-art applications, as well as eco-friendly

---

* Corresponding authors.
E-mail addresses: ebrochima@gmail.com (E.C. Okpara), c.banks@mmu.ac.uk (C.E. Banks).

https://doi.org/10.1016/j.ccr.2025.216837
Received 12 April 2025; Accepted 18 May 2025

catalytic procedures and viable technologies for developing synthetic strategies for catalysts, have attracted significant interest from researchers. As a result, systematic enquiry is continuously directed towards promoting and supporting the design of new and advanced materials and applications [104]. Noble metal nanoparticles (NMNPs) possess a reasonable amount of functionality owing to their exceptional physicochemical qualities [105]. The surface modification, easy chemical synthesis, and high stability make NMNPs, such as silver, gold, and

Table 1

A collection of organic pollutants, their abbreviations, chemical structures, and adverse health effects.

Organic pollutants	Abbreviation	Chemical structure	Adverse health effects	Reference
Dyes				
Orange II	O-II	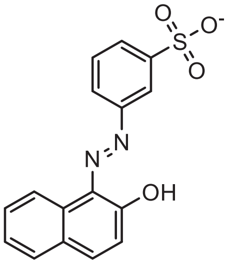	Reduces red blood cells and cell volume.	
Malachite green	MG	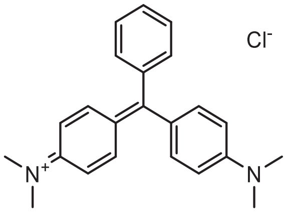	Organ damage, mutagenic, carcinogenic, and developmental abnormalities.	
Acid orange 7	AO-7	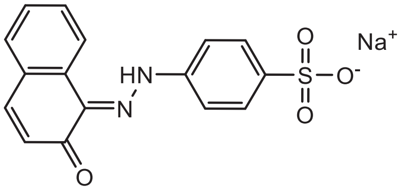	Carcinogenic in humans and harmful to aquatic habitats.	
Methyl orange	MO	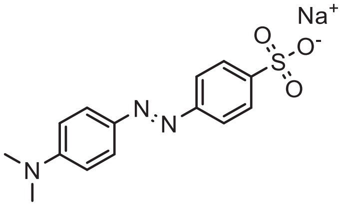	Genotoxic effects damage humans' eyes, skin, and digestive and respiratory systems.	
Methyl blue	MB	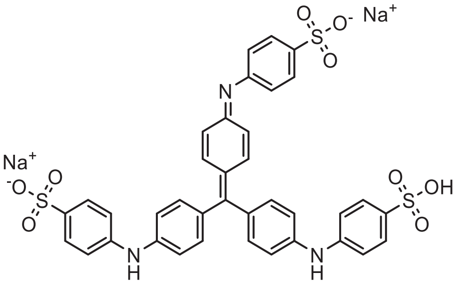	Reduces total dissolved oxygen (TDO), lowers the diversity and aesthetics of the biota, as well as high phototoxicity. Causes: nausea, diarrhoea, vomiting, urine discoloration, irritation of the bladder, skin, mouth, throat, oesophagus, and stomach,redness, itching, dizziness, headache, fever, and anaemia in humans.	
Methyl violet	MV	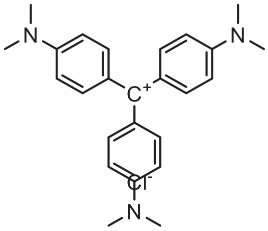	Vomiting and diarrhoea.	

(continued on next page)

Table 1 (*continued*)

Organic pollutants	Abbreviation	Chemical structure	Adverse health effects	Reference
Congo red	CR	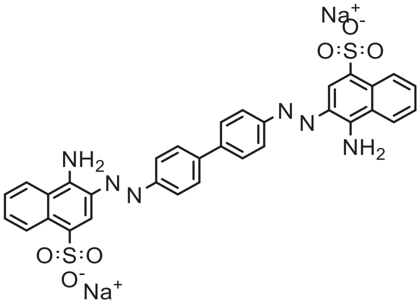	Carcinogenic, mutagenic, and allergen in humans, causing infertility in water fleas, increases COD, poor surface aesthetics, and phototoxicity in plants.	
Thymol blue	TB	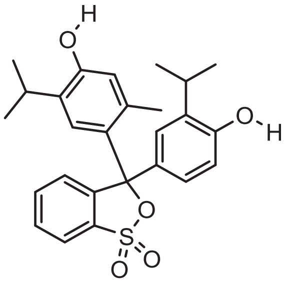	Painful to the skin and eyes, disturbance to the gastrointestinal tract, and can cause disorders in the respiratory system.	
Rhodamine B	RhB	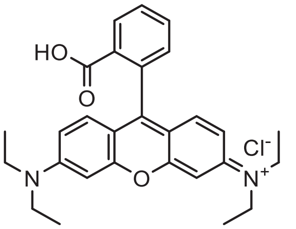	Causes eye and skin irritation, thyroid, and liver damage. Potentially toxic, particularly carcinogenic and neurotoxic to animals and humans.	
Basic blue 41	BB-41	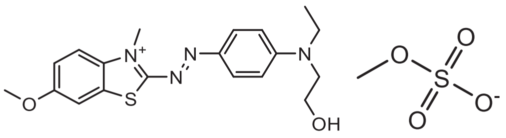	It causes allergies, dermatitis, skin irritation, and cancer in humans, poor surface water aesthetics, phototoxicity, toxic effects on aquatic flora and fauna, and decreased gas solubility in water.	[5,6]
Acid orange 8	AO-8	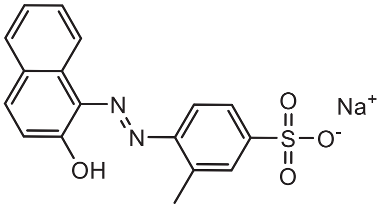	Carcinogenicity, mutagenicity, and allergies.	[7]
Direct red 16	DR-16	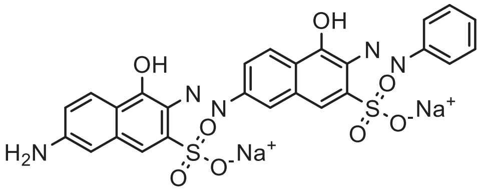	Mutagenic.	[8,9]
Acid violet 7	AV-7	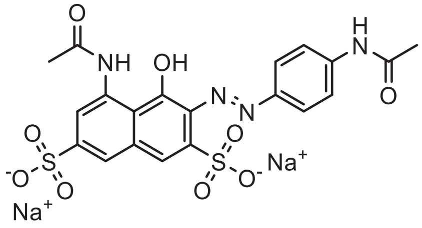	Genotoxic, with significant ability to induce chromosome alteration, lipid peroxidation, and inhibitory impact on acetylcholinesterase.	[10,11]

(*continued on next page*)

Table 1 (*continued*)

Organic pollutants	Abbreviation	Chemical structure	Adverse health effects	Reference
Acid brown 14	AB-14	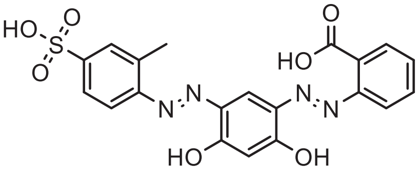	Poor surface water aesthetics, phototoxicity, and perturbation of aquatic life may cause stomach discomfort, respiratory, eye, and skin irritation (for sensitive individuals).	[12][13]
Acid red 14	AR-14	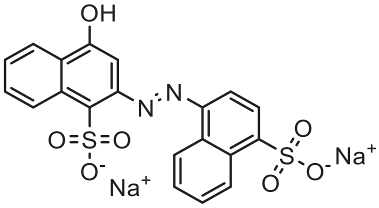	Aesthetic problems, carcinogenic, neurological, and reproductive disorders in humans and aquatic life.	[14]
Acid red 88	AR-88	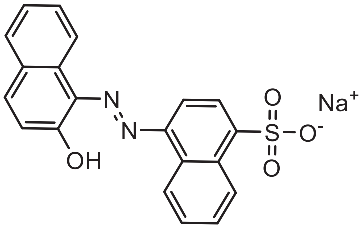	Aesthetic problems, mutagenic, and carcinogenic	[15]
3 Brilliant red	3BF	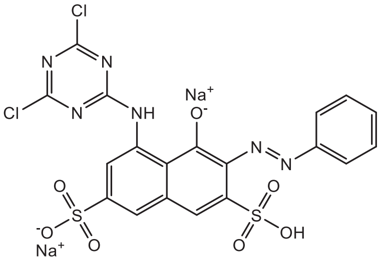	Potential to produce toxic byproducts during degradation and its adverse effects on aquatic life	[16,17]
Direct blue 71	DB-71	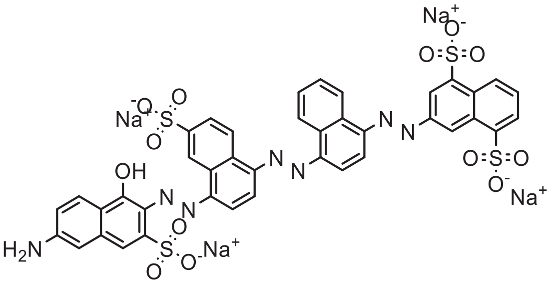	Mutagenic, poor surface water aesthetics, phototoxicity, and carcinogenic.	[18]
Acid red 1	AR-1	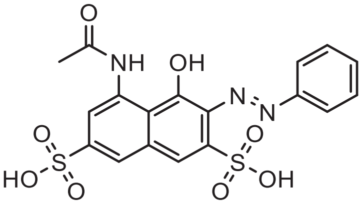	Impedes the transparency and aesthetic quality of surface waters, mutagenic and carcinogenic	[15]

(*continued on next page*)

Table 1 (*continued*)

Organic pollutants	Abbreviation	Chemical structure	Adverse health effects	Reference
Acid black	AB	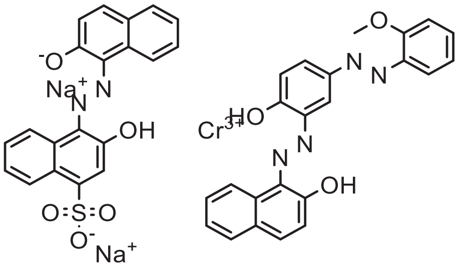	Malfunctioning of the kidney and reproductive system at elevated concentrations. Long-term exposure may cause increased lipid peroxide formation, alteration in cytoskeleton protein formation, deficiency of G6PD, gas transport, immune responses, disturbance in ion transport, failure of tubulin polymerization, and altered ion permeability of the cell membrane in fishes.	[19,20]
Acid blue 92	AB-92	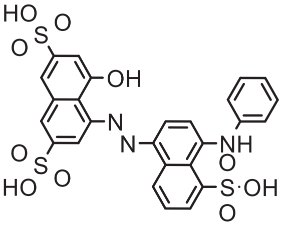	Toxic, mutagenic, and carcinogenic in humans and oxidative stress in plants.	[21,22]
Reactive black-5	RB-5	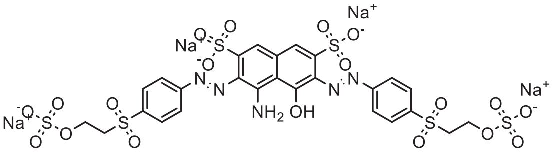	Blocks light in ecological waters even in trace quantities, thus harming the growth of aquatic plants, lowering TDO, and ultimately leading to eutrophication; long-term and continuous exposure could result in bladder cancer, aberration, skin rashes chromosomal, kidney and respiratory failure, asthma cardiovascular collapse, blindness, shock, and aesthetic problems in surface water.	[23]
Fast green dye (FCF)	FG	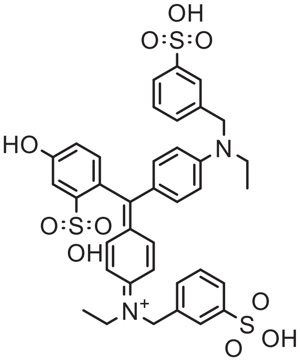	It impairs hepatic functions, inhibits synaptic activity, causes phototoxicity, and has poor water aesthetics. It also modifies the direct allergic response when orally ingested in food.	[24–27]
Rose bengal dye	RB	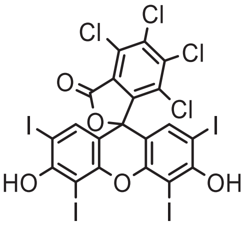	It causes irritation, itchiness, blistering, and reddening. Its effects on the eyes include severe damage to corneal epithelium, inflammation, itching, and redness.	[28]
Phenol Group				
Nitrophenol	NP	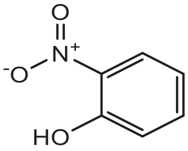	Oxidative stress in microalgae and inhibits the production of cell constituents.	[29–32]

(*continued on next page*)

Table 1 (*continued*)

Organic pollutants	Abbreviation	Chemical structure	Adverse health effects	Reference
Bisphenol-A	BPA	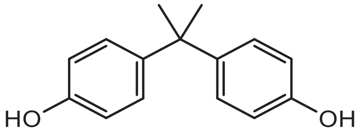	Carcinogenicity, mutagenicity, and geno- and cytotoxicity effects raise the chances of numerous health-related challenges in humans (e.g., diabetes, obesity, and cardiovascular diseases, with endocrine-disrupting properties.	[33–35]
Tetrabromobisphenol A	TBBA	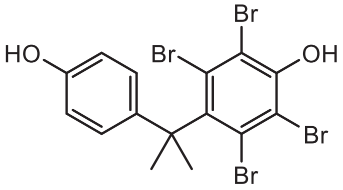	May adversely affect aquatic life, such as retarding developments and deformation, reproductive toxicity, nephrotoxicity hepatotoxicity, endocrine disruption, and neurotoxicity in mammals.	[36]
Phenol		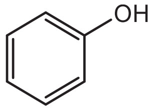	Chronic exposure causes several symptoms such as anorexia, muscle pain, headache, and gastrointestinal pain, which will then lead to cancer. It can also cause skin damage and even lead to death.	[37–40]
Phenol red	PR	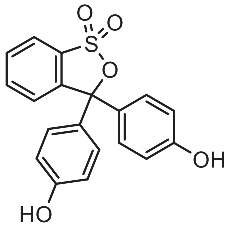	Aesthetic problem. They are also hepatotoxic and hematotoxic, and could be mutagenic and carcinogenic in other living organisms and humans.	[15,41]
p-nitrophenol	p-NP	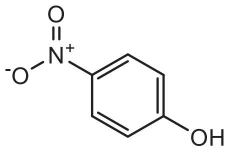	Can promote mutation of genes, aberration of chromosomes, carcinogenesis, and oxidative damage to DNA above 1–20 mg/L.	[42,43]
2,4-dichlorophenol	2,4-DCP	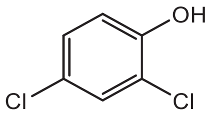	Risk of thyroid cancer, morbidity due to asthma, total serum levels of immunoglobulin E in patients with immediate allergy, and a history of olfactory dysfunction, wheezing, and an enhanced incidence of food allergies.	[44–46]
Pharmaceutical and Personal Care Products				
Sulfamethazine	SMZ	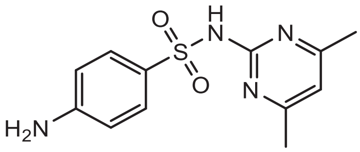	Ability to inhibit the denitrifying microorganisms, reproductive toxicant and toxic to aquatic living systems.	
Amlodipine	AD	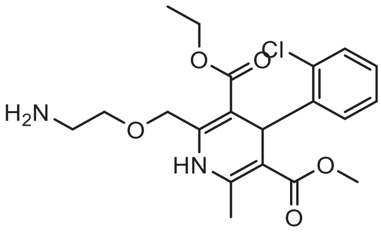	Hypotension and dysrhythmia.	[47]
Naproxen	NPX	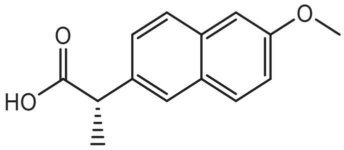	Genotoxicity, peroxidation of lipid and carbonylation of protein, rise in catalase and superoxide dismutase activity, and drop-in Glutathione peroxidase activity in freshwater invertebrates.	[48,49]

(*continued on next page*)

Table 1 (*continued*)

Organic pollutants	Abbreviation	Chemical structure	Adverse health effects	Reference
Salicylic acid	SAA	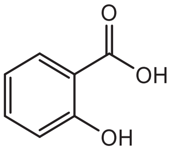	Salicylism and even death in tropical applications and acute aquatic toxicity.	[50,51]
Alachlor	–	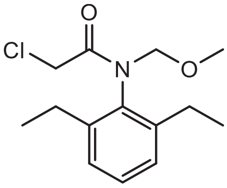	Acute neurological and cardiovascular outcomes may develop in humans.	[52,53]
Phenanthrene	PHE	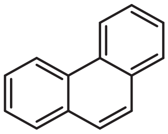	Mutagenic and/or carcinogenic to microorganisms might disrupt reproduction in fish.	[54–56]
Levofloxacin	LFX	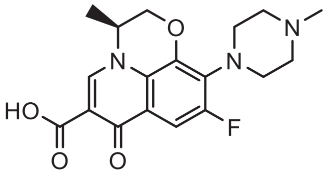	May cause some gastrointestinal (e.g., nausea, diarrhoea) disorders and CNS events (e.g., headache, insomnia) in humans.	[57,58]
Acetaminophen	ACT	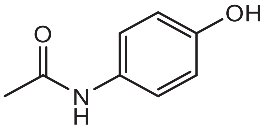	Hepatic dysfunction and renal failure, long-term exposure can be carcinogenic, result in endocrine disruption, resistance to antibiotics, and numerous chronic diseases, as well as toxicity to the aquatic ecosystem.	[59,60]
Sulfamethoxazole	SMX	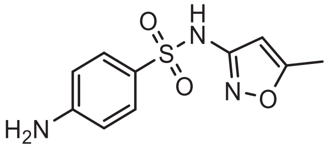	Third-class carcinogen, toxic effects on some freshwater habitats, and adversely affects chlorophyll content by blocking photosynthesis.	[61]
Carbamazepine	CMZ	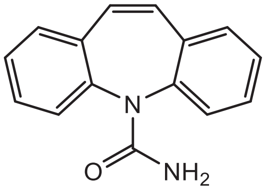	Toxic to freshwater invertebrates and causes congenital abnormalities in human offspring.	[62–64]
Tetracycline hydrochloride	TCH	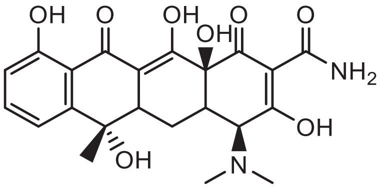	Can have adverse effects on aquatic and terrestrial lives, such as growth inhibition. It may also be harmful to developing foetuses, inhibiting their skeletal development. It can also lead to permanent teeth discoloration and enamel hypoplasia, whereas long-term exposure may lead to microscopic brown-black thyroid gland discoloration.	[65,66]
Oxytetracycline	OTC	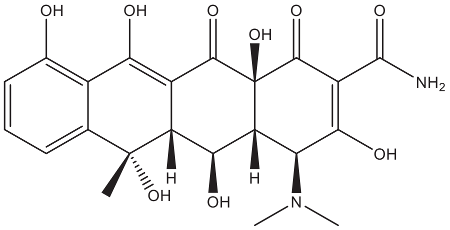	May affect thyroid function and neurobehaviour at high cocentrations in Zebrafish.	[67]

(*continued on next page*)

Table 1 (*continued*)

Organic pollutants	Abbreviation	Chemical structure	Adverse health effects	Reference
Tetracycline	TC	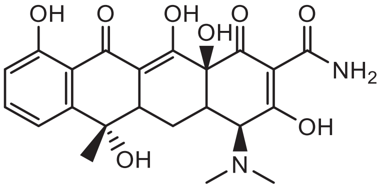	It can chelate calcium ions and integrate them into bone, cartilage, and teeth, thereby causing discoloration of the teeth. Minocycline hydrochloride, a semisynthetic product of TC, is notorious for pigmentation of numerous tissues, including thyroid, skin, teeth, nails, sclera, bone, and conjunctiva.	[68,69]
4-(2-hydroxyethyl)-1-piperazineethanesulfonic acid	HEPES	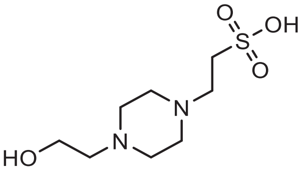	Promotes endothelial cells to generate toxic oxygen metabolites, contributing to the inhibition of cell growth.	[70]
Ciprofloxacin	CIP	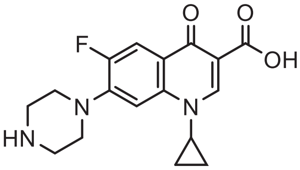	It can adversely affect human tenocytes, inhibit microbial growth, and present a significant hazard to the ecosystem, specifically soil microbial ecology. It can also negatively impact microbial ecosystem services.	[71,72]
Agricultural Products				
p-arsanilic acid	p-ASA	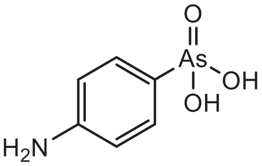	Causes an increase in arsenic concentration, which is harmful to aquatic life and increases the risk of cancer in humans.	[73,74]
Chlorpyrifos	CPF	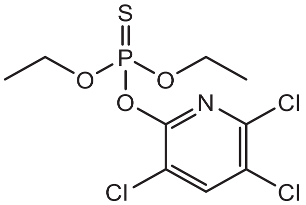	Demonstrates neurotoxicity, reproductive toxicity, and genotoxicity.	[75]
Atrazine	ATZ	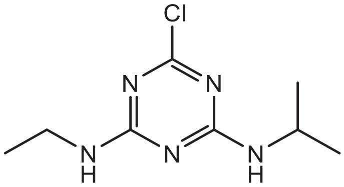	Inhibition of the intestinal cell maturation and decreased transepithelial electrical resistance in humans.	[76]
Triclopyr	TCP	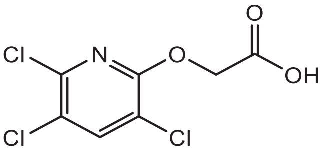	Aggressive eye irritation, carcinogenic in mammals, and threatens aquatic plant species.	[77,78]
Violet 3	V-3	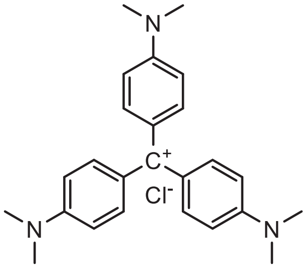	Strong lethal effects on freshwater microbiota.	[79]

(*continued on next page*)

Table 1 (*continued*)

Organic pollutants	Abbreviation	Chemical structure	Adverse health effects	Reference
Monocrotophos pesticide	MCP	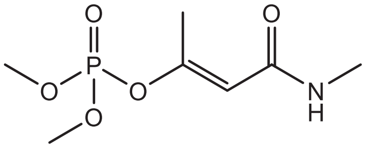	Abnormality, ranging from mild to severe confusion, agitation, hypersalivation, convulsion, pulmonary failure, senescence in mammals and insects, inhibits the activity of the acetylcholine esterase enzyme in humans, and is toxic to aquatic life.	[80–82]
Other organic products				
Benzophenone	BP	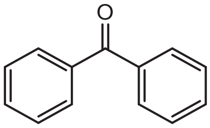	Kidney and liver disorders at higher concentrations.	[83]
Nitrobenzene	NB	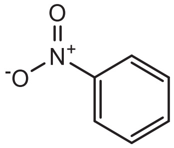	Reduces the ability of blood to carry oxygen because it causes methemoglobinemia. Continuous exposure to a high amount of 1,3-DNB and 1,3,5-TNB (derivatives of NB) could result in anaemia, a rise in bluish skin colour, dizziness, sleepiness, grouchiness, nausea, vomiting, headache, and weakness. 1,3-DNB and 1,3,5-TNB damage the male reproductive system and may lower sperm production. 2-CNB is a significant hepatotoxicant, whereas 4-CNB has been identified as a potential hepatotoxicant.	[84–88]
N, N-diethyl-*p*-phenyl diamine	DPD	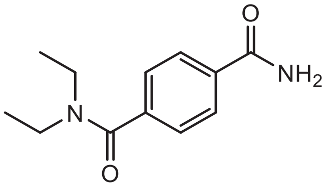	Allergic dermatitis in humans.	[89]
Benzotriazole	BTA	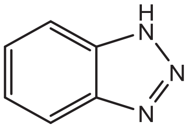	Neurotoxicity, endocrine disturbing effects, hepatotoxicity, and, as well as the capacity to heighten the endometrial carcinoma development.	[90]
1,4-dioxane	1,4-D	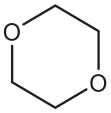	Probable carcinogen.	[91]
Toluene	–	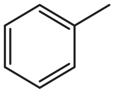	Distortion of embryonic axis, dysfunctional development of cardiovascular and circulatory system, hydration and swelling of the pericardial coelom, haemorrhaging, an overall stunted appearance, microphthalmia, and a unique migration of the ventrally located yolk syncytial layer and its associated nuclei.	[92]
Phthalic acid	PHT	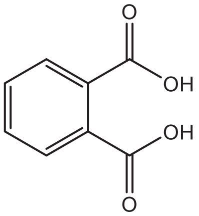	Prolonged exposure to phthalates can disrupt the endocrine system and impair the normal function of various organs, leading to long-term adverse effects on pregnancy outcomes, child development, and the reproductive health of both children and adolescents.	[93]

References for the uncited dyes can be found under “Further Readings” in the References section.

platinum nanoparticles (NPs), attractive for numerous functionalities [106].

However, their high cost and limited availability have prompted an increasing shift towards earth-abundant alternatives. In particular, copper-based nanomaterials have emerged as attractive substitutes due to their low cost, natural abundance, rich redox chemistry, and well-defined coordination environments [107]. Their utility has been explored in diverse applications spanning electronics, energy systems, pharmaceuticals, and environmental catalysis. The potential to modulate copper's oxidation states (Cu^0, Cu^+, Cu^{2+}) and coordinate it with a range of ligands or substrates further underpins its catalytic adaptability. In parallel with these advances, the incorporation of copper nanostructures into carbon-based frameworks, forming copper–carbon heterojunctions, has gained traction, offering synergistic effects that enhance catalytic performance, charge separation, and material stability in aqueous-phase reactions.

The urgency of global water scarcity, driven by mounting pollution, climate variability, and population growth, necessitates the development of scalable and sustainable water treatment technologies [108,109]. In this context, Cu—C heterojunctions represent an emerging class of materials with significant promise due to their synergistic catalytic and adsorptive capabilities, earth-abundant composition, and low-cost fabrication potential (see Table 2) [110,111]. The creation of copper–carbon heterojunctions has been reported to increase the surface area of copper-based catalysts, enhance their stability in environmental applications, and improve overall catalytic performance [112–117]. Compared to conventional nanomaterials such as TiO_2, ZnO, and noble metal-based systems, CCNHs stand out for their visible-light activity, high surface area, and dual-functionality in degrading organic pollutants while capturing contaminants through adsorption [118]. Furthermore, the potential to synthesize these materials from waste-derived carbon sources supports circular economy practices and positions CCNHs as a green alternative in decentralized water treatment systems [119]. These attributes align directly with the United Nations Sustainable Development Goals, particularly SDG 6 (Clean Water and Sanitation) and SDG 12 (Responsible Consumption and Production), highlighting the broader environmental and societal relevance of advancing CCNH-based technologies [120,121].

This review will consider copper-carbon heterojunction nanostructured materials applied in water treatment using various technologies, explore the possible mechanism of organic pollutant removal, and address future perspectives. Overall, this review comprehensively

Table 2
Selected practical applications of Cu—C heterogeneous catalysts in water purification processes.

Cu—C Nanostructure	Synthesis	Solvent	Reducing agent /Stabilizer	Technique	Product morphology	Application					Ref
						[Cu—C]	Pollutant	[P]	DE (min)	kinetics	
Cu doped ZnO-MWCNT	Facile chemical route	Water	PAH	Photocatalysis	20 nm spherical CuZnO NPs spread on the surface of the MWCNTs	5 mg	RhB, phenol, and OTC	0.01 ppm, 1 ppm, and 50 ppm respectively	79 %, 91 %, and 55 % (240)	$k = 0.00485\ min^{-1}$ for RhB	[94]
nZVC-CNT filter/PMS	Facile approach	Water	$NaBH_4$	PMS activation	0.2 mM $CuCl_2$ solution (500 mL) passed through a pre-formed CNT filter for Cu^{2+} grafting. Further passing of 0.5 M $NaBH_4$ solution through CNT-$COOCu^{2+}$ system to reduce Cu^{2+} to Cu^0	0.2 mM	CR	0.015 mM	100 % (2 s)	–	[95]
CuFe-MCs/H_2O_2	"One-pot" block-copolymer self-assembly strategy	Water	–	Fenton-like process	1.0 g Pluronic F127 was dissolved in 20 g of ethanol to generate a transparent solution at 35 °C. Then, 30.2 mg $Cu(NO_3)_2·3H_2O$ and 101 mg $Fe(NO_3)_3·9H_2O$ and (molar ratio 2:1) added to dark solution. 5.0 g Resol precursor solution added and stirred for 10 min, dried at 100 °C after ethanol evaporation, and pyrolyzed at 800 °C for 4 h.	300 ppm	BPA	100 ppm	93 % (60)	$k = 2.8\ h^{-1}$	[96]
N-doped CNTs stabilized Cu_2O	–	Water	PVP	Adsorption	–	2.0 g/L	TBBPA and MG	100 ppm	>99 % for MG and 80 % for TBBPA	$Q_{max} =$ 116.72 and 1495.46 mg g^{-1}	[97]
CuHCF	-	-	-	Copper ion resin	Commercial IX resin rich in carboxyl group used as the substrate immobilization of PBA	1 g/L	NH_4^+	25 mg NH_4^+-N/L		47.07 mg NH_4^+ per g of catalyst	[98]

Key: PAH: Poly(allylamine) hydrochloride; [P]: pollutant concentration; [Cu—C]: Catalyst concentration; DE: Degradation efficiency.

examines the definition, surface modification, and factors influencing the catalytic performance of CCNH in enhancing catalytic function, efficiency, stability, reusability, and selectivity in water treatment. It begins with an overview of water pollution, various organic contaminants, and the associated risks of exposure beyond targeted applications. Next, the vital roles of low-cost metal nanoparticles in environmental remediation are emphasized, focusing on the definition, advantages, synthesis methods, and advancements in using CCNHs to remove organic pollutants from water. Subsequently, we explore the approaches to enhance the stability and reusability of these nanocomposites. In Section 4, the mechanisms for the removal of organic pollutants from water systems are discussed. We conclude by addressing the challenges that hinder industrial-scale applications of these catalysts, along with perspectives, recommendations, and a summary of our findings on the potential impact of CCNH in the water treatment sector.

1.2. *Defining copper-carbon nanostructure heterojunctions (CCNHs)*

Copper-carbon nanohybrid heterojunctions (CCNHs) are advanced materials that combine copper-based nanostructures, such as Cu, CuO, Cu_2O, Cu_3N, CuS, and CuSe, with carbonaceous materials like carbon nanotubes (CNTs), graphene, biochar, and activated carbon [122]. This integration results in coordination interactions and synergistic effects that enhance charge separation, improve electrical conductivity, and significantly boost adsorption capabilities compared to their individual components [123]. The coordination interaction between copper-based nanostructures and carbon materials optimizes the physicochemical properties of CCNHs, facilitating efficient catalytic oxidation, accelerating electron transfer processes, and enhancing chemical stability. Additionally, CCNHs exhibit superior structural attributes, including high specific surface area, tailored pore structures, and abundant active sites, all of which are critical for the effective degradation of pollutants. These unique properties position CCNHs as promising candidates for environmental remediation applications, particularly in wastewater treatment and advanced oxidation processes (AOPs) [124,125]. Building upon the multifunctional advantages of copper-carbon nanohybrids, the strategic engineering of semiconductor heterojunctions further enhances their catalytic performance through improved charge dynamics and light absorption.

1.3. *Heterojunction engineering for enhanced catalytic performance in copper-carbon nanohybrids*

Constructing semiconductor heterojunctions through the direct interface of two distinct semiconductors offers a strategic approach to overcoming the performance constraints associated with individual semiconductor materials [21]. In heterostructure design, extended charge carrier lifetime, increased charge carrier separation, and expanded solar light absorption are facilitated by the coupled semiconductors' appropriate band edge positions. Fig. 1 illustrates different types of electronic band structures at material interfaces, including semiconductor-semiconductor heterojunctions, metal-semiconductor Schottky barriers, and ohmic contacts. These band alignments play a crucial role in charge transfer, space charge region formation, and overall material performance in catalytic applications. The formation of semiconductor heterojunctions encompasses several critical stages. First, prior to contact (A), the p-type and n-type semiconductors exhibit distinct Fermi levels and band structures. Upon the establishment of the junction (B), charge transfer occurs, leading to band bending and the formation of a depletion region. This region of depletion is critical, as it promotes charge separation. This phenomenon is particularly significant in Cu-based semiconductors, such as Cu_2O and CuO, which can effectively generate heterojunctions with C-materials, including graphene and CNTs. The heterojunctions thus formed boost charge separation, thereby limiting the tendency of electron-hole recombination, which in turn amplifies the efficiency of catalytic water treatment applications. Moreover, the region of depletion is pivotal in the promotion of redox reactions, prompting the effective breakdown of organic pollutants.

On the other hand, ohmic contacts are generated when a semiconductor with a higher work function contacts a metal of lower work function (i.e., $\Phi m < \Phi s$). Before this contact (E), the difference in the work function between the metal and the semiconductor is apparent. However, once the junction is created (F), a region of space charge is formed, which promotes the migration of free electrons and results in the generation of an ohmic contact [127,128]. In relation to Cu—C, this pattern can lead to electrical conductivity, thus enhancing the efficient transfer of electrons during catalytic reactions. Such behaviours are beneficial in electrocatalytic water treatment, where effective transport of charge is required for the degradation of pollutants [127].

Therefore, the implications these mechanisms have on water treatment are crucial. The generation of heterojunctions or Schottky barriers in Cu—C materials limits the recombination of charges [129–131], thereby promoting photocatalytic efficiency for the degradation of pollutants. In addition, depending on the energy band alignments, the Cu—C interfaces can facilitate redox reactions [132,133], optimize electron transfer [134,135] and improve the electrochemical water treatment process [135]. Furthermore, the Cu—C interaction contributes to an increase in structural stability, forestalling aggregation of NPs or deactivation during prolonged use.

For instance, Toloman et al. [94], investigated the photocatalytic degradation efficiency of Cu-doped ZnO-MWCNT nanocomposites under visible light. The formation of a heterojunction between ZnO and multi-walled carbon nanotubes (MWCNTs) significantly enhanced photocatalytic performance. ZnO, recognized as a well-known n-type semiconductor with a wide bandgap of approximately 3.3 eV [136], tends to limit visible-light absorption. However, incorporating MWCNTs, which are known for their excellent conductivity, improved charge transport within the system [137,138]. The ZnO-MWCNT composite was doped with Cu, creating impurity levels that reduced the bandgap [139], thereby facilitating better visible-light absorption. When ZnO and MWCNTs form a heterojunction, as illustrated in Fig. 1, the charge transfer processes are notably enhanced, effectively preventing electron-hole recombination. This interface development leads to improved separation of photogenerated charge carriers due to the bending of energy bands, while the presence of MWCNTs acts as an electron acceptor. This dual effect minimizes recombination and extends the light absorption range into the visible spectrum, ultimately improving the degradation efficiency of organic pollutants.

Doping with copper played a crucial role in the modification of the electronic properties of the ZnO/MWCNT system by adding mid-gap states that serve as charge-capturing centers. The interaction between ZnO and Cu leads to the creation of a Schottky barrier [140,141], which consequently boosts the rate of charge transfer [142]. This process is required to generate oxidative species, such as hydroxyl radicals (*OH), which are effective in the degradation of the target pollutants including RhB, OTC, and phenol [143,144]. Furthermore, Cu doping promotes electron-hole separation by modifying the pathways of charge transport [139,145]. The Cu acts as a co-catalyst, boosting the production of reactive oxygen species (ROS), further expediting the breakdown of organic pollutants [143,146]. The MWCNTs create a conductive network resembling an ohmic contact, accelerating fast electron transfer while limiting recombination, which amplifies efficiency of catalysis. This interaction is pivotal in amplifying the photocatalytic degradation efficiency of the target pollutants. Therefore, the superior performance of Cu-doped ZnO-MWCNT composites can be attributed to several factors. The formation of a heterojunction reduces recombination losses, leading to enhanced reaction efficiency. Additionally, Cu doping introduces intermediate energy levels that significantly boost photocatalytic activity under visible light. Finally, the combination of CNTs and Cu doping contributes to increased stability, improved structural durability, and enhanced conductivity, resulting in a highly efficient and reusable photocatalyst.

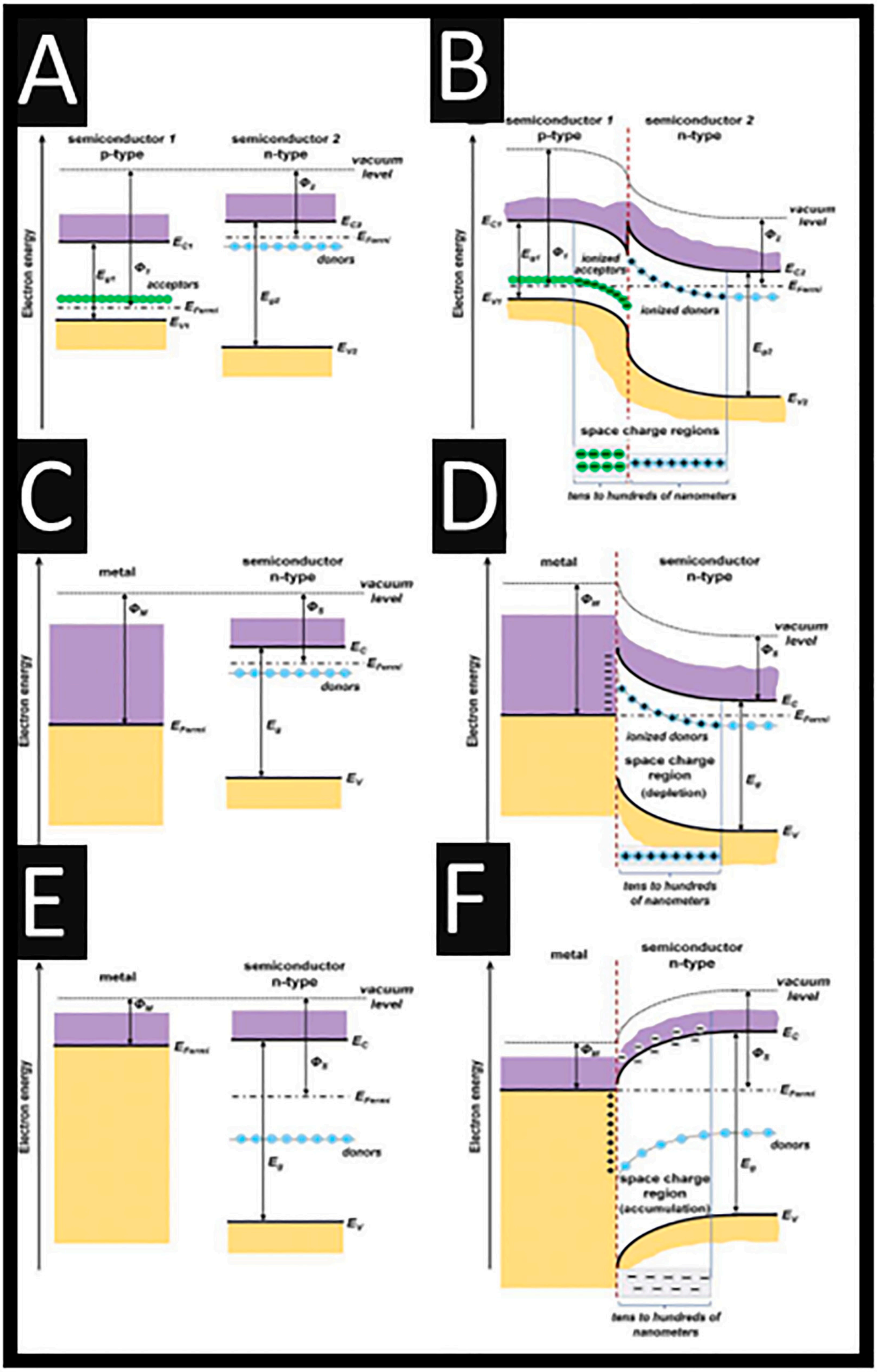

Fig. 1. Examples of junction band diagrams. (A) p- and n-type semiconductors before contact and (B) after heterojunction formation. (C) Metal (with higher work function ΦM) and n-type semiconductor (with lower work function ΦS) before contact and (D) after formation of the Schottky barrier. (E) Metal and n-type semiconductor (in the case where ΦM < ΦS) before contact and (F) after making an ohmic junction. (E_g, band gap; E_{Fermi}, Fermi level; and EC and EV, lower edge of the conduction band and upper edge of the valence band, respectively). Figure reproduced from reference [123].

Another study by Wan and team members [119] employed a wood waste-derived biochar catalyst doped with copper heteroatoms and processed under a CO_2 atmosphere. The copper-doped graphitic biochars (Cu-GBCs) were subjected to a series of comprehensive characterizations, including X-ray diffraction (XRD), Fourier-transform infrared spectroscopy (FTIR), Raman spectroscopy, and X-ray photoelectron spectroscopy (XPS). These analyses revealed significant modifications in the specific surface area and pore structure of the Cu-GBCs, as well as enhancements in their graphitization and the presence of active sites such as defective sites and ketonic groups. These changes are attributed to the synergistic effects resulting from the loading of Cu species, alongside the reformation of the carbon matrix induced by copper in a CO_2-rich environment during the pyrolysis process. This approach significantly enhanced oxygen functionalities, defective sites, and a highly ordered sp^2-hybridized carbon matrix. The Cu-GBCs demonstrated superior catalytic abilities in activating peroxydisulfate (PDS) for the removal of RhB, phenol, BPA, and 4-chlorophenol, achieving a degradation rate of 0.0312 min^{-1}. The combined effects were attributed to evolved ketonic groups, abundant unconfined π-electrons, and Cu heteroatoms within the carbon lattice. This study emphasized sustainable and selective non-radical pathways, such as singlet oxygenation and transfer of electron, mediated by Cu-induced metastable surface complex.

2. Advancements and performance of copper-carbon nanostructures

Recent research has shown that the CCNHs afford improved catalytic efficiency, essentially attributed to the synergistic interaction between rich redox activity of Cu and the unique electrical conductivity of carbon. These heterojunctions offer a crucial role in various catalytic processes, such as energy conversion and environmental applications. The main innovations in this field include optimizing Cu particle size and carbon substrate distribution, enhancing the stability of the catalyst under operational conditions, and the creation of novel synthesis methods that enabled better integration of carbon and Cu. These developments not only amplified catalytic activity but also paved the way for the design of next-generation catalysts with tuned properties for specific reactions. Key advancements include:

2.1. Doping and surface modification

Enhancing the efficiency of electron transfer processes is critical for numerous applications in the field of energy conversion and environmental remediation. By optimizing these processes, the selectivity towards target pollutants can be significantly enhanced for effective environmental remediation efforts. This involves the development of advanced materials and methods that can differentiate between harmful pollutants, thereby certifying that the removal process attacks only the target pollutants while limiting the impact on target substances. Improving electron transfer and amplifying the selectivity of pollutants opens the door for more sustainable and efficient solutions in environmental applications.

2.1.1. Transition metal doping

Recent research has demonstrated that doping CCNH with transition metals (TMs) can significantly enhance its performance in various photocatalytic applications. Examples include CuCo/Carbon Dots utilized in photocatalysis [147], Fe/$CuFe_2O_4$ embedded in porous carbon composites for the removal of TET and Ag-Cu/rGO applied in the catalytic degradation of dyes [148]. Additionally, novel amino-functionalized and starch-coated $CuFe_2O_4$-modified magnetic biochar composites have shown effectiveness in removing Pb^{2+} and Cd^{2+} from wastewater [149]. Other notable developments include Type-II $CuFe_2O_4$/g-C_3N_4 heterojunctions that exhibited high-efficiency photocatalysis [150], carbon nitride compounds-complexed Cu(II)-$CuAlO_2$ for dual-reaction-centre Fenton-like degradation of BPA over a wide pH range, [151] along with flexible rGO/Cu/Ni/ZnO nanocomposites that possess enhanced optoelectronic, anticorrosive, photocatalytic, and magnetic properties [152]. These modifications robustly alter the electron transfer properties and selectivity in diverse catalytic processes, leading to increased electron mobility and catalytic activity, ultimately improving efficiency and selectivity in chemical reactions.

In a particular case study [153], integrating Fe—Cu into CCNHs significantly advanced catalytic water purification through oxidative degradation and adsorption processes. A primary advantage of Fe—Cu bimetallic systems lies in their synergistic redox interactions, which enhance performance in both Fenton and PMS activation. A notable characteristic of these systems was the mutual regeneration of Fe^{2+} and Cu^{+}, with Cu^{+} facilitating the conversion of Fe^{3+} back to Fe^{2+}. This process maintains the presence of active species that generate reactive radicals, enabling continuous radical generation and thereby improving catalytic efficiency.

Furthermore, Fe—Cu catalysts broaden the operational pH range compared to traditional Fe-based systems, achieving high oxidative efficiency even under neutral and alkaline conditions, making them well-suited for real-world wastewater treatment applications [154]. Their dual-site nature allows for simultaneous degradation pathways, effectively utilizing both radical and non-radical species to enhance pollutant breakdown [151]. Additionally, anchoring Fe—Cu onto conductive supports such as biochar or graphene oxide improves metal dispersion and minimizes leaching, thereby extending catalyst longevity and enhancing environmental safety. The coupled adsorption-catalysis effect, as demonstrated in systems like Fe/$CuFe_2O_4$@C, reflects efficient pollutant degradation. Moreover, the intrinsic magnetism of $CuFe_2O_4$ facilitates easy recovery and reuse, supporting sustainable water treatment solutions.

2.1.2. Nitrogen doping

Doping Cu—C nanohybrids with nitrogen have been explored for the degradation of water pollutants, leveraging their improved electrocatalytic qualities. The integration of nitrogen introduces defects and functional groups within the carbon matrix, enhancing electron transfer and overall reactivity, which are crucial for the degradation of pollutants. Nitrogen-doped biochars (NBCs) have been robustly investigated for their ability to activate persulfate, resulting in the generation of ROS, capable of degrading organic contaminants in wastewater. The nitrogen functionalities within the biochar improved electron transfer processes, enhancing the degradation efficiency of pollutants. An exhaustive review highlighting the methods of preparation, catalytic performance, and the mechanism by which NBCs initiate the oxidative degradation has been published [155].

Tang and Zhang [156] have shown that doping C- electrodes with nitrogen can effectively activate persulfate under electrochemical conditions, resulting in the degradation of organic pollutants such as p-nitrophenol. The nitrogen doping improves the production of reactive radicals, including hydroxyl radicals ($^{\bullet}OH$) and sulfate radicals ($SO_4^{\bullet-}$), which are instrumental in breaking down complex organic molecules in water. Another study by [157] synthesized Co—Cu embedded nitrogen-doped carbon nanostructures derived from metal–organic frameworks (MOFs) for catalytic applications. These materials exhibited efficient electrochemical conversion capabilities, which are linked to the architecture of this composite as well as the presence of N-species (pyridinic and graphitic nitrogen) within the carbon matrix, which could facilitate CO_2 adsorption and the subsequent generation of intermediates and products from the reduction reaction. While the primary focus was on oxygen reduction reactions, the structural characteristics, such as high surface area and enhanced electron transfer capabilities, suggest potential applicability in the degradation of organic pollutants in aqueous environments.

2.1.3. Surficial vacancy engineering

Surface vacancies on copper-based nanostructures, for example, in Cu_2ZnSnS_4/CdS photocathodes, play a crucial role in accelerating electron transfer and optimizing product selectivity during photoelectrochemical CO_2 reduction. By carefully tailoring the sulfur vacancies through specific heat treatments, researchers have demonstrated the ability to enhance selectivity towards desired reduction products. This vacancy engineering approach helps to create active sites that can direct the reaction pathways more favorably, providing a strategy to synthesize valuable hydrocarbons from CO_2 with improved efficiencies [158–160]. This approach can also be extended to the degradation of organic pollutants in water.

2.1.4. Mesoporous structures with copper doping

The doping of mesoporous TiO_2 with copper has shown significant promise in boosting photocatalytic properties for environmental applications. The unique mesoporous architecture increases the surface area and provides ample space for photocatalytic reactions. At the same time, introducing Cu enhances electron transfer mechanisms and the overall degradation efficiency of pollutants. Studies have indicated substantial improvements in the breakdown of organic dyes, such as methyl orange, under UV light exposure, showcasing this method's potential to address water pollution and contribute to the advancement of sustainable cleaning technologies [161].

2.2. Structural control

Recent studies have investigated the structural control of CCNHs to engineer porosity and morphology, optimizing active sites for the removal of organic pollutants in water. For example, a novel copper molybdate ($CuMoO_4$) decorated polymeric graphitic carbon nitride (g-C_3N_4) heterojunction nanocomposite was synthesized using a solvothermal method. The resulting flower-like nanostructure, with sizes ranging from 10 to 15 nm, exhibited enhanced photocatalytic degradation efficiencies of 98 % for RhB and 97 % for CIP in 35 and 60 min, respectively under visible light irradiation. The improved performance is attributed to the engineered porosity and optimized active sites facilitated by the unique nanostructure morphology [162]. A comprehensive review highlighting the progress of copper-based nanocatalysts in advanced oxidation processes for wastewater treatment has been reported by Li et al. [163]. The study highlighted the significance of structural modifications, such as controlling porosity and nanostructure morphology, to improve the catalytic activity and specificity. The optimization of these structures is an essential step for enhancing the efficiency of degrading organic pollutants in water.

2.3. Hybrid compositions

Hybrid compositions incorporating elements like sulfur and nitrogen into CCNHs have revealed significant enhancements in both stability and catalytic activity, especially in removing organic contaminants in water. These improvements are critical to the development of more effective water treatment technologies. Numerous studies have emphasized the benefits of these hybrid systems. For example, the introduction of nitrogen can modify the electronic structure of the nanostructure [126,164] and promote the formation of coordination bonds with metal centers, thereby resulting in higher adsorption capabilities for various organic pollutants. Meanwhile, sulfur can play a critical role in enhancing catalytic efficiency and stimulating faster degradation of contaminants through improved reaction pathways [165]. Research has demonstrated that these modified nanostructures not only retain structural integrity under diverse environmental conditions but also afford sustained catalytic performance over prolonged periods. This synergy of stability and activity makes them promising composites for real-world applications in environmental remediation.

Lin and team members [126], synthesized a novel heterogeneous Fenton-like catalyst by co-loading Cu and Co onto sulfur-doped carbon nitride (SCN) (see Figs. 2 and 3). The addition of sulfur enhanced the efficiency of electron transport and increased the specific surface area of the catalyst. The CuCo/SCN composite demonstrated superior catalytic activity and stability across a wide pH range, effectively achieving 100 % degradation of MO within 60 mins in water. In another study by Jia

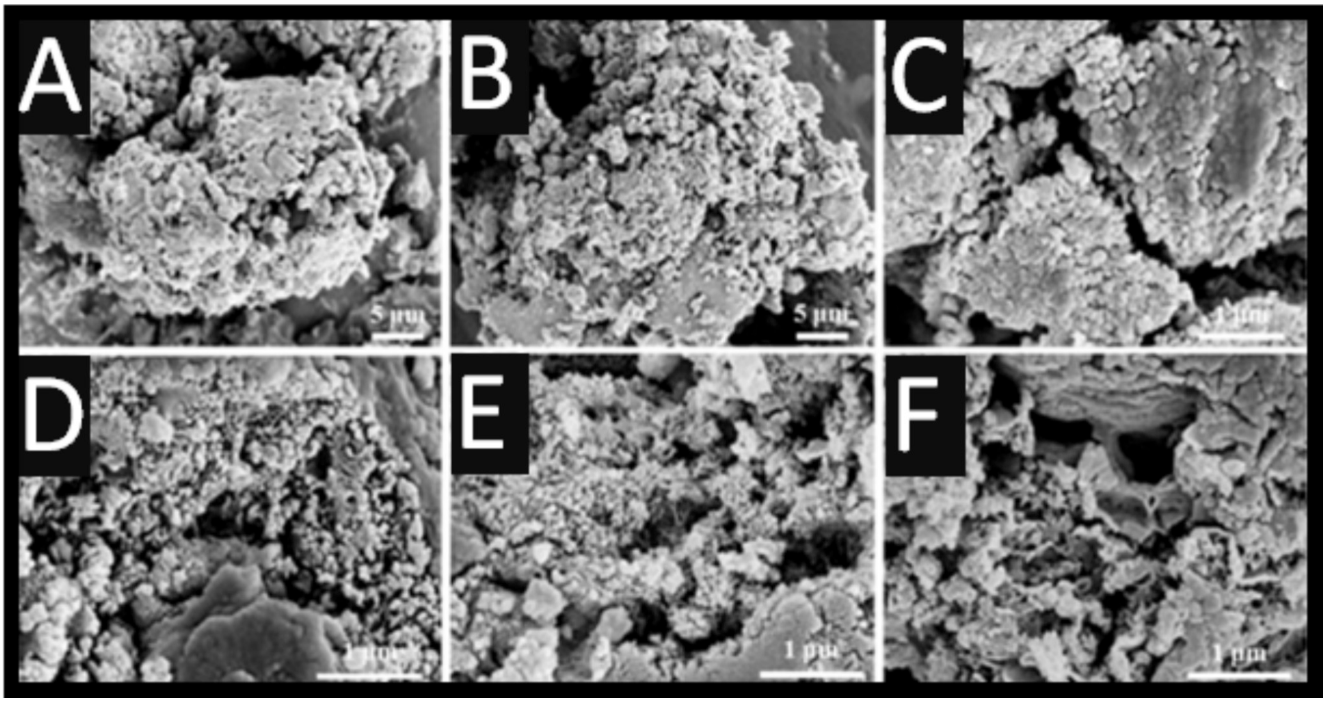

Fig. 2. SEM image of (A) CN, (B) SCN, (C) Cu/SCN, (D) Co/SCN, (E) CuCo/CN, and (F) Cu. Figure reproduced from reference [126].

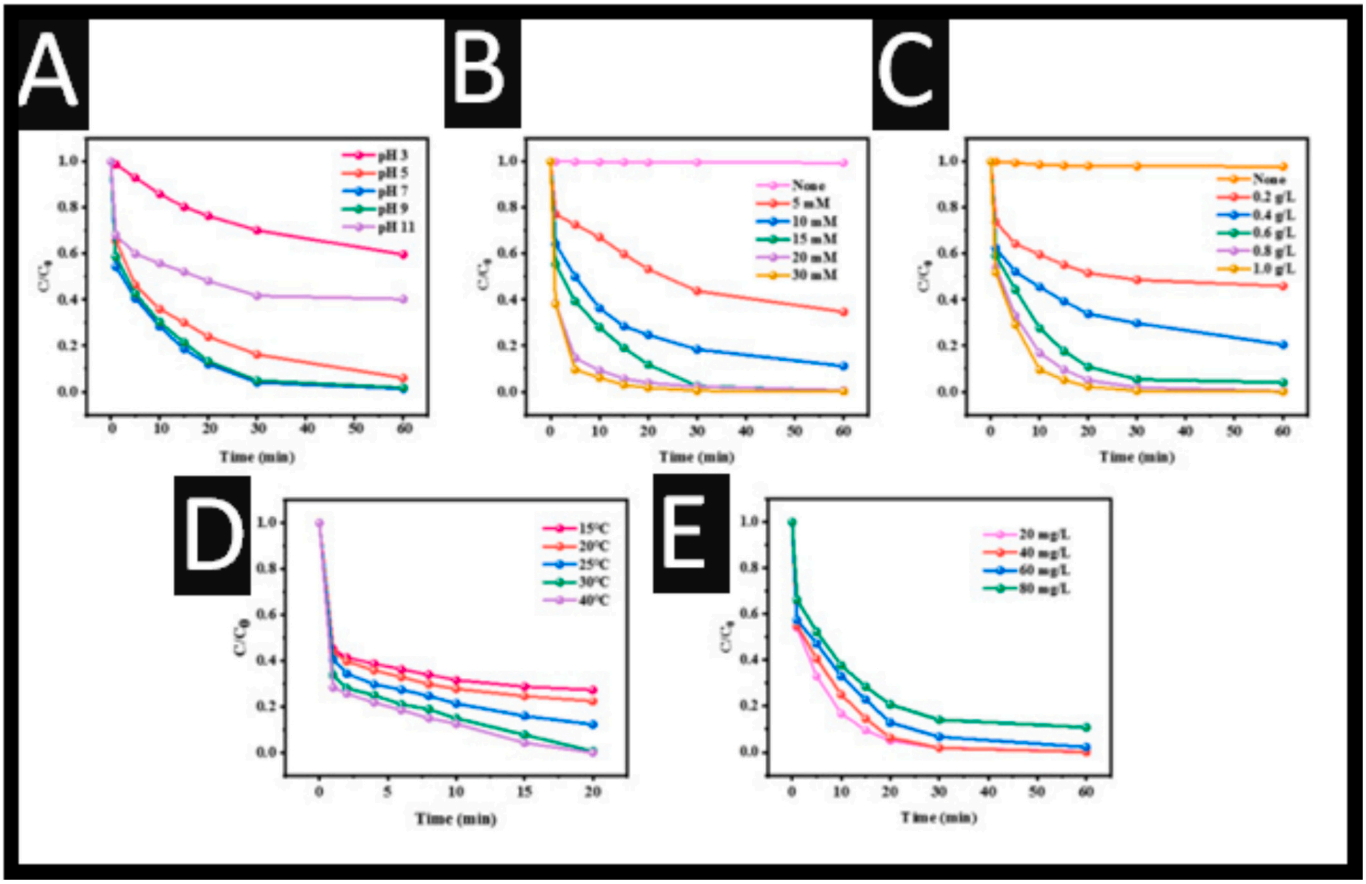

Fig. 3. Effect of (A) initial pH, (B) H_2O_2 dosage, (C) catalyst dosage, (D) reaction temperature, and (E) initial MO concentration on the removal of MO. Figure reproduced from reference [126].

and co-workers [166], a novel catalyst was prepared by encapsulating copper nanoparticles within nitrogen-doped porous carbon. Nitrogen doping facilitated the development of a mesoporous structure and better dispersion of Cu NPs, resulting in superior catalytic activity for reducing 4-nitrophenol. The catalyst also exhibited excellent reusability over multiple cycles.

3. Synthesis and characterization Cu—C based heterostructures

The copper-carbon heterostructures have been synthesized using ultrasonic impregnation method [167], sol-gel, chemical vapor deposition (CVD), simple liquid approach [168], chemical oxidative copolymerization [169], reflux scheme [170], chemical reduction [171],

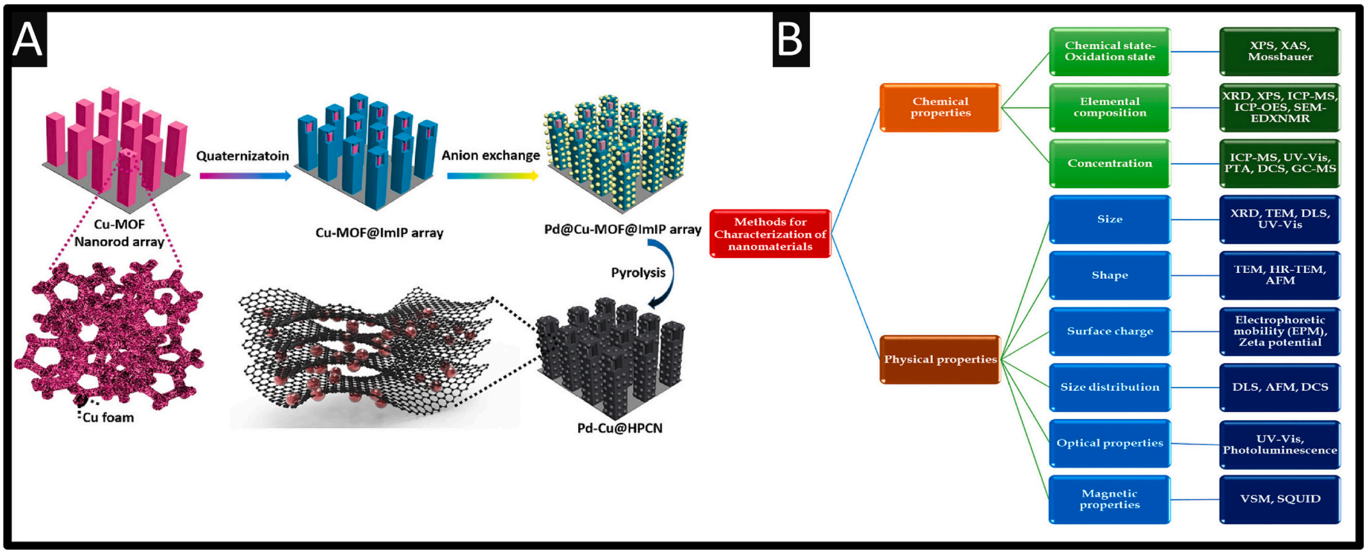

Fig. 4A. Schematic overview for the preparation of the hollow carbon nanopillar arrays embedded with Pd—Cu alloy NPs. Figure reproduced with permission from reference [179]. Copyright 2023 American Chemical Society. **B:** Various techniques for characterization of Cu—C nanocomposites. Figure reproduced with permission under a Creative Commons attribution-type BY from reference ([180]). Copyright 2023 MDPI.

simple chemical reduction [172], hydrothermal synthesis [173,174], microwave irradiation [175], ultrasonication [176], simple physical mixing [177], and the coprecipitation technique [178]. The cited sources provide details on the synthesis conditions that are not covered in this review. For instance, Fig. 4A illustrates the assembly of a core-shell architecture involving a MOF@imidazolium-based ionic polymer (ImIPs) pattern. Conversely, the characterization of the CCHNs is presented as outlined in Fig. 4 B.

3.1. Factors influencing the properties of copper-carbon nanostructures

The coordination bonding between copper and carbon materials significantly influences their performance in water purification. This interaction between copper and carbon materials is influenced by several factors such as the synthesis method, surface functionality, structural and electronic properties, stability, and reusability (see Table 2).

3.1.1. Synthesis method

The synthesis method employed for the CCNHs significantly influences their crystallinity, surface morphology, and particle size, which in turn affect their efficacy in removing organic pollutants from water. In a hydrothermal synthesis, for example, high-temperature and high-pressure aqueous solutions were utilized to synthesize nanomaterials [173]. This technique permits precise control of morphology and crystal size, resulting in highly stable nanostructures. Moreover, hydrothermally synthesized CuO nanostructures have shown efficient photocatalytic degradation of organic dyes, attributed to their tuned morphology and crystallinity [181]. The synthesis method determines:

3.1.1.1. Physical properties. The methods of synthesis utilized in the fabrication of CCHN have a significant impact on their physical properties, which are in turn instrumental in water treatment applications. Key properties such as surface morphology, particle size, and crystallinity are pivotal in the determination of the activity of these nanostructures [182].

3.1.1.2. Crystallinity. The degree of crystallinity in these materials is important, as increased crystallinity is usually linked with enhanced electron mobility [183]. This improved mobility reduces the rates of recombination of electron-hole pairs, usually limiting photocatalytic activity [184]. Hence, nanostructures possessing high crystallinity manifest superior efficiency in catalytic processes, making them more relevant in the degradation of water pollutants. The dependence of photocatalytic performance on the crystallinity of materials is attributed to the presence of fewer defects and grain boundaries in highly crystalline materials, which can function as recombination centres for charge carriers that are photogenerated [185]. When an incident light is absorbed by a photocatalyst, electrons are excited from the VB to the CB, generating an electron-hole pair. For the photocatalytic processes to be efficient, these charge carriers must migrate to the surface of the catalyst to participate in redox reactions that can degrade pollutants [186,187]. For a low-crystalline material, the large defects and grain boundaries hinder the migration of electrons, leading to electron-hole recombination before they reach the surface. [188]. This process of recombination emits energy as heat [189], lowering the number of charge carriers available for pollutant degradation [182,190]. Therefore, nanostructures with high crystallinity demonstrate robust photocatalytic efficiency, which makes them more useful in the degradation of organic water pollutants [191,192]. The improved electron mobility in highly crystalline catalyst materials inspires a more efficient separation of charges and transport, resulting in a greater number of electron-hole pairs for redox reactions [193].

3.1.1.3. Surface morphology. The surface structure design, including properties like roughness, porosity, and specific surface, is vital for CCNHs [194,195]. Tuning these surface properties can significantly increase the availability of active sites for chemical reactions, which results in enhanced interaction with various pollutants. For example, higher surface roughness may improve adsorption capacity, permitting the nanostructures to trap and react with a broader range of contaminants [196]. Rough surfaces can also enhance light scattering, improving the amount of light absorbed by the photocatalyst. Surface morphology is critical in photocatalysis, as it manipulates the adsorption of reactants and the transport of products. A porous structure delivers a high specific area, which improves the number of active sites available for adsorption of contaminants [197]. This is particularly crucial for diluted solutions of pollutants, where the adsorption step can be rate-limiting. The increased surface area permits more contaminant molecules to come into contact with the photocatalyst, improving the overall reaction rate. Therefore, optimizing the structure of the photocatalyst is crucial in maximizing the efficiency of the nanostructure in practical applications. By manipulating the surface morphology, it is possible to fabricate catalysts with advanced adsorption, charge transport features, and light harvesting, resulting in enhanced contaminant degradation efficiency.

3.1.1.4. Particle size. The particle size of CCNHs is another crucial parameter influencing their activity in water purification applications [198,199]. Smaller particle sizes return a larger surface area to volume, which has the advantage of better adsorption capacities and catalytic performance. This pattern means that the smaller the particle size, the higher the available surface area and active sites for interaction, resulting in improved reactivity [200]. This is especially significant in heterogeneous photocatalysis, where the reaction occurs at the interface between the contaminant and photocatalyst [201]. With a higher surface area, more contaminant molecules can be absorbed and react at the photocatalyst surface. However, it is crucial to note that exceptionally small particle size can result in agglomeration, which lowers the active sites, thus hampering photocatalytic performance [202,203]. As a result, the choice of particle size is critical in optimizing the activity of the CCNHs in water purification processes and minimizing aggregation effects. By meticulously tuning the particle size during synthesis, it is possible to manipulate the properties of the CCNHs for specific water treatment applications. Kang et al. [204] reported that the catalytic activity of Cu NPs can be significantly enhanced through a reduction process. In their study, Cu NPs (with an average size of 2.0 ± 0.4 nm) were uniformly distributed on reduced graphene oxide (rGO) using laser ablation followed by a reduction treatment, which ensured structural stability. The resulting Cu/rGO nanocomposites were employed as catalysts for the reduction of 4-NP, achieving impressive results with a mass-normalized rate constant (k/m) of 3.118 s^{-1} $mgCu^{-1}$ and a turnover frequency (TOF) of 2.987×10^{-4} mmol $mgCu^{-1}$ s^{-1}. Additionally, the strong interface between rGO and the ultrafine Cu NPs provided the Cu/rGO catalysts with remarkable stability, maintaining a conversion efficiency of over 92.0 % for 4-NP even after 10 consecutive reaction cycles. Therefore, the relationship between crystallinity, surface morphology, and particle size determines the efficiency of CCNHs in water treatment processes, underscoring the significance of careful design and synthesis methods in developing effective catalytic materials. The combined effect of these features ensures that the nanostructures demonstrate improved light absorption, surface reactivity, and charge separation, resulting in enhanced degradation efficiency of pollutants.

3.1.2. Surface functionalization

The functionalization of the surface of the CCNH entails the strategic integration of specific functional groups onto their surfaces, which can efficiently enhance their electron transfer capacities and efficiency of adsorption [205]. Modifying with these functional groups is critical in eliminating organic contaminants in water. The attachment of functional groups such as amino ($^{-}NH_2$), carboxyl ($^{-}COOH$), or hydroxyl (^{-}OH) to the carbon substrate increases the surface reactivity of the material and creates more active sites for adsorption of pollutants [205,206]. In addition to facilitating robust interaction between the carbon-copper materials and pollutants, this alteration in surface reactivity improves the ability of the material to engage in electron transfer reactions. Hence, surface functionalized CCNH exhibits profoundly increased activity in advanced water purification applications. Their improved features, including the formation of coordination bonds between active sites and pollutant molecules, enable more efficient binding of organic pollutants, resulting in increased decontamination efficiency and rapid adsorption kinetic processes. In the long run, these modifications facilitate more sustainable and reliable technologies for water purification that address environmental concerns associated with organic pollutants. Below is how the surface reactivity of the CCNHs can be influenced by modification:

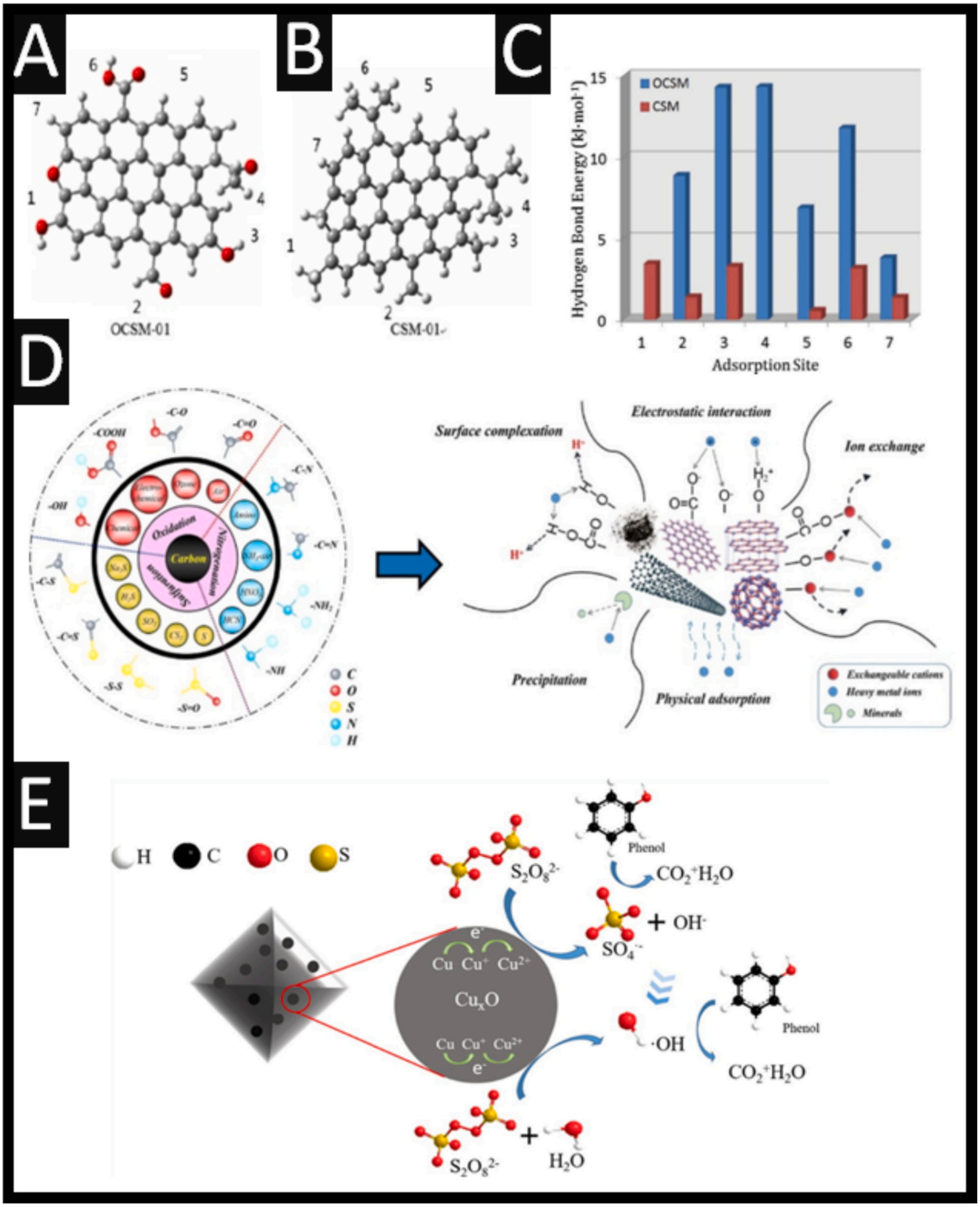

Fig. 5. Theoretical models for (A) oxygen- containing carbon surface and (B) pure carbon surface (red ball: oxygen atom; grey ball: carbon atom; small grey ball: hydrogen atom). (C) Hydrogen bond energies at different adsorption sites [208]. (D) Modification techniques to functionalize carbon adsorbents with various functional groups [210]. (E) The mechanism of the degradation of phenol in the presence Cu-CuxO NPs on porous carbon [211]. (For interpretation of the references to colour in this figure legend, the reader is referred to the web version of this article.)

3.1.2.1. Addition of oxygen-containing functional groups. Introducing oxygen-reach functional groups like carboxyl (-COOH), carbonyl (C═O), and hydroxyl ($^{-}$OH) [207], onto carbon surfaces significantly improved their surface polarity, which subsequently increases interactions with polar organic contaminants. These functional groups play an essential role in improving the performance of the carbon surface by facilitating the generation of hydrogen bonds and electrostatic interactions with diverse pollutants (see Fig. 5(A-C)) [208]. Consequently, the efficiency of adsorption of these contaminants is profoundly advanced. Furthermore, these oxygen-rich groups can affect the distribution of charge and density of electrons on the surface of carbon [209]. This modification supports more efficient electron transfer during catalytic procedures, which is critical in improving the overall effectiveness of CCNH materials in environmental applications, such as pollutant degradation and wastewater treatment. The ability to modulate the surface features of carbon materials through the introduction of these functional groups forms platforms (Fig. 5D), for the optimization of their activity in various catalytic and adsorption applications. This makes them viable candidates for addressing a wide range of environmental challenges [209,210].

For example, $CuCo_2O_4$ was supported on AC in heterogeneous catalysis that effectively removed Brilliant red 3BF (3BF) as a probe compound using peroxymonosulfate (PMS) activation [216], CuO anchored on/AC in catalyzing ozonation degradation of heavy oil refinery wastewater [217], and highly dispersed Cu-Cu_xO NPs on porous carbon for the advanced persulfate activation towards the degradation of phenol (Fig. 5(E)) [211].

3.1.2.2. Sulfur and nitrogen functionalization. Integrating sulfur and nitrogen atoms into the carbon matrix facilitates coordination bonding with metal centers or pollutant molecules, thereby improving the interaction of materials with organic contaminants. Nitrogen-containing functional groups, particularly pyridinic nitrogen and amines, enhance the carbon surface's basicity and total electron-donating ability. These modifications with nitrogen generate active sites to aid stronger interaction with electron-poor organic contaminants, such as halogenated compounds or some aromatic hydrocarbons (HC). These interactions can be credited to improved charge transfer mechanisms, making it less difficult for contaminants to adsorb onto or react with the altered carbon structure. Moreover, sulfur-rich functional groups also contribute to the chemical reactivity of carbon materials. The availability of sulfur supports the generation of strong covalent bonds with specific pollutants, as well as π-π interactions that can improve adsorption. This is especially useful for targeting contaminants like polycyclic aromatic HCs (PAHs) or heavy metals, where the unique electronic features of sulfur can enhance binding affinity. Through the promotion of both covalent and non-covalent interactions, modifications with sulfur can further optimize the capacity of the material to trap and retain a broad spectrum of environmental contaminants [218–220].

The functionalization of carbon materials with sulfur and nitrogen significantly enhances their adsorption capabilities and reactivity, broadening the spectrum of contaminants that these materials can effectively target. This functionalization strategy is crucial for the development of advanced materials aimed at ecological remediation and the removal of pollutants from contaminated environments [218–220]. In one study, Wang et al. [212] incorporated copper into a nitrogen-doped carbon matrix derived from metal-organic frameworks (MOFs) to improve peroxide production and electro-Fenton catalysis. (see Fig. 6) Another study [221] detailed the creation of nitrogen and sulfur co-doped carbon embedded with high-density cobalt single atoms (Co-SAs/NSC), which was employed for the electro-oxidation of organic sulfides using water as a feedstock. The catalyst demonstrated a high conversion rate of thioethers, achieving both absolute selectivity and impressive Faraday efficiency for sulfoxide production.

3.1.2.3. Plasma treatment for surface activation. Treatment with plasma is a very effective technology employed in the activation of carbon surfaces, supporting the integration of functional groups while retaining the integrity of their bulk qualities. This advanced technique uses ionized gas (plasma) to tune surface features at the molecular level

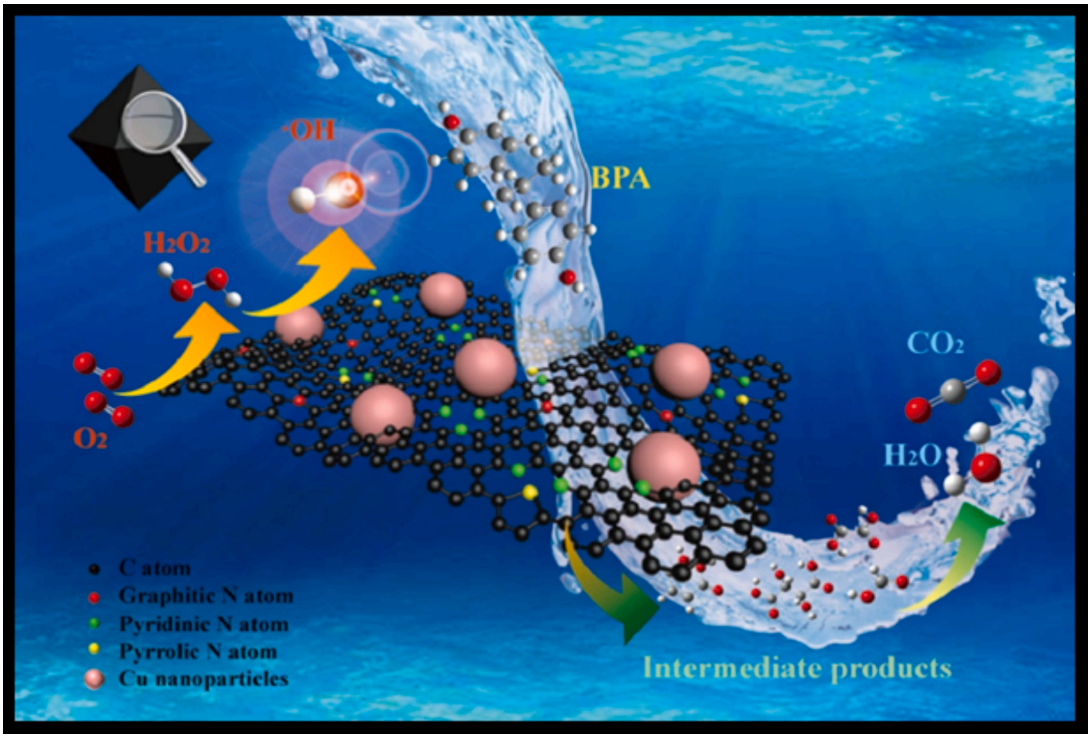

Fig. 6. Copper incorporated into a N-doped carbon matrix derived MOFs to improve peroxide production and electro-Fenton catalysis. Figure reproduced from reference [212].

[222]. Using this process, different collections of oxygen-containing functional groups including carboxyl, carbonyl, and hydroxyl groups, are introduced onto the carbon surface [223,224]. The addition of these functionalities substantially improves the acidity of the surface of the carbon materials, which in turn increases their ability to adsorb organic contaminants. This improvement plays an important role in applications in ecological remediation, where the removal of toxic substances is required [225]. Additionally, the modified surfaces exhibit advanced electron transfer characteristics, which are especially beneficial in catalytic degradation procedures. The enhancement of electron transfer supports more efficient reactions, which makes surface treatment with plasma specifically significant for applications in heterogeneous catalysis and wastewater treatment processes [226–228]. In general, treatment with plasma not only transforms the surface chemistry of carbon materials but also results in significant enhancements in their functional activities in numerous industrial and environmental applications [229].

3.1.2.4. Surfactant modification. The functionalization of carbon materials with surfactants is a crucial approach for improving their dispersibility in diverse media while concurrently generating extra active sites for the adsorption of contaminants [230]. Surfactant molecules, which have both hydrophobic and hydrophilic components, can add significant functional groups that radically change the surface features of carbon materials [231]. This modification permits more effective targeting of specific organic contaminants, as the tailored surfaces can interact with water-soluble or oil-soluble pollutants more favorably, depending on the nature of surfactants employed [232]. Furthermore, integrating surfactants can affect the dynamics of electron transfer of carbon materials [233]. By changing the surface charge and tailoring the electronic environment, surfactants can accelerate or hamper interactions with contaminants, possibly improving the adsorption efficiency of contaminants [234].

This alteration results in better catalytic activity towards applications in environmental remediation and present opportunities for engineering advanced materials with tailored reactivity and selectivity for complex systems of organic contaminants. Overall, surfactant functionalization of carbon material using methods such as dry oxidation, surfactant wet oxidation, and adsorption features a robust strategey to boosting their abilities in environmental management and control of pollution [218,230]. Although there is limited direct literature on the functionalization of copper-carbon heterogeneous materials with surfactants for water treatment, integrating these approaches holds promise for developing advanced materials aimed at water remediation. Future research could concentrate on investigating the synergistic effects of copper, carbon, and surfactant functionalization to create highly efficient and stable catalysts for water treatment applications.

3.1.2.5. Ligand functionalization. The coordination of specific ligands to carbon surfaces is instrumental in generating selective binding sites that effectively target and trap contaminants through stable ligand-metal interactions. For example, integrating ligands capable of creating coordination bonds with metal ions sufficiently enhances the decontamination efficiency of metal-containing organic contaminants. This functionalization not only improves binding interactions but also alters the electronic features of the carbon surface. By modifying the electron density, the carbon material can accelerate oxidation-reduction reactions better, which are critical for the degradation of diverse contaminants. Such alternation aids the carbon surfaces to originate chemical transformations, breaking down toxic substances into less harmful or unreactive forms. Ultimately, the strategic design of these ligands and their interaction with carbon substrate can result in advanced materials with improved catalytic activity in ecological remediation applications [218].

In a particular study, Garcia-Martin et al. [235] introduced a novel method for functionalizing the graphitic layers of activated carbons. They incorporated N-(4-amino-1,6-dihydro-1-methyl-5-nitroso-6-oxo2-pyrimidinyl)-L-lysine (AMNLY) and N-(4-amino-1,6-dihydro-1-methyl-5-nitroso-6-oxopyrimidin-2-yl)-N-[bis(2-aminoethyl)] ethylene diamine (AMNET) into basic activated carbon that has low levels of oxygen and nitrogen. This modified carbon was employed to remove chromate (VI) from water. The researchers suggested that AMNLY and AMNET could enhance the π-electron density within the graphene layers, thereby boosting adsorption capabilities through π-dispersive and/or donor–acceptor interactions between the pyrimidine group and basic arene centers. The adsorption capacity of Cr(VI) on AMNET-supported activated carbon increased by 1.7 times compared to untreated activated carbon, due to strong interactions between chromate anions and NH_3^+ groups. Conversely, the introduction of AMNLY reduced Cr(VI) uptake by 75 %, as it hindered the interaction between chromate anions and NH_3^+ groups because of the presence of a negatively charged carboxylate center nearby.

Thus, surface functionalization of copper-carbon materials by introducing specific functional groups can significantly enhance their electron transfer capabilities and adsorption efficiency, thereby improving the removal of organic pollutants from water [236,237]. For instance, in what could be regarded as copper bridging mechanism [236], the presence of Cu ions served as a bridge between organic pollutants and functionalized CNTs, to enhance the adsorption of chlorinated phenols and 1-naphthylamine onto surface-modified CNTs by complexing with functional groups on the CNT surface, thereby facilitating electron transfer and adsorption efficiency [238]. Moreso, by carefully selecting and introducing appropriate functional groups, the electron transfer abilities and adsorption efficiencies of copper-carbon-based materials can be tailored to target specific organic pollutants, leading to more effective water purification strategies [239].

3.1.3. Structural and electronic properties

The interface between carbon and copper in composite materials is essential to their performance, particularly in the context of eliminating organic contaminants from wastewater. This interaction can robustly impart the efficacy of catalytic process. Diverse structural properties, such as the availability of defects—like dislocations or vacancies—and the tailored integration of dopants, change the electronic and chemical characteristics of these materials.

These modifications can improve the active sites vacant for reaction, enhancing the overall catalytic activity of the composites. Moreover, the specific morphology and distribution of copper within the carbon matrix is crucial in influencing the availability of contaminants and the performance of the catalytic reactions. By exploring these complexities, it can be better understood how composite materials are optimized for efficient wastewater treatment. These structural properties can be modified using:

3.1.3.1. Copper-doped mesoporous polyimide nanocomposites. A study reported the development of copper-doped mesoporous polyimide (Cu-MP) nanocomposites that demonstrated high activity in Fenton-like processes for degradation of organic contaminants across a broad range of pH [240]. Through the C–O–Cu bridges, copper atoms bind with aromatic rings of the polyimide substrate, stimulating cation-π interactions. This bonding generated electron-rich centers around the copper atoms and electron-poor centers on the aromatic rings aiding the transfer of electrons during degradation of contaminants. The π–π stacking interactions between the aromatic rings of the Cu-MP nanocomposites and the contaminants further improved adsorption and electron donation, fast-tracking the catalytic cycle. Deng et al. [213] also described the formation of a C–O–Cu bond bridge on the catalyst surface, which induces an electron polarization distribution. This results in a non-equilibrium surface characterized by electron-rich and electron-poor microregions, as confirmed by a series of characterization techniques (see Fig. 7).

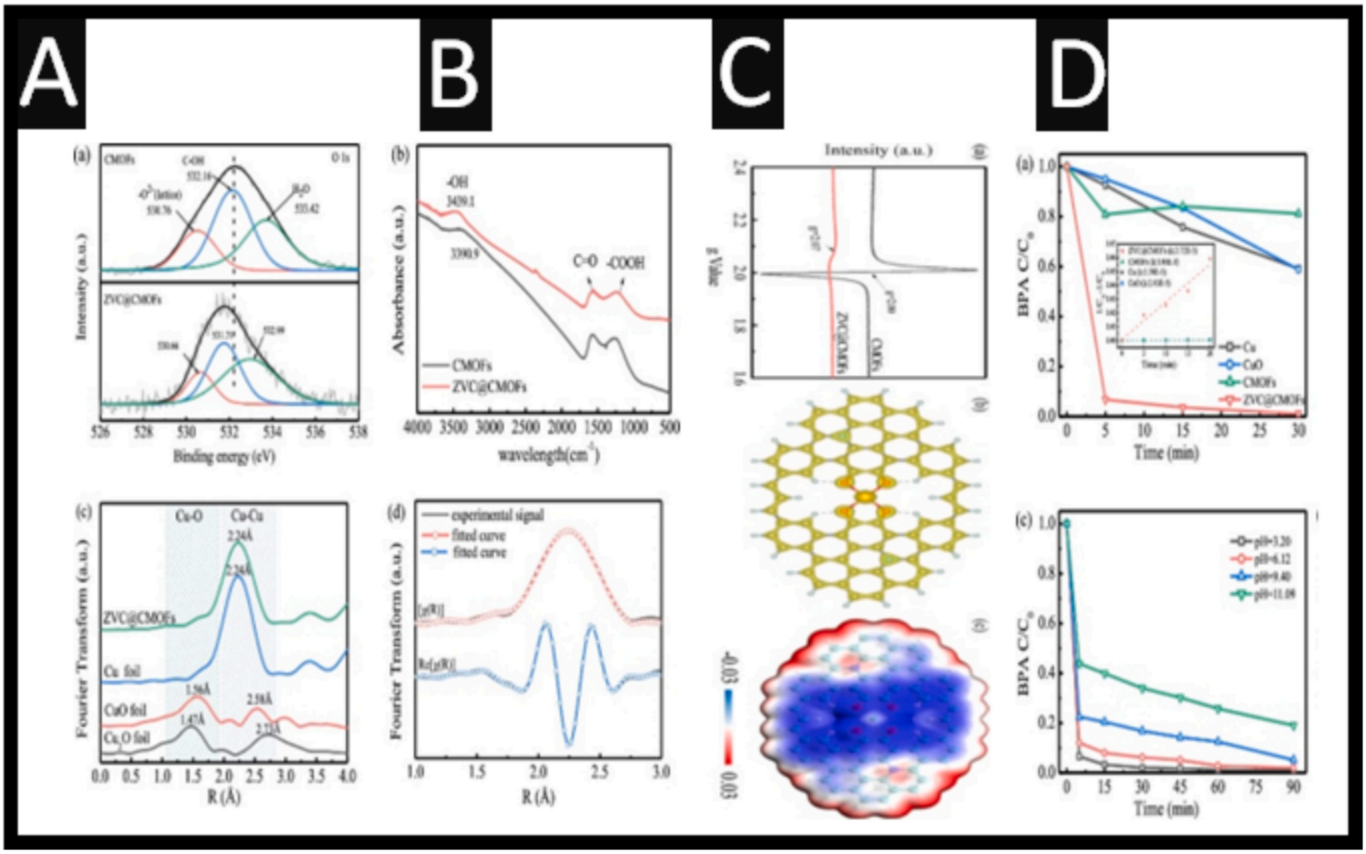

Fig. 7. (**A**) O 1 s XPS spectra and Fourier transforms of k^3-weighted EXAFS oscillations obtained at the Cu K-edge of Cu foil, CuO, Cu_2O, and ZVC@CMOFs. (**B**) FTIR patterns of CMOFs and ZVC@CMOFs and EXAFS curve fittings of ZVC@CMOFs on [$\chi(R)$] and Re[$\chi(R)$]. (**C**) Solid EPR spectrum of CMOFs and ZVC@CMOFs, valence electron density (the yellow area around the atom represents the electron density) andESP map of the ZVC@CMOF model fragment. (**D**) Degradation of BPA in various suspensions with H_2O_2 (the inset shows the corresponding second-order dynamical curve) and degradation curves of different pollutants (10 mg/L) in the ZVC@CMOF/H_2O_2 system. (For interpretation of the references to colour in this figure legend, the reader is referred to the web version of this article.). Figure reproduced from reference [213]. Copyright 2021, ACS.

3.1.3.2. Graphene oxide and reduced graphene oxide composites. Graphene oxide (GO) and reduced graphene oxide (rGO) have emerged as promising materials for supporting MNPs, significantly enhancing their catalytic activity in various applications. The unique properties of GO arise from its rich functional group content, which includes hydroxyl, epoxy, and carboxyl groups. These oxygen-containing functional groups improve the material's hydrophilicity and facilitate its dispersion in aqueous environments, thereby enhancing its interactions with a range of pollutants. When MNPs, such as copper, are incorporated into these graphene-based composites, they not only retain the advantageous properties of GO but also benefit from the material's structural characteristics. The strong interactions between the metal nanoparticles and the functional groups on the GO surface promote improved electron transfer processes. For example, in a photo-Fenton advanced oxidation process, the epoxide groups on GO can efficiently interact with H_2O_2, resulting in the creation of *OH radicals. This process is important as *OH radicals are strong oxidizing agents which have the capacity to degrade a broad range of contaminants [241]. Graphene-incorporated Cu_2O nanocomposites (GCC), synthesized via a precipitation method, have also demonstrated high photocatalytic degradation efficiencies of 97.9% for methylene blue (MB) and 96.1% for methyl orange (MO) within 160 and 220 minutes, respectively (see Fig. 8) [214].

Further, the combined impact of the embraced MNP and the GO matrix unlocks new pathways for electron transfer, which improves the general efficacy of catalytic reactions. This has pronounced implications for ecological remediation techniques, which suggests that rGO and GO composites could function as promising catalysts for the degradation of toxic substances in wastewater treatment, and other applications in pollution control [242–250].

3.1.3.3. Copper-doped graphitic carbon nitride (g-C_3N_4). Doping the graphitic carbon nitride (g-C_3N_4) structures with Cu significantly improved the ultrasound-assisted Fenton-like degradation of dyes [215]. The integration of Cu ions into the g-C_3N_4 medium creates more active sites, which are instrumental in accelerating the formation of ROS. The ROS, including the *OH radical, are very efficient in breaking down complex organic contaminants. This alteration not only enhances the efficiency of degradation of various organic dyes but also affects the electronic features of the g-C_3N_4 material. As a result, the enhanced electronic conductivity and efficient charge separation strengthen the overall catalytic activity of a material. The improvement of the photocatalytic activity can be ascribed to the improved band structure and energy levels, which synergistically support a more efficient interaction with light, thereby promoting better adsorption and degradation of contaminants (see Fig. 9).

3.1.3.4. Copper-doped carbon dots. Copper-doped carbon dots (CuCDs) were prepared using a one-step hydrothermal technique, returning a material that demonstrated improved Fenton reaction activity for the breakdown of organic dyes like RhB [251]. The integration of Cu into the carbon matrix facilitated the process of electron transfer on the surface of the CuCDs, resulting in the creation of •OH and $^1O_2$ radicals.

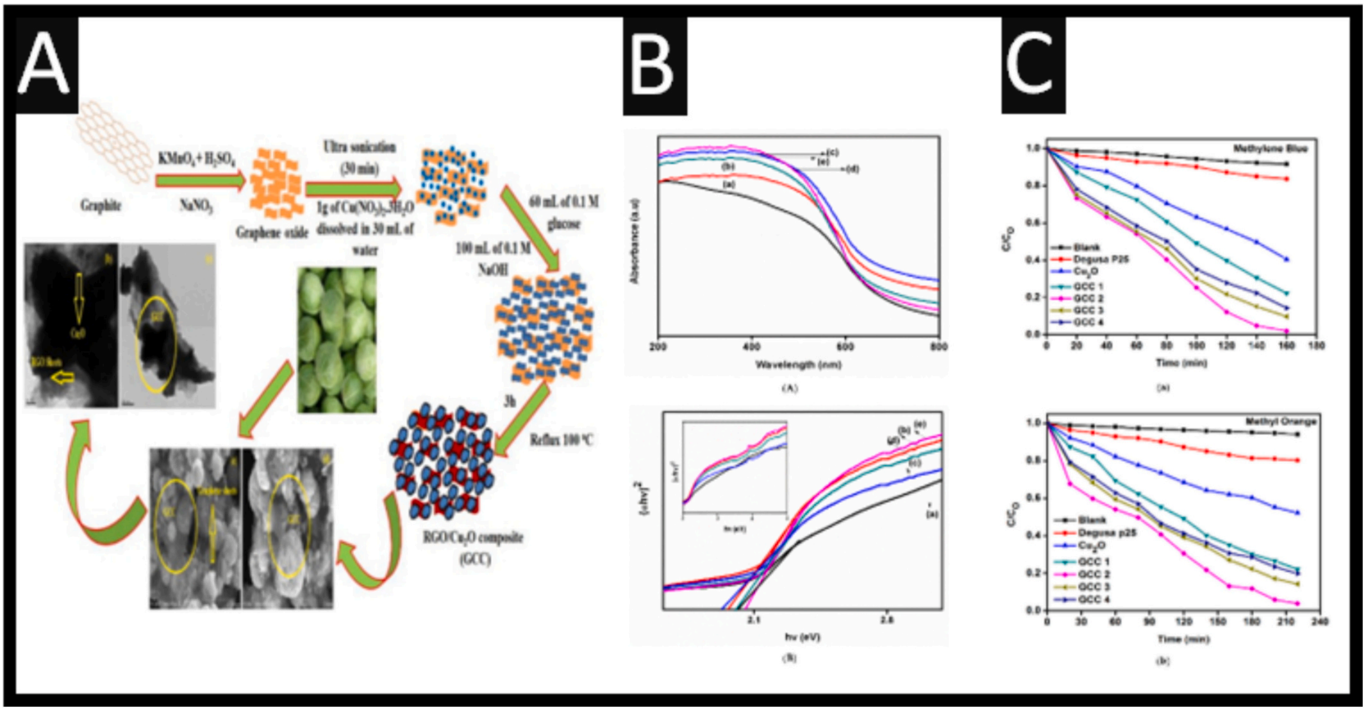

Fig. 8. (A) Synthesis of RGO/Cu$_2$O composite (GCC), Effect of GO loading on the (B) electronic properties of the GCC, (C) photocatalytic degradation of MB and MO (Different wt% 1 %, 2 %, 3 %, and 4 %) of GO were employed for the synthesis of various GCC composites as GCC 1, GCC 2, GCC 3, and GCC respectively). Figures reproduced from reference [214].

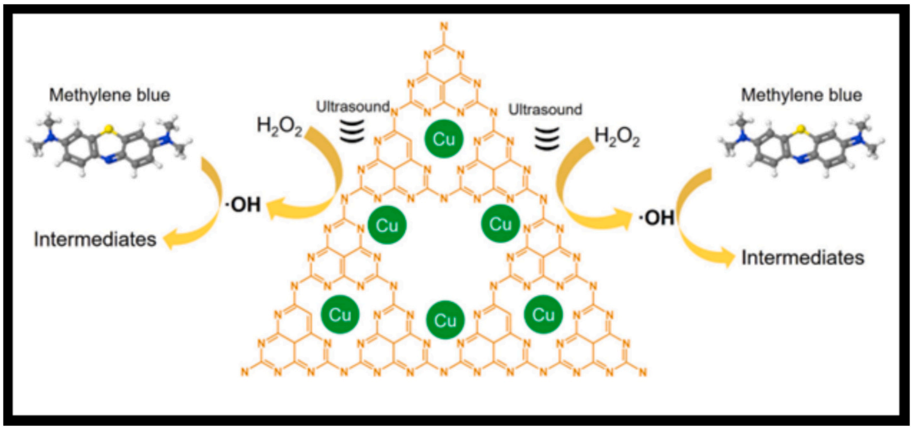

Fig. 9. Schematical scheme of plausible catalytic mechanism in Cu-C$_3$N$_4$/H$_2$O$_2$/ultrasound system. Reproduced with permission from ref. [215]. Copyright 2021, IWA Publishing.

The study also underscored that factors, such as CuCDs loading, pH, temperature, metal ions, the presence of O$_2$, and polymers can facilitate catalytic performance, highlighting the relevance of optimizing these parameters for effective wastewater treatment.

3.1.3.5. Role of defects in catalytic performance. Internal defects of carbon structure, including distortions, dopants, and vacancies, act as active sites for catalytic reactions. These imperfections generate regions of improved chemical reactivity, which robustly enhance the adsorption of contaminants by supplying extra surface area and energies that support interaction with adsorbates. Furthermore, the availability of these defects can accelerate the electron transfer process, which is critical for efficient catalytic performance [252–254]. Nonetheless, the relations between defects and catalytic performance are not fully understood. It is crucial to retain an optimized balance in the nature and concentration of the defects. While some defects can improve catalytic performance by increasing available reaction sites and advancing the transfer of charges, too many defects can undermine the structural integrity of carbon material [255]. This results in poor stability and potential degradation of the performance of catalysts over time [255]. Thus, meticulous characterization and control of defects are crucial for harnessing their catalytic ability without compromising the overall stability and effectiveness of the materials.

3.1.3.6. Negative effects of certain dopants. While doping can enhance catalytic activity, the choice of dopant is crucial. For example, introducing non-reducible dopants like gadolinium into ceria supports has been shown to negatively affect the catalytic performance of copper-ceria catalysts in CO preferential oxidation reactions. Such dopants can hinder the redox equilibrium essential for catalytic activity, leading to decreased efficiency. This finding emphasizes the need for careful selection and optimization of dopants to achieve the desired catalytic properties [256].

Tailoring the structural and electronic properties at the copper-carbon interface through the strategic introduction of defects and appropriate dopants offers a promising pathway to enhance the catalytic degradation of organic pollutants in wastewater. However, to optimize catalytic performance and ensure structural stability, it is essential to consider the type and concentration of dopants, as well as the nature of defects.

3.1.4. *Stability and reusability*

The catalytic performance of Cu—C heterojunction in closely connected with their structural stability, a feature largely influenced by the surrounding environmental conditions [257]. These heterojunctions which combine the properties of copper and carbon-based materials, are viable catalysts for numerous applications including water purification and photocatalysis [258,259]. Nonetheless, the very conditions that support catalytic performance can also stimulate degradation, requiring a robust comprehension of these effects [260]. The poor stability of copper-based catalysts can be major impediment to their broad engagement in industrial applications [261]. The compromise in structural integrity happening during catalysis, such as metal oxidation, sintering, or leaching, can significantly change the catalytic performance and selectivity of the material. Environmental factors such as fluctuating pH levels [262], the presence of reactants and products, and variations in temperature [263] can all contribute to these alterations, ultimately resulting in a decline in catalytic activity. The vulnerability of Cu-C heterojunction to harsh conditions stems from several factors. The interface between Cu and C materials is one significant area, susceptible to degradation due to variations in thermal expansion coefficient and electrochemical potential [259,264,265]. Secondly, exposure to alkaline or acidic systems can result in corrosion of the copper component, leading to dissolution of copper ions and concomitant loss of active sites. Exposure to acidic [266] or alkaline [267] environments can corrode the copper component, leading to the dissolution of copper ions and subsequent loss of active sites.

Therefore, improving the reusability and stability of the CCNH is crucial for their efficient application in wastewater purification, as these materials deteriorate after prolonged usage. This deterioration not only limits their efficiency but also raises operational costs. To overcome these problems, researchers explore several approaches, including protective coatings, which act as hindrances to corrosion and potential leakage of active components, and doping modifications, which entail the integration of foreign elements to enhance the chemical and mechanical features of the nanostructures. Recent progress in these areas includes:

3.1.4.1. Nitrogen doping for stabilization. Doping carbon supports with nitrogen has been established to profoundly improve the dispersion and stabilization of Cu NPs, which hinders deactivation and sintering, thus enhancing their catalytic activity and durability. A significant study explored the decomposition of formic acid over copper catalysts anchored on nitrogen-doped mesoporous carbon [268]. This result showed that doping with nitrogen resulted in strong interaction between copper species and the support, leading to the stabilization of copper in the shape of clusters less than 5 nm and even as a single atom. These single copper atoms were observed in significant ratios, credited to their strong coordination with pyridinic nitrogen atoms at the edges of the graphene sheet within the support. This robust coordination hindered deactivation and sintering of the Cu NPs, thus improving the catalyst's activity and stability.

In a study conducted by Wang et al. [269], an N-doped carbon layer was applied to Cu_2O nanowires to improve the stability and conductivity of electrodes used in filtration devices. This enhancement led to an impressive antimicrobial efficiency of 99.9 % at a flow rate of 1200 mL/min and a voltage of 10 V (Fig. 10). Compared to Cu_2O, the work function of the N-doped Cu_2O structures is measured at 3.623 eV, indicating that these electrodes can effectively inhibit the recombination of electron-hole pairs, thereby enhancing carrier transport efficiency. Additionally, Mulliken charge density analysis revealed that the N-doped Cu_2O structure reduced the oxidation tendency of the copper

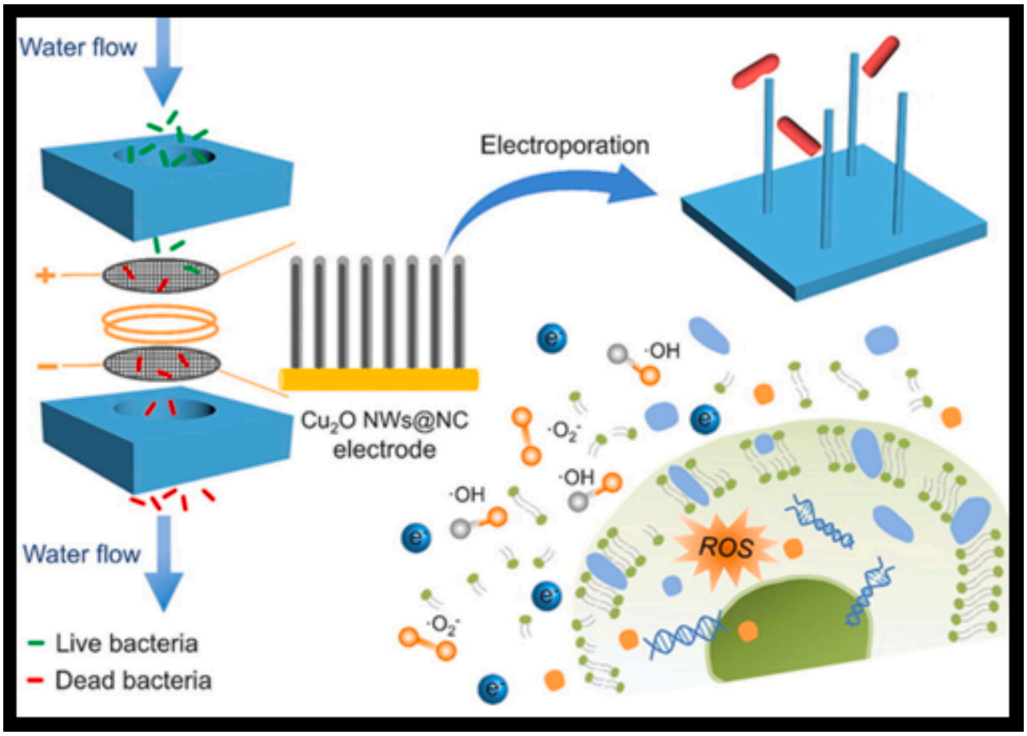

Fig. 10. The set-up of the bacterial water disinfection system [269]. Copyright 2022 Elsevier.

atoms and increased the stability of the electrodes. The mechanism by which this antibacterial effect occurs involves the synergistic action of ROS, *OH and $^1O_2$, alongside the process of electroporation.

Noh and colleagues [157], attributed the enhanced catalytic performance and stability of carbon nanostructures doped with nitrogen and containing cobalt and copper nanoparticles, which were pyrolyzed at 750 °C (CoCu@NC-750), to several factors. These include the increased oxygen adsorption facilitated by the nitrogen-doped carbon layer, resulting from localized changes in electron density, as well as the improved stability of the bimetallic core.

3.1.4.2. *Carbon Nanotube (CNT) Reinforcement.*

Adding CNTs into copper matrices has been broadly investigated to improve stability and mechanical properties [277–279]. Recent studies have concentrated on interface regulation strategies, including chemical bonding [280,281], physical interfaces [282,283], and metallurgical bonding [284], to increase performance by enhancing structural stability, charge transfer efficiency and active site exposure in catalytic systems. A novel approach involving the use of amorphous CNTs to create a nanoscale composite, resulted in improved stability and recyclability of the material [122]. However, effective regulation of the interface is critical in the optimization of the mechanical features of CNT-reinforced copper composites. The van der Waals forces determine the physical interfaces between the copper matrix and CNTs, which may mean weak interfacial bonding. Chemical bonding techniques entail functionalization of the CNTs to generate stronger covalent bonds with the copper matrix, thus improving the load transfer and mechanical strength. Metallurgical bonding, derived through processes like sintering of spark plasma, enables atomic-level bonding between copper and CNTs, resulting in robust interfacial strength and enhanced mechanical properties [122].

3.1.4.3. *Hollow Nanotube Carbon Nitride Anchored with High-Density CuNx Sites.*

As discussed in the previous sections, stabilizing copper-based catalysts by forming well-dispersed Cu—N (CuNx) coordination sites has emerged as a viable strategy to suppress metal leaching and improve catalytic durability. By anchoring copper atoms within nitrogen-rich frameworks, particularly in carbon nitride (CN) structures, researchers have demonstrated the formation of Cu—N heterostructures that reduce the presence of unstable Cu^{2+} surface species and promote stronger metal–support interactions [285–290]. Despite these advantages, conventional Cu–Nx site catalysts often suffer from disordered morphologies, leading to low specific surface area, poor porosity, and inefficient charge transport, which critically limit their applicability in advanced water treatment processes. To address these limitations, structural tuning via morphological engineering has gained increasing attention. Notably, size reduction and dimensional control at the nanoscale can induce quantum confinement effects, producing highly anisotropic, low-dimensional materials with significantly altered electronic structures and physicochemical behaviours [291,292]. Among such morphologies, hollow nanostructured materials, and in particular hollow carbon nitride nanotubes (HNCNs), offer a compelling platform for heterogeneous catalysis. Their unique architecture enhances light trapping and promotes effective spatial separation of oxidative and reductive species [293], thereby increasing photocatalytic efficiency.

Compared to bulk or disordered carbon nitride, hollow nanospheric and tubular CN structures demonstrate substantially higher charge separation efficiencies due to reduced recombination of photogenerated carriers [294]. Additionally, the curvature and internal void of hollow structures induce multiple internal reflections of incident light, which boosts photon absorption and expands active site exposure. Constructing 1D hollow CN nanotube**s** further amplifies these advantages by increasing the specific surface area and providing continuous pathways for directional electron transport, both essential for accelerating redox reactions [295,296]. By anchoring Cu species onto such hollow CN nanotube carriers (Cu–HNCN), researchers can leverage a synergistic set of properties: (1) enhanced visible-light absorption and utilization, (2) maximized exposure of active metal sites, (3) strong interfacial interactions between Cu species and the CN matrix, and (4) rapid and efficient charge transport [297,298]. Nevertheless, the fabrication of such catalysts remains technically challenging, particularly due to the difficulty in achieving uniform coatings on highly curved hollow surfaces [299]. However, when successfully synthesized, Cu–HNCN catalysts stand out as promising environmentally functional materials with substantial potential in wastewater treatment and other photocatalytic applications.

A recent illustration of the practical application of hollow carbon nitride nanotube-supported catalysts is demonstrated by the utilization of Cu–HNCN materials in the degradation of antibiotic pollutants through a hybrid photo-Fenton (PF) catalysis [270]. In this study, catalysts featuring highly dispersed CuNx active sites, anchored within hollow CN nanotubes, were synthesized and employed for the removal of TET, a representative and persistent pharmaceutical contaminant. Comprehensive characterization revealed that the unique morphology of Cu–HNCN, characterized by a high surface area, rich porosity, and strong capability for visible-light trapping, significantly enhanced catalytic efficiency. The Cu–HNCN/PF system achieved an impressive 96.0 % degradation of TET within 50 min, while also demonstrating broad-spectrum efficacy against other antibiotic compounds. Investigations into reaction parameters, including variations in H_2O_2 concentration, catalyst loading, pH, contaminant concentration, and water matrix composition, provided valuable insights into the operational robustness of the system.

Furthermore, DFT calculations (Fig. 11) confirmed that the hollow structure facilitated charge transfer, and the presence of short Cu—N bonds contributed to excellent structural stability and reduced copper leaching. Analyses of active species, coupled with liquid chromatography-mass spectrometry (LC-MS) and frontier electron density (FED) modeling, supported the elucidation of a reaction mechanism and degradation pathway. Together, this case study reinforces the potential of Cu–HNCN catalysts as highly efficient, structurally stable, and environmentally benign materials for advanced water treatment applications.

4. Mechanism of pollutant removal

Potable water recycling requires wastewater treatment systems to effectively remove a wide range of contaminants, including organic compounds, inorganic substances, heavy metals, and pathogenic microorganisms. Traditional treatment methods such as coagulation-flocculation, conventional successive oxidation pre-treatment, disinfection techniques (like chlorination), filtration, and sedimentation have been extensively utilized in the wastewater treatment sector. However, these traditional technologies often struggle to eliminate persistent contaminants fully and may inadvertently create secondary waste streams that complicate the treatment process. For example, pre-chlorinating contaminated water to promote oxidation can unintentionally create harmful by-products, including genotoxic, mutagenic, and carcinogenic chlorine derivatives. Furthermore, alternative oxidative treatments like ozonation have produced mixed outcomes. At the same time, they can be effective in certain scenarios, but residual ozone may inadvertently foster the growth of pathogenic microorganisms, thereby heightening public health concerns.

In contrast, heterogeneous catalytic water treatment processes, especially those utilizing copper-carbon (Cu—C) nanostructured heterojunctions, have surfaced as promising alternatives due to their superior degradation capabilities and enhanced mineralization potential. Recent research has yielded profound insights into the molecular-level mechanisms that govern these improvements. The synergistic interactions among various copper oxidation states (Cu^0, Cu^+, and Cu^{2+}) and carbonaceous supports, such as graphene, CNTs, and biochar, play a crucial role in facilitating multi-electron transfer processes. This

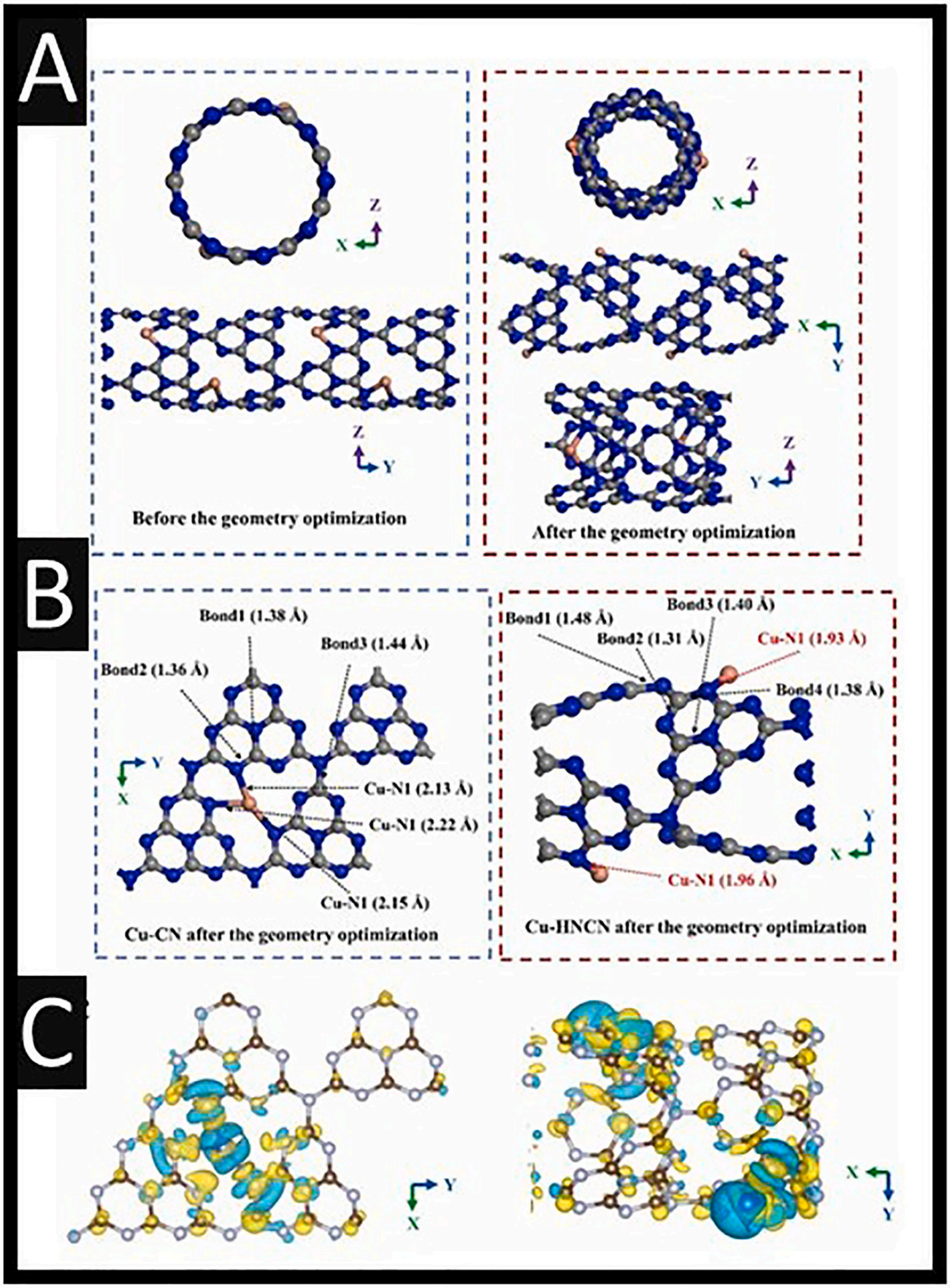

Fig. 11. (A) Atomic model of the Cu-HNCN before and after geometric optimization. (B) The atomic model of Cu-CN and Cu-HNCN after geometric optimization and the corresponding bond length. (C) Calculated charge density difference of Cu-CN and Cu-HNCN (the yellow and cyan areas indicate charge accumulation and depletion, respectively). Reproduced with permission from the ref. [270]. Copyright 2022 Elsevier. (For interpretation of the references to colour in this figure legend, the reader is referred to the web version of this article.)

interaction significantly enhances the generation of ROS like $^{\bullet}$OH, $O_2^{-\bullet}$), and $^1O_2$, all of which are vital for the oxidative degradation of organic pollutants during photocatalytic and Fenton-like reactions.

Advanced characterization and simulation techniques have provided compelling evidence supporting these mechanisms. For example, Density Functional Theory (DFT) simulations reveal critical charge redistribution dynamics and enhanced interfacial coupling at the Cu—C interface. These phenomena lead to improved electron–hole separation and the formation of preferred pollutant adsorption sites. Additionally, in situ spectroscopic techniques, including electron spin resonance (ESR), liquid chromatography–mass spectrometry (LC-MS) [300], X-ray photoelectron spectroscopy (XPS) [301], and X-ray absorption near-edge structure (XANES) [302], have been instrumental in tracking transient intermediate species and monitoring the redox transformations of copper catalysts throughout various processes. These studies illustrate a dynamic redox cycling mechanism, particularly evident during the activation of oxidants such as PMS and H_2O_2, where Cu^+/Cu^{2+} pairs effectively drive the catalytic cycles.

Such comprehensive molecular-level insights validate the enhanced catalytic activity of Cu—C heterojunctions and furnish a foundational framework for the rational design of next-generation water purification systems. By thoroughly understanding the underlying mechanistic pathways, future research endeavors can be better aligned to optimize material composition, enhance surface functionality, and refine process conditions. This strategic approach further elevates advanced pollutant removal technologies' selectivity, efficiency, and safety, ultimately contributing to a more sustainable and secure water supply for diverse applications.

Leveraging on these insights, we examined the core mechanisms by which Cu—C heterojunctions drive pollutant degradation, including photocatalysis, Fenton-like reactions, persulfate activation processes, etc.

4.1. Photocatalysis

Copper-based heterogeneous catalysts in photocatalysis have been extensively applied owing to their copious availability, low cost, good selectivity, excellent photocatalytic activity, and easy technique for the formation of the semiconductor layer [303–305]. Cupric oxide (Cu_2O/CuO) is a well-known p-type semiconductor used as photo-electrodes in the decomposition of contaminants because of its smaller band gap (E_g = 2.17 eV) [306,307]. These Cu-based photocatalysts could of a photosensitizer to support the photocatalytic performance of semiconductor catalysts with a broad E_g by increasing their capacity to absorb visible light. This could be attributed to the ability of Cu NPs to form localized surface plasmon resonance (LSPR) when irradiated with visible light of a specified wavelength [308]. However, a narrow E_g promotes rapid charge carrier recombination, which undermines the photocatalytic activity of copper oxide catalysts. Hence, doping and co-doping of Cu—O catalysts to create a heterojunction has become an efficient means of reducing the effect of charge carrier recombination. This approach increases the transfer of interfacial charge carriers, and enhances the absorption of visible light by generating defect states in the band gap position [309]. Such defect sites trap VB holes and CB electrons, thus inhibiting the recombination effect and boosting the photocatalytic efficiency of the catalyst [310]. In a copper-carbon-based nanostructure heterojunction, the Cu acts as a visible-light-responsive photocatalyst, while the carbon material reduces the bandgap, allowing visible light to be utilized. The system generates ROS such as $^{\bullet}OH$, $O_2^{\bullet-}$, and H_2O_2, which oxidize and degrade pollutants.

The reaction pathway for pollutant degradation [154]:

1. Excitation stage: $CuO/Cu_2O + h\nu \rightarrow e^- + h^+$
2. Transfer of electron to carbon material:
   e_{CB}^{-} → carbon material (e.g., MWCNT/rGO/Grephene) → hinders recombination
3. ROS generation: $h^+ + H_2O \rightarrow {}^{\bullet}OH + H^+$
   $e^- + O_2 \rightarrow O_2^{\bullet-}$

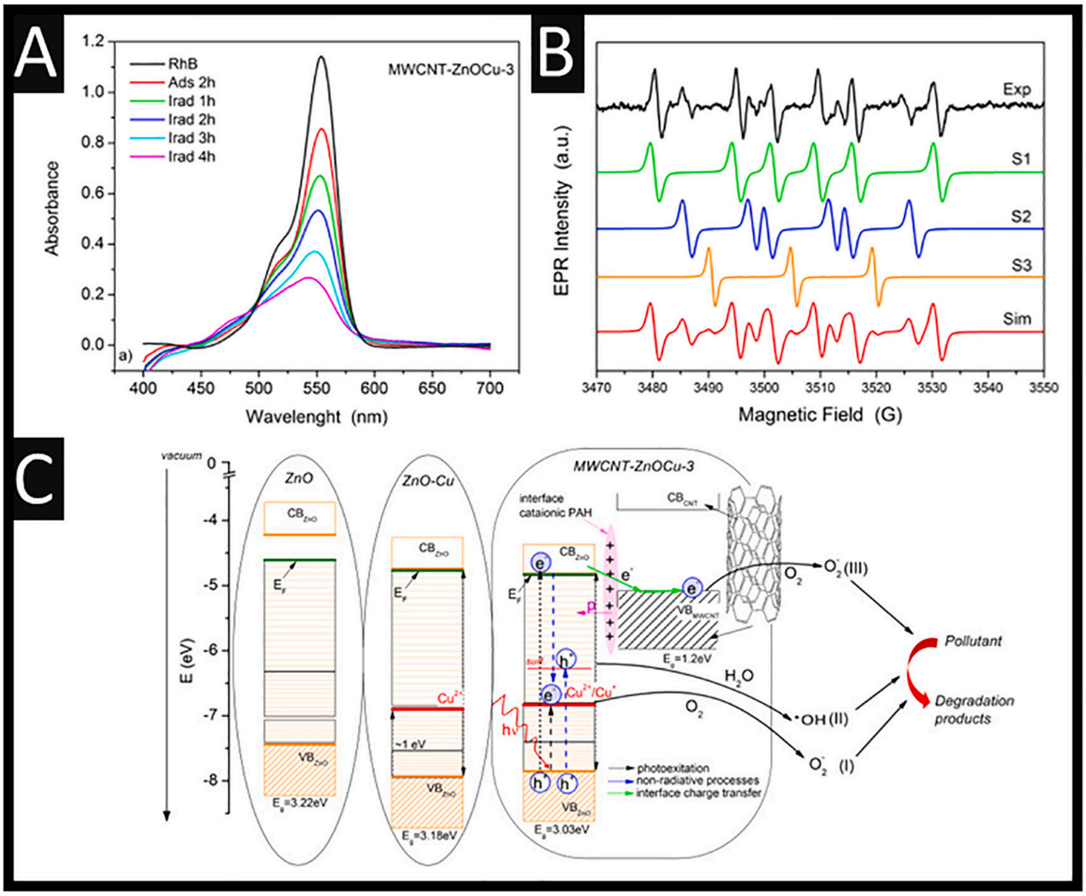

Fig. 12A. The RhB solution absorbance in the presence of MWCNT-ZnOCu-3 sample with diverse irradiation time intervals; **B:** Electron spin resonance (ESR) spectrum of the MWCNT-ZnOCu-3 sample under visible light irradiation in dimethyl sulfoxide (DMSO) with 5,5-dimethyl-1-pyrroline N-oxide (DMPO) as a spin-trapping agent. The experimental spectrum was simulated as a linear combination of the following spin adducts: •DMPO–CH_3 (S1: $a_N = 14.45$ G, $a_H = 21.4$ G, $g = 2.0101$, $\Delta H = 1.42$ G; relative concentration 65 %), •DMPO–OOH (S2: $a_N = 14.6$ G, $a_H = 21.7$, 0.8 G, $g = 2.0095$, $\Delta H = 1.5$ G; relative concentration 30 %), and a nitroxide-like radical (S3: $a_N = 14.6$ G, $g = 2.0098$, $\Delta H = 1.0$ G; relative concentration 5 %). The presence of •DMPO–CH_3 confirms •OH radical formation via reaction with DMSO. The nitroxide-like radical arises from N—C bond cleavage and DMPO ring opening, while the •DMPO–OOH adduct results from protonation of superoxide radicals; **C:** The overview of photodegradation mechanism mediated by MWCNT-ZnOCu nanocomposites; Figures reproduced from reference ([94]). Copyright 2021 Elsevier.

4. Pollutant degradation: pollutant $+ {}^{\bullet}OH + O_2^{\bullet-} \rightarrow CO_2 + H_2O$

According to Toloman et al. [94], doping ZnO- MWCNT with Cu improved the photocatalytic performance of the ZnOCu system towards the degradation of an antibiotic OTC, a dye (RhB and aromatic phenol (Fig. 12A). At optimal conditions of MWCNT/ZnOCu (1:3), rates of degradation of 76 %, 91 %, and 55 % were realized for RhB, phenol, and OTC, respectively, under visible light irradiation. This study provides a compelling molecular-level demonstration of these dynamic redox cycling mechanisms using a ZnO-Cu/MWCNT heterostructure. In this system, visible light excites electrons from the ZnO valence band to its conduction band, where they are transferred to Cu^{2+}, forming Cu^{+} ions. These Cu^{+} ions then reduce adsorbed O_2 to form $O_2^{-}\bullet$ radicals. Simultaneously, the photogenerated holes in ZnO's valence band oxidize water molecules to generate •OH radicals [311] (Eq. (1)–(5)). The addition of MWCNTs introduces multiple non-radiative excitation channels, enabling faster charge transport and further suppression of electron-hole recombination. MWCNTs act as electron sinks, and their high electrical conductivity provides an efficient escape route for charge carriers, thereby sustaining the generation of ROS at the catalyst surface [94].

$$h\upsilon + \mathrm{ZnOCu} \rightarrow e^{-} + h^{+} \tag{1}$$

$$e^{-} + h^{+} \rightarrow Cu^{+} \tag{2}$$

$$Cu^{+} + O_2 \rightarrow O_2^{-}\bullet \tag{3}$$

$$h^{+} + H_2O \rightarrow \bullet\, OH \tag{4}$$

$$e^{-}_{MWCNT} + O_2 \rightarrow O_2^{-} \tag{5}$$

To validate the roles of these active species, the study employed targeted scavengers, ammonium oxalate (h^{+}), vitamin C ($O_2^{-}\bullet$), and tert-butanol (•OH), and showed that suppression of ROS significantly decreased the degradation rates of RhB, phenol, and OTC. The most notable inhibition occurred with vitamin C and ammonium oxalate, confirming the importance of both $O_2^{-}\bullet$ and h^{+} in the photocatalytic degradation of RhB. All scavengers significantly suppressed activity in phenol degradation, emphasizing a broader ROS involvement. For OTC, superoxide radicals were the dominant oxidative species.

Further, ESR studies combined with DMPO spin-trapping revealed the formation of •OH and $O_2^{-}\bullet$ radicals [312–314], with •OH species present at approximately twice the concentration of superoxide radicals (Fig. 12B). This ratio was attributed to the high density of defect states in ZnO and low Cu doping levels (1/200), both of which favor •OH generation [94]. This case study exemplifies the critical role of defect engineering, interface design, and redox dynamics in enhancing ROS production and pollutant degradation efficiency at the molecular level, core principles for advancing copper-carbon nanostructure-based water purification technologies.

Another study by Haldorai et al. [315] described a simple sol-gel-assisted method for synthesizing CuO NPs dispersed on a rGO composite to facilitate the removal of MB dye under solar light. The TEM images revealed that the CuO NPs, which averaged 30 nm in diameter, were spread across the rGO surface. The composite photocatalyst achieved a 92 % degradation rate for the MB dye. Moreover, the study showed the loading of photocatalysts influences MB degradation, the concentration of MB, and pH levels. Research on radical scavenging indicated that the formation of superoxide radicals was the primary factor driving the degradation of MB. The stability assessment showed that the degradation efficiency of MB did not significantly decrease after four successive cycles.

An Ag-Cu_2O@rGO composite demonstrated outstanding photocatalytic efficiency, achieving complete degradation of MB dye within 60 min. This performance surpassed that of Cu_2O and Ag-Cu_2O counterparts, attributed to its enhanced charge separation and light absorption capabilities. Additionally, the composite exhibited exceptional stability and reusability, maintaining its catalytic effectiveness over six consecutive photodegradation cycles. Evaluating the photocatalytic mechanism of Ag-Cu_2O@rGO under visible light, radical scavenger experiments were conducted using benzoquinone ($O_2^{-}\bullet$), benzoic acid (•OH), and EDTA (h^{+}) at 1 mM concentration. The addition of these scavengers significantly suppressed the photocatalytic degradation efficiency from 99 % (no scavenger) to 38 %, 56 %, and 44 %, respectively. These results indicated that •OH were the dominant reactive species driving pollutant degradation, followed by photogenerated holes and superoxide anions [316].

The covalent organic frameworks (COFs) are unique due to the ability to predesign the π-electronic frameworks with knot and linker, as well as linkage, and therefore, present a well-structured molecular platform for scheming the highest occupied molecular orbital (HOMO) and lowest unoccupied molecular orbital (LUMO) levels to manipulate semiconducting features. Moreover, the COFs have been engineered into donor-acceptor structures [224], which offered robust heterojunctions for dividing excitons into electron-hole pairs, while the donor and acceptor π-columns support the migration of holes and electrons, respectively. These unique properties are not available in other molecular architectures and polymeric skeletons. Therefore, the COFs are very promising in designing photocatalysts. As a result, a squaraine-linked copper porphyrin (CuP-SQ) COF (Fig. 13) photocatalyst was designed based on COFs that activated molecular oxygen to singlet oxygen under visible light. Due to the π-coupled squaraine linkage and well-defined π-columns, CuP-SQ COF demonstrated robust photocatalytic performance, relative to the monomeric copper porphyrin complex [317].

4.2. PMS activation

The peroxymonosulfate (PMS)-based AOPs have been broadly investigated for water treatment using non-radical and radical pathways [318,319]. The radical pathway entails sulfate radicals $SO_4^{\bullet-}$ and ${}^{\bullet}OH$ generation using external stimuli, for instance, photo, electricity, heat, and radio, or through a single-electron reduction process to integrate the peroxide O—O on a catalyst [320–323]. Contrarily, the organic substrates function as donors of electrons to release sacrificial electron(s) to the PMS surface-activated system in a non-radical mechanism. This results in the oxidation of the pollutant through a charge transfer process [324].

Cu-based catalysts, in particular, nanoscale zero valence copper (nZVC), have since been investigated as a promising alternative towards the activation of PMS owing to their high reactivity, low toxicity, and broad working pH range. However, the practical application of a Cu-based catalyst in PMS activation is limited by the slow-moving kinetics of Cu^{2+}/Cu^{+} redox cycles and the poor recyclability of the nano-dimensioned catalyst. The slow Cu^{2+}/Cu^{+} recycling commonly results in poor reaction rate and low efficiency of degradation since Cu leaks into the solution from the surface of the solid catalyst. Various strategies have been investigated to increase the Cu^{2+}/Cu^{+} kinetics such as adding small-molecule reductants like hydroxylamine. The second problem related to poor recyclability has been tackled through the anchor of active supports to improve the architectural strength and realize less difficult regeneration and recycle. Additionally, the kinetics of oxidation and adsorption in typical batch reactors are characteristically restrained by mass transfer. This is because of the time-consuming PMS diffusion to the surface of the catalyst and the reaction of the produced ROS with aimed contaminant within the bulk solution. Therefore, the use of a flow-through system can contribute to faster mass transfer, resulting in improved degradation efficiency [325]. Carbonaceous CNTs are popular to stimulate an electron-transfer reaction from the organic donor to the C-activated PMS to complete a redox cycle.

In a report by Zheng et al [95], a hybrid electrochemical, catalytic oxidation, and nanofiltration systems were integrated for catalytic PMS activation and decomposition of aqueous micro-contaminants using

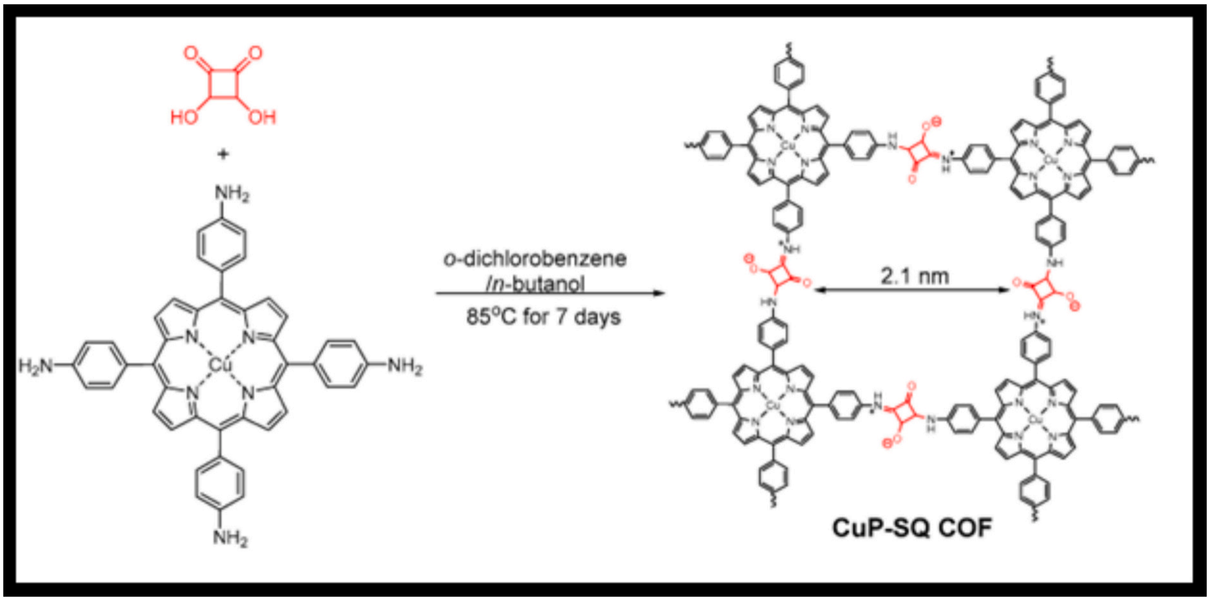

Fig. 13. Synthetic reaction of squaraine-linked COFs (CuP-SQ COF). Reproduced with permission from ref. [271]. Copyright MDPI 2017.

nZVC/CNT composite as electrode, filtration, and high-performance catalyst simultaneously (Fig. 13). The purification followed both non-radical and radical mechanisms, which had a huge synergistic impact on the decomposition of target pollutants. Total degradation of CR ($\tau < 2$ s) was achieved through a single-pass via the nZVC/CNT nano-filter at a pH of 7 and enjoyed rapid degradation kinetics over a broad pH window (3.0–7.0), in complex media (e.g., lake water, and tap water). The superior performance of nZVC/CNT was attributed to the enhanced Cu^{2+}/Cu^{+} redox cycles in the presence of an external electric field. The flow-through system significantly outstripped the traditional batch system because of the mass transport promoted by convection. Further mechanism investigation indicated that the electrophilic oxygen and carbonyl group of CNTs functioned as electron acceptors and electron donors, respectively, in the PMS activation to generate $^1O_2$ and $^{\bullet}OH$ through single-electron transport. The electron-deficient atoms of Cu are disposed to react with PMS through the surface OH group to generate aggressive intermediates (Cu^{2+}-O-O-SO$_3^-$) and subsequently generate $^1O_2$ by cracking the metastable intermediate coordination bond.

The mechanism of activation of PMS by the nZVC/CNT composite to generate the respective ROS for the degradation of CR is represented in Eq. (6)–(11).

$$\left[Cu^{2+}\text{—}OH\right]^{+} + H\text{—}O\text{—}O\text{—}SO_3{}^{-} \rightarrow \left[Cu^{2+}\text{—}O\text{—}O\text{—}SO_3{}^{-}\right] + H_2O \tag{6}$$

$$2\left[Cu^{2+}\text{—}O\text{—}O\text{—}SO_3{}^{-}\right] + 3H_2O + HSO_5{}^{-} \rightarrow 2\left[Cu^{+}\text{—}OH\right] \tag{7}$$

$$+ 3SO_4{}^{2-} + 2O_2{}^{\bullet -} + 5H^{+}$$

$$\left[Cu^{2+}\text{—}O\text{—}O\text{—}SO_3{}^{-}\right] + O_2{}^{\bullet -} + OH^{-} \rightarrow \left[Cu^{2+}\text{—}OH\right] \tag{8}$$

$$SO_4{}^{2-} + 3^1O_2$$

$$2O_2{}^{\bullet -} + 2H_2O \rightarrow 2^1O_2 + H_2O_2 + 2OH^{-} \tag{9}$$

$$HSO_5{}^{-} \rightarrow SO_5{}^{\bullet -} + H^{+} + e^{-} \tag{10}$$

$$2Cu^{2+} + 2SO_5{}^{\bullet -} \rightarrow 2Cu^{2+} + 2SO_4{}^{2-} + {}^1O_2 \tag{11}$$

The DFT simulations revealed that the Cu centres preferentially adsorb PMS, facilitating the generation of ROS (.Fig. 14A). The CNTs were found to enhance the adsorption of PMS through electron donation, promoting the activation process (Fig. 14B). The XPS analysis confirmed the presence of Cu^{2+} and Cu^{+} states on the catalyst surface, supporting the proposed redox mechanisms (Fig. 14C).

The EPR spectroscopy, employing DMPO and 2,2,6,6-tetramethyl-4-piperidinol (TEMP) as spin-trapping agents, revealed the generation of $^1O_2$ as the dominant ROS. A clear three-line TEMP-$^1O_2$ signal (1:1:1) and a weak four-line DMPO-•OH signal (1:2:2:1) were observed (refer to ref. ([95] for Figure), suggesting that $^1O_2$ was primarily produced through the slow decomposition of PMS in water. The presence of CNTs enhanced the yield of $^1O_2$ and •OH radicals, whereas the application of a weak electric field had minimal influence. The speciation of PMS is strongly pH-dependent: HSO_5^- dominates in weakly acidic environments, while SO_5^{2-} is more prevalent under mildly alkaline conditions. The $^1O_2$ is formed through a nucleophilic attack of SO_5^{2-} on HSO_5^-. Comparisons of EPR spectra between CNT/PMS and nZVC–CNT/PMS systems confirmed that the copper species served as the primary driver of $^1O_2$ generation. While transition metals are widely known to activate PMS via radical generation, in this case, the system mainly followed a non-radical pathway. $SO_4\bullet^-$ was not detected in EPR spectra, likely due to its rapid conversion or low yield, but DMPO-X signals (hyperfine splitting products of DMPO oxidation) confirmed the presence of strong oxidants.

Although $O_2\bullet^-$ formation was indicated in quenching experiments, its detection via EPR in water was hindered by high disproportionation rates. This limitation was overcome by conducting EPR in absolute methanol, where $O_2\bullet^-$ was stabilized, and its characteristic DMPO–$O_2\bullet^-$ signal was detected. Further mechanistic analysis revealed that PMS activation in the CCNH system proceeded via inner-sphere complexation, as confirmed by ionic strength studies: increasing $NaClO_4$ concentration (1–10 mM) had no impact on degradation efficiency. XPS analysis showed a decline in surface hydroxyl content after reaction, indicating that Cu–OH sites are actively involved in PMS activation. According to proposed mechanisms, electron-deficient surface Cu atoms bind PMS via Cu–OH groups to form metastable intermediates (e.g., Cu^{2+}–O–O–SO_3^-), which subsequently decompose to generate $^1O_2$. Additional $^1O_2$ may form through the coupling of $O_2\bullet^-$ radicals or by reactions involving $SO_5\bullet^-$. This dual contribution from radical (•OH, $O_2\bullet^-$) and non-radical ($^1O_2$) pathways enables robust pollutant degradation. Notably, a chemical oxygen demand (COD) removal efficiency of 78.9 % for Congo red was achieved, demonstrating the practical potential of this PMS activation route in advanced water treatment.

Another notable example is the use of $CuFe_2O_4$ magnetic

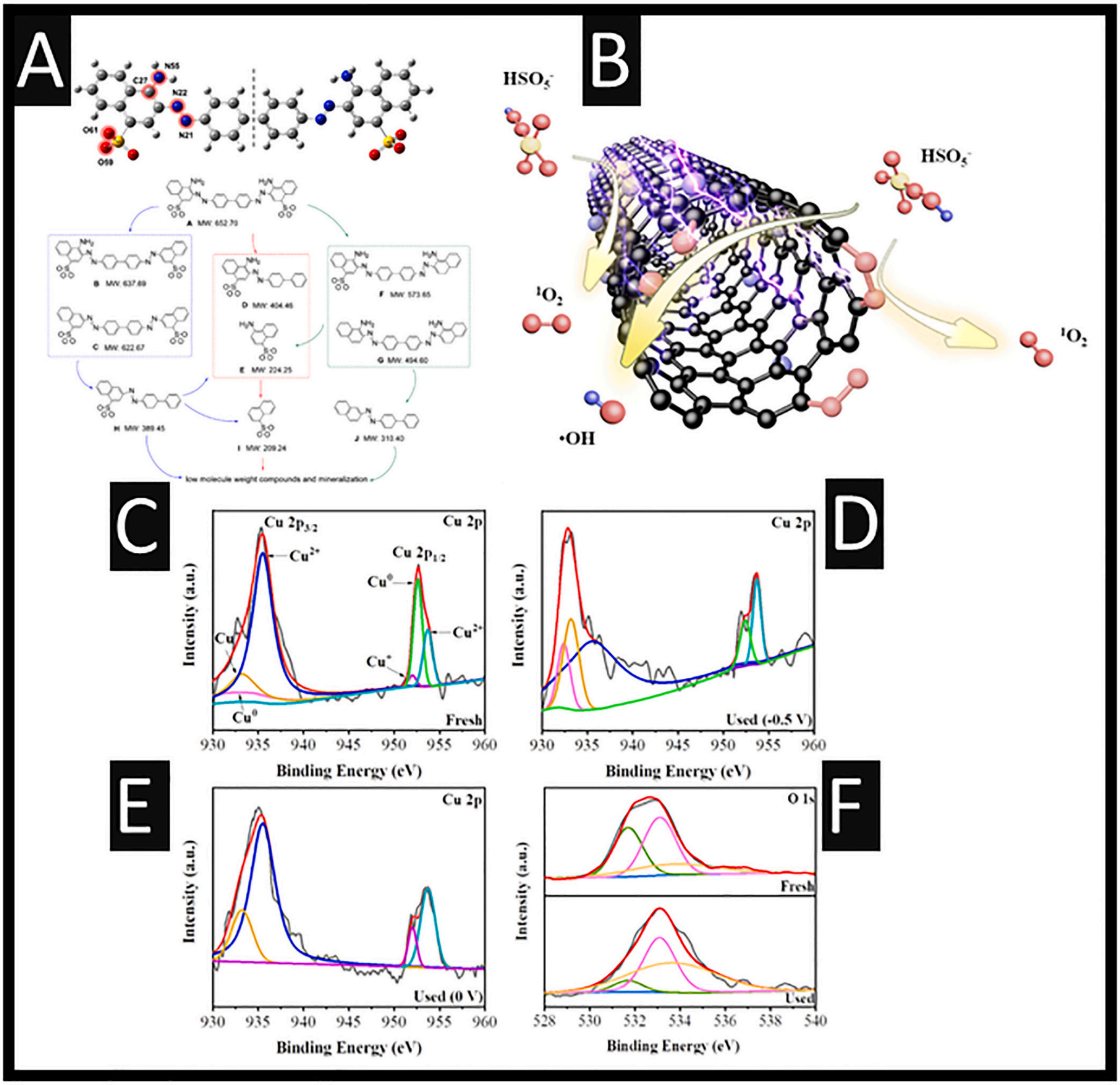

Fig. 14A. DFT calculations on CR molecule reactive sites at the B3LYP/6–31 + G (d, p) level; Chemical structure of CR (red circles signify the reactive sites); Also shown is the schematic representation of the probable mechanism of activation of PMS based on the electrochemical nZVC/CNT nano filter system; **B**: The CR proposed pathway of degradation mediated by DFT calculation. XPS spectra of nZVC–CNT before and after filtration. Deconvolution of the Cu 2p peak (C) before and (D) after reaction at −0.5 V or (E) without applied voltage. (F) Deconvolution of the O 1 s before and after reaction. Figures reproduced with permission from the reference ([95]). Copyright 2021 Elsevier. (For interpretation of the references to colour in this figure legend, the reader is referred to the web version of this article.)

nanoparticles supported on CNTs for PMS activation in BPA degradation [326]. The catalyst demonstrated nearly complete BPA removal within 60 min and 84.0 % total organic carbon (TOC) removal in 120 min at neutral pH. EPR spectroscopy and XPS confirmed the generation of •OH, indicating the involvement of radical pathways in the degradation process. The study proposed a mechanism where surface-bound redox cycles between Fe(III) and Cu(II) species on the $CuFe_2O_4$/CNT catalyst facilitate PMS activation, leading to BPA mineralization.

4.3. Fenton-like reaction

Standard homogeneous Fenton reaction (HoFR) has been identified as a strong and extensively used AOPs for the purification of wastewater polluted with refractory organic contaminants like organic synthetic dyes, PPCP, herbicides, and pesticides [22]. However, the key setback in practical applications of the HoFR is that it involves a high amount of Fe salt-based sludge present in the effluents, and excess use of H_2O_2, which requires additional post-treatment purification steps to remove. In addition, a small pH window (pH 2–3) can contribute to the limitations of the HoFR applications [23,24]. Moreover, the next-generation Fenton systems, such as photo-Fenton, electro-Fenton, and ultrasonic Fenton, though effective, present economic and operational challenges due to their energy-intensive requirements [102].

Recent studies have demonstrated that catalytic performance in Fenton-like systems can be significantly enhanced through the strategic design of dual reaction centers (DRCs), which are formed by inducing polarized charge distributions across catalyst surfaces. This approach has proven effective in improving hydrogen peroxide (H_2O_2) utilization and extending catalytic activity across a broader pH range [327–332]. For example, Deng et al. [327] reported that cation–π structures, such as V–S–C(π) and V–O–C(π) bridges, facilitated direct electron transfer from carbon π-systems to vanadium centers, thereby accelerating redox reactions. Similarly, Jiang and team members [329] confirmed that DRCs formed on Cu-doped carbon nitride surfaces substantially improved Fenton-like activity. These systems establish efficient electron transport pathways, wherein electrons migrate from electron-deficient sites to electron-rich centers, allowing H_2O_2 and DO to act as effective electron acceptors, yielding reactive oxygen species like •OH and O_2•⁻.

According to Wang et al [96], Fe—Cu bimetallic NPs were encapsulated within a structured mesoporous carbon composite catalyst (CuFe-MC) for the catalytic degradation of eight (8) model non-biodegradable organic pollutants. Effective total organic carbon (TOC) elimination of the contaminants was realized by employing the as-prepared CuFe-MC, which enhanced degradation efficiency relative to the Fe^{2+} ion under the same reaction conditions. The reduced Fe leaching in the CuFe-MC catalyst supported its good stability. In addition, the recovery of the catalyst was done easily by employing an external magnet at the end of the process and maintained useful performance following 5 cycles, which underscores its potential long-term useful life in wastewater purification. Fig. 15 shows the morphological properties of the fabricated catalyst and the pathway of the BPA degradation.

The possible mechanism of the heterogeneous Fenton reaction catalysed by CuFe-MC proceeded through surface reactions which involve both Fe and Cu active sites as represented by Eq. (12–16) and Eq. (17–19) for Fe and Cu activation of H_2O_2 to generate OH radical respectively.

$$\equiv Fe^0 + 2H^+ \rightarrow \equiv Fe^{2+} + H_2 \tag{12}$$

$$\equiv Fe^{2+} + H_2O_2 \rightarrow \equiv Fe^{3+} + {}^{\bullet}OH + OH^- \tag{13}$$

$$\equiv Fe^0 + H_2O_2 + 2H^+ \rightarrow \equiv Fe^{2+} + 2H_2O \tag{14}$$

$$\equiv Fe^{3+} + H_2O_2 \rightarrow \equiv Fe^{2+} + HOO^{\bullet} + OH^- \tag{15}$$

$$2 \equiv Fe^{3+} + \equiv Fe^0 \rightarrow 3 \equiv Fe^{2+} \tag{16}$$

$$\equiv Cu^+ + H_2O_2 \rightarrow \equiv Cu^+ + {}^{\bullet}OH + OH^- \tag{17}$$

$$\equiv Cu^{2+} + H_2O_2 \rightarrow \equiv Cu^+ + HOO^{\bullet} + OH^- \tag{18}$$

$$\equiv Fe^{3+} + \equiv Cu^+ \rightarrow \equiv Fe^{2+} + \equiv Cu^{2+}; \Delta E^0 = 0.6\ V \tag{19}$$

The standard reduction potential of Cu^{2+}/Cu^+ and Fe^{3+}/Fe^{2+} redox pairs are 0.17 V and 0.77 V respectively, therefore the oxidation of Cu^+ by Fe^{3+} (Eq. (14) is thermodynamically favourable, which benefits the redox cycles of Cu^{2+}/Cu^+ and Fe^{3+}/Fe^{2+}. Therefore, through the contribution of Cu^{2+}/Cu^+ and Fe^{3+}/Fe^{2+} pair, the electron transfer at the interface is significantly improved in the CuFe-MC system.

To probe the generation of •OH radicals during the reaction, ESR analysis was conducted using DMPO as a spin-trapping agent. The ESR spectra showed (refer to reference ([96] for Figure), a clear four-line signal characteristic of DMPO–•OH adducts with an intensity ratio of 1:2:2:1, confirming the production of •OH. Among the tested catalysts, Cu-MC, Fe-MC, and CuFe-MC, CuFe-MC-1-800 exhibited the most intense DMPO–•OH signal, indicating superior catalytic activity and efficient H_2O_2 activation. To quantitatively assess •OH generation, benzoic acid was employed as a probe molecule, with hydroxylation products monitored by high-performance liquid chromatography (HPLC). The CuFe-MC-1-800 catalyst produced up to 325 μM of •OH within 60 min, nearly tenfold higher than the 32.9 μM reported for mesoporous $CuFe_2O_4$ [333], and significantly higher than Fe-MC-1-800 (112 μM) and Cu-MC-1-800 (55 μM). These results underscore the dominant role of •OH in the degradation pathway and the enhanced radical generation efficiency of the bimetallic system.

At the molecular level, the proposed mechanism involves surface-mediated redox reactions where zero-valent iron (Fe^0) is oxidized to Fe^{2+}, which in turn activates H_2O_2 to produce •OH via the Haber–Weiss mechanism. Concurrently, Cu species (Cu^+/Cu^{2+}) also participated in H_2O_2 activation and facilitated the regeneration of Fe^{2+} from Fe^{3+}, sustaining the catalytic cycle. The ordered mesoporous carbon support enhances surface area and active site dispersion and promotes electron transfer between metal centers, thereby lowering the activation energy for H_2O_2 decomposition. The CuFe-MC-1-800 catalyst exemplifies how

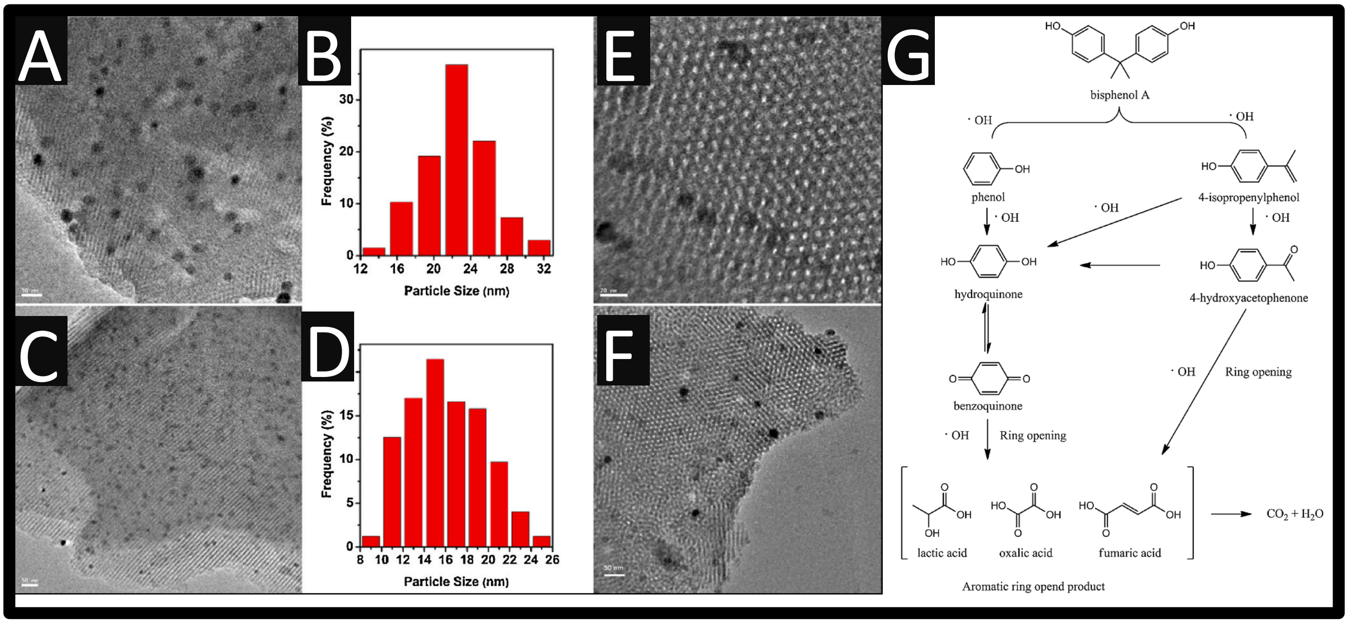

Fig. 15. TEM images of CuFe-MC-1-800 (**A** and **E**) and Fe-MC-1-800 (**C** and **F**) viewed along the [93] (**A** and **C**), and [001] (**E** and **F**) directions, respectively. The central (**C** and **D**) are the size distribution histograms of metal NPs calculated from A and C, respectively; **G**: Proposed degradation mechanism of bisphenol A. Reproduced with permission from reference ([96]). Copyright 2014 Elsevier.

CCNH-based systems can be engineered to maximize Fenton-like reactivity through strategic metal synergy and carbon support design. This molecular-level understanding supports the development of robust, recyclable, and highly active catalysts for pollutant degradation in water treatment applications.

As mentioned in a previous section, Deng and the team members [213], explored the development and application of ZVC@CMOFs as a catalyst for BPA degradation in aqueous solutions. The ZVC@CMOF catalyst exhibited a unique dual-reaction-center (DRC) Fenton-like mechanism. Electron-rich zero-valent copper (ZVC) centers facilitated the reduction of hydrogen peroxide (H_2O_2) to •OH, while electron-poor carbon (C(π)) centers adsorbed pollutants like BPA through π–π interactions. This electron transfer from C(π) to Cu enhanced the catalyst's reactivity, enabling the generation of reactive ROS such as $O_2•^-$, $^1O_2$, and •OH, which collectively degrade pollutants. The ZVC@CMOFs catalyst achieved a 93.2 % BPA degradation within 5 min, surpassing Cu and CuO, which reached 40.8 % and 41.2 % degradation, respectively, over 30 min. The catalyst maintained over 80 % degradation efficiency after multiple cycles, indicating excellent reusability. Most importantly, it demonstrated effective pollutant removal across a broad pH range (3.20–11.09), reassuring its applicability in varying environmental conditions.

The XPS analysis revealed the formation of C–O–Cu bonds, which indicates strong interactions between copper and the carbon matrix. Additionally, DFT calculations showed that both O_2 and H_2O_2 preferentially adsorb at the electron-rich copper centers. At the same time, pollutants tend to adsorb at the electron-poor carbon (π) centers (Fig. 16A). Moreover, Raman spectroscopy demonstrated shifts in the D and G bands upon the adsorption of pollutants, further confirming the interaction between these pollutants and the catalyst's surface (Figs. 16 (B—D). Lastly, EPR spectroscopy detected signals for $O_2•^-$, $^1O_2$, and •OH, thereby confirming the generation of multiple ROS during the catalytic process (Figs. 16(*E*-G). This arrangement facilitates efficient electron transfer and the generation of ROS.

The ZVC@CMOF catalyst demonstrated significant potential for environmental applications, particularly in the degradation of persistent organic pollutants like BPA. Its high efficiency, stability, and adaptability across a wide pH range make it a promising candidate for wastewater treatment processes. The catalyst's ability to utilize natural dissolved oxygen and pollutants as electron donors further enhances its sustainability and applicability in real-world scenarios.

Another recent work by Liao et al. [102], has demonstrated a cost-effective and environmentally sustainable alternative through the development of copper-species-doped graphene-like catalysts (Cu-GCD

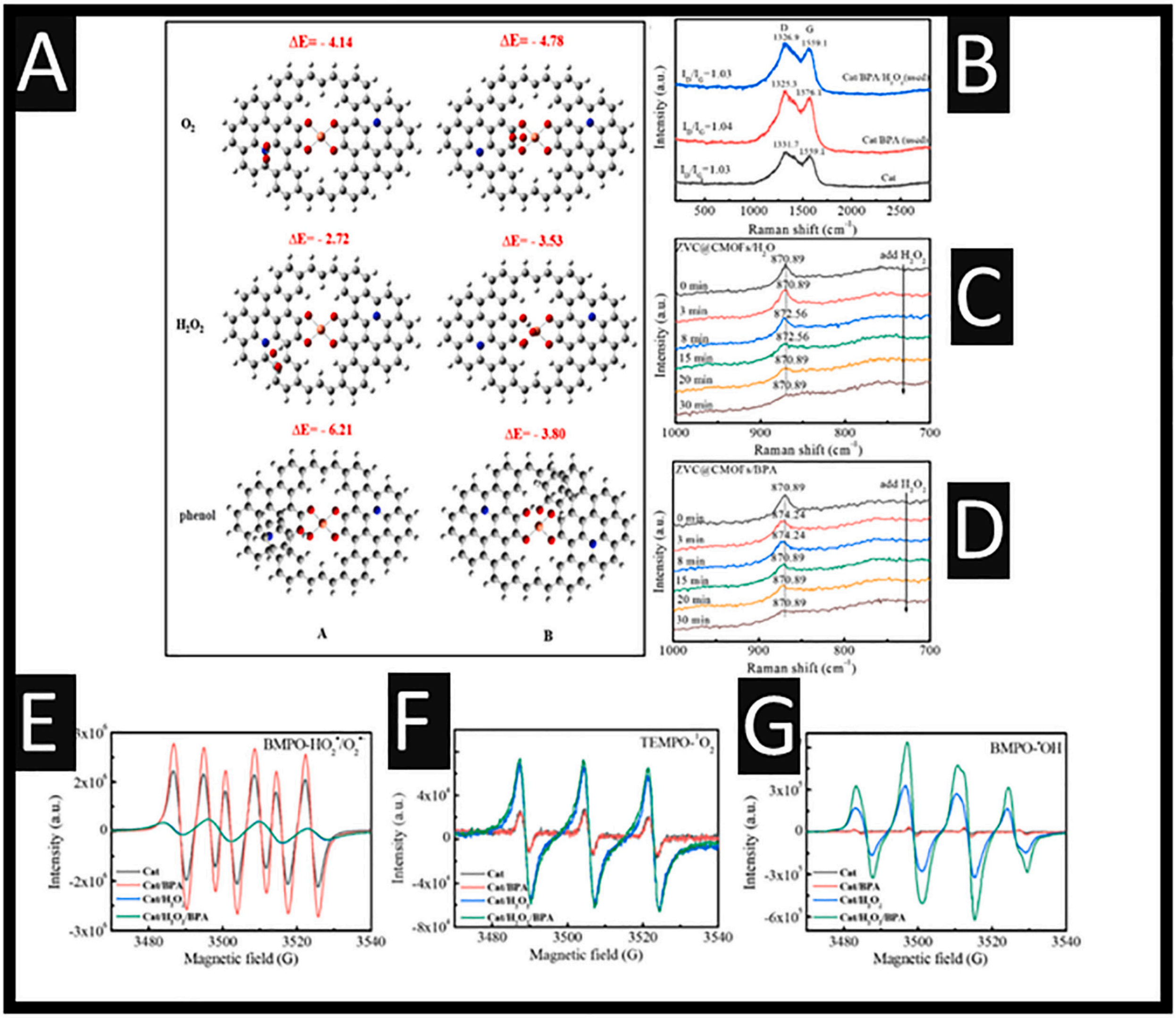

Fig. 16. (A) Adsorption energy of O_2/H_2O_2/phenol in A and B positions of the ZVC@CMOF model calculated by DFT. (B) Raman spectra of ZVC@CMOFs obtained under different conditions. (C) In situ Raman spectra of ZVC@CMOF/H_2O and (D) ZVC@CMOF/BPA dispersions recorded at different times after adding H_2O_2. Spin-trapping EPR spectra for (E) $HO_2^\bullet$/$O_2^{\bullet-}$, (F) $^1O_2$, and (G) $^\bullet OH$ in various systems. Reproduced with permission from reference ([213]). Copyright 2014 Elsevier.

NSs), synthesized via a carbothermal reduction of a β–cyclodextrin–copper complex. In this system, copper is coordinated to carbon in C–O–Cu bonds, forming dual reaction centers (DRCs) with polarized charge distributions. These DRCs promote directional electron flow—electron donors such as pollutants bind at electron-deficient graphene-like π-centers, while electron acceptors like H_2O_2 and dissolved O_2 interact with the electron-rich copper sites. This facilitates efficient generation of reactive oxygen species (•OH and $O_2•^-$), enhancing Fenton-like degradation under near-neutral conditions.

The Cu–GCD NSs catalyst achieved nearly complete degradation of BPA and other refractory pollutants within 90 min, demonstrating both high efficiency and reduced oxidant consumption. Specifically, 69.2 % of BPA was degraded within the first 15 min, with complete removal achieved by 90 min in the Cu–GCD NSs/H_2O_2 system, in stark contrast to the negligible degradation observed in the absence of H_2O_2. Moreover, traditional Fe_3O_4-based Fenton catalysts exhibited almost no catalytic activity for BPA degradation under neutral conditions [334], underscoring the advantage of the Cu–GCD NSs system in a wider pH range. Beyond BPA, the catalyst demonstrated robust performance across a spectrum of refractory contaminants: PHT was fully removed within 90 min, while CIP, DP, and IBU were oxidized by 100 %, 92.6 %, and 62.7 %, respectively, within 120 min. Notably, the system exhibited diminished dependence on oxidant dosage; ~90 % of BPA was removed within 120 min using just 2 mmol/L H_2O_2, illustrating improved utilization efficiency of the oxidant. Density functional theory and in situ spectroscopic analysis confirmed that optimized adsorption and interfacial charge transfer are central to the enhanced performance.

These findings highlight the potential of earth-abundant Cu—C coordination architectures in constructing robust, low-cost, and pH-tolerant Fenton-like systems, operating under environmentally benign conditions, for real-world wastewater treatment.

4.4. *Adsorption*

Carbon nanotubes (CNTs) have attracted significant attention due to their potential usefulness in environmental remediation promoted by their small size, layered and hollow structure, and large specific surface area. They have been used as potential adsorbents for the removal of organic compounds [335], heavy metals [336], dye [337] and gas [338]. Nonetheless, the adsorption activities of CNTs towards the target contaminant are not sufficient, which could be attributed to the significant agglomeration of nano-dimensioned CNTs, weak interface between adsorbate and CNTs, and insufficient presence of active sites on the surface of CNTs. Therefore, creating a heterojunction with other inorganic and organic materials has been investigated for enhanced adsorption. The resultant composites would incorporate the advantages and properties of each component and make the composite manifest complementary or synergistic functions. The properties and structure of CNTs allow them to be employed as a supporter for anchoring or coating diverse types of earth-abundant and inexpensive materials metal oxide NPs. According to Li et al [97], Cu_2O NPs were anchored on PVP-stabilized CNT for adsorption of TBBPA and Malachite Green (MG). The O- and N-possessing functional groups in the PVP complexed with the Cu_2O to generate coordinate complexes. This efficiently reduced the agglomeration of CNTs, and as a result, gave high reactivity of the composite adsorbent. The introduction of PVP also provided active sites for organic pollutant adsorption. At optimal conditions, the hybrid mesoporous adsorbent demonstrated exceptional adsorption activity for TBBPA and MG. The maximum adsorption of TBBPA and MG by the as-prepared PVP@CNTs-Cu_2O were 116.72 and 1495.46 mgg^{-1}, which is remarkedly greater than that of pristine CNTs (68.03 and 417.58 mgg^{-1}, respectively). The experimental data fitted the Freundlich isotherm model for both TBBPA and MG which indicates the heterogeneous surface of PVP@CNTsCu_2O. The mesoporous adsorbents exhibited a rapid rate of adsorption for both TBBPA and MG, and their adsorption kinetics followed pseudo-second-order models, indicating a chemical reaction-controlled system [339]. The catalyst demonstrated rapid kinetics, enhanced reusability and high adsorption capacity.

The functionalization of carbon-based materials with $CuFe_2O_4$ nanostructures presents a promising strategy for the efficient adsorptive removal of heavy metals from aqueous systems. In a recent study, novel magnetic biochar composites, SFeCu@SBCO and FeCu@SBCO-NH_2, were synthesized by modifying oxidized sawdust biochar (SBCO) through co-loading with Fe/Cu, followed by starch coating or surface amination [149] (see Fig. 17). The materials were thoroughly characterized using FTIR, XRD, BET, SEM-EDS, and XPS to confirm successful incorporation of $CuFe_2O_4$ and surface modifications. Adsorption experiments demonstrated remarkable capacities for Pb^{2+} and Cd^{2+} removal, reaching 184.26/173.35 mg g^{-1} for SFeCu@SBCO and 201.43/190.81 mg g^{-1} for FeCu@SBCO-NH_2, respectively,values over five times greater than those of the pristine SBC. This enhancement was attributed to the synergistic effects of the $CuFe_2O_4$ nanoparticles and the functional groups (hydroxyl, amino) introduced via starch coating and amination. These modifications increased the density of active sites and improved metal ion affinity.

Mechanistically, the adsorption of Pb^{2+} and Cd^{2+} was governed primarily by monolayer chemisorption, as indicated by Langmuir isotherm modeling, and was endothermic. Complexation with amino/hydroxyl groups and electrostatic attraction to negatively charged oxygen-containing functional groups were identified as dominant interactions. Secondary mechanisms such as ion exchange and physical adsorption also contributed to the overall process. Importantly, the composites exhibited excellent reusability and anti-interference performance, maintaining adsorption efficiencies across multiple cycles and in the presence of competing cations. The magnetic properties imparted by $CuFe_2O_4$ further enabled facile separation and regeneration. These findings underscore the potential of CCNH-enhanced biochars as sustainable, high-efficiency adsorbents for the remediation of heavy metal-contaminated waters, while also valorizing agricultural biomass waste.

4.5. *Copper ion resin*

Ion resin technology represents an innovative and non-destructive methodology designed for the efficient treatment of wastewater. This technique utilizes various specialized materials, including selective resins, chelating resins, macroporous resins, polymer-based hybrid adsorbents, and other polymeric adsorbents. In practice, the treatment process involves pressurizing the contaminated water through beds of these resins, facilitating the exchange of harmful contaminants with more suitable ions, thereby purifying the water. One of the key advantages of this technology is the ability to backflush and reuse saturated resin beds, which enhances economic and environmental sustainability [340]. The application of ion resin technology has gained widespread acceptance in wastewater treatment for several compelling reasons. It demonstrates exceptional treatment performance and high purification efficiency, making it applicable in both batch and continuous processing systems. This versatility allows for the concentration of various types of pollutants, showcasing rapid adsorption kinetics and yielding high-quality effluent [341].

A notable study conducted by Kang et al. [98] explored the effectiveness of a copper hexacyanoferrate (CuHCF) absorbent integrated with a weak acidic cation (WAC) exchange resin to facilitate the removal of ammonium ions without any prior treatment. Physiochemical analyses revealed that CuHCF specifically localized on the surface of the WAC, enhancing its capability to adsorb ammonium (NH_4^+). The adsorption kinetics conformed to a pseudo-second-order model, suggesting that the adsorption process predominantly involved chemisorption. Furthermore, the study established that the Langmuir isotherm provided the best fit for the adsorption data, indicating monolayer adsorption on a surface with a finite number of identical sites.

Under the optimal reaction conditions identified in the study, the maximum adsorption capacity (qmax) for NH_4^+ reached 47.07 mg per

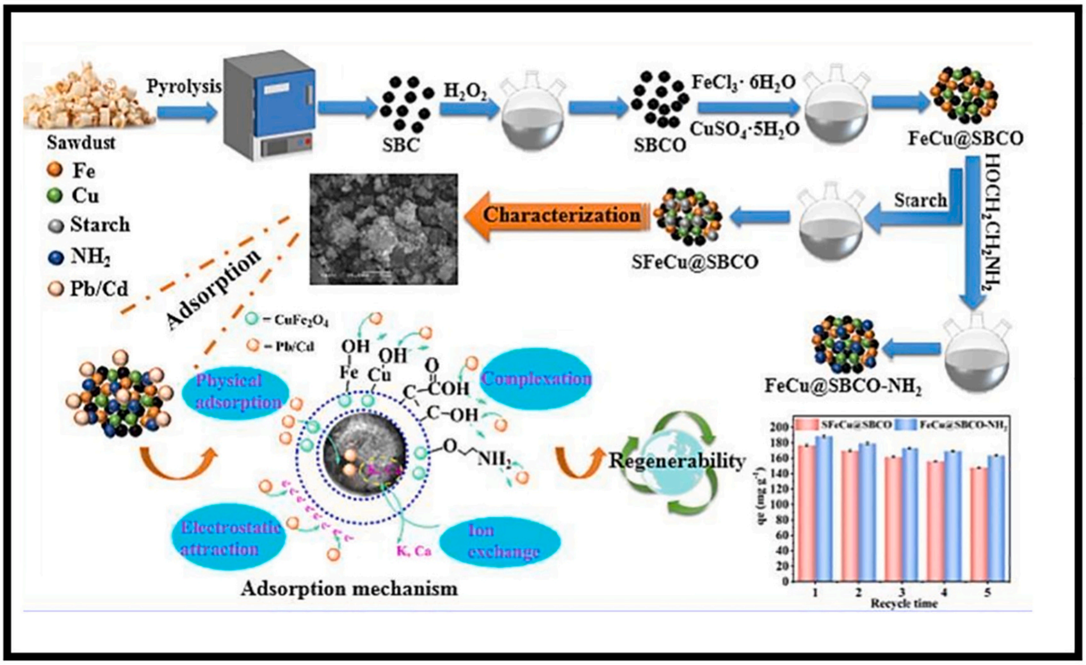

Fig. 17. The synthesis, application and regerability of FeCu@SBCO-NH_2. Reproduced with permission from ref. [149]. Copyright 2024 Elsevier.

gram of WAC-CuHCF at a pH level of 6.5. Interestingly, the presence of potassium ions (K^+) in the solution resulted in approximately a 10 % reduction in the efficiency of NH_4^+ adsorption, while the presence of sodium ions (Na^+) posed a minimal threat to the removal rate of ammonium pollutants. The study also delved into the regeneration and recycling of the WAC-CuHCF adsorbent, revealing promising results. The regenerated adsorbent retained nearly identical catalytic performance levels as observed during its initial application, indicating the potential for sustained use and reusability in wastewater treatment processes. This finding underscores the practicality and effectiveness of ion resin technology in environmental management and pollution control.

4.6. Microbial disinfection

The problem of achieving suitable disinfection without generating obnoxious disinfection by-products from traditional disinfectants. In addition, the growing dependence on point-of-use or decentralized water purification and recycling systems demands new technologies for effective microbial control and disinfection. Numerous natural and synthetic nanostructures have exhibited significant antimicrobial activities through different mechanisms including photocatalytic generation of ROS that attack and destroy cell components and viruses. The key mechanism of antimicrobial activities of nanomaterials as reported in the literature is represented in Fig. 18. The NPs can either directly attack the microbial cells by interrupting the transmembrane transfer of electrons, penetrating/disrupting cell envelop, oxidizing components of the cell, or generating secondary products like ROS or dissolved heavy metal ions which damage the cell [342]. For instance, Li et al. [343] studied the mechanism of antimicrobial performance of graphene films (GF) on diverse substrates. The findings revealed that GF on the copper conductor and germanium semiconductor substrates remarkably inhibited bacterial growth, whereas the same film treated with SiO_2 showed no visible antimicrobial activity. With no copper leaking, the antimicrobial behavior of the graphene@copper film was as a result of the transfer of electrons from the bacteria surface via graphene to the conductor substrates, which ultimately destroyed the integrity of the microbial membrane, disruption of the electron transport and mortality of the microbial cell [343,344].

4.7. Towards practical deployment: pilot studies on Cu—C nanohybrids for water purification

While extensive laboratory research has showcased the remarkable catalytic, adsorptive, and antimicrobial properties of copper–carbon (Cu—C) nanohybrids, the challenge of translating these materials into scalable, real-world applications remains critical. Recent pilot-scale demonstrations represent a significant advance towards addressing this gap, illustrating the practical feasibility and operational stability of Cu—C nanohybrids in dynamic water purification settings. These studies emphasize the material's performance under continuous flow conditions, energy-independent operation, and long-term effectiveness in removing microbial and organic contaminants. By validating Cu—C systems beyond controlled experimental environments, these pilot projects provide essential groundwork for their future integration into decentralized and sustainable water treatment technologies. A few examples are represented below:

4.7.1. Continuous flow column with Ag–Cu–activated carbon

Biswas and Bandyopadhyaya [345] developed a composite material consisting of Ag and Cu NPs supported on activated carbon (referred to as Ag–Cu–AC), which was utilized in a continuous flow column reactor for the effective treatment of contaminated water. Operating at a flow rate of 5.32 L/h, the system demonstrated a remarkable ability to achieve a 4-log reduction in *Escherichia coli* (*E. coli*) concentrations within just 7 min of contact time. This swift and efficient bactericidal action highlights the potential of the Ag–Cu–AC composite in water purification processes. Furthermore, the antibacterial efficacy of the composite was rigorously tested and sustained over 5 consecutive days, underscoring its excellent operational durability. The steady state concentrations of Ag and Cu in the treated water were 23 and 56.4 μg/L, respectively, which are well within the permissible limits of 100 and 1000 μg/L for Ag and Cu, respectively. These results suggest that the synergistic effects between the Ag and Cu NPs significantly enhanced the antibacterial performance beyond what could be achieved by either metal individually. The robust performance of the Ag–Cu–AC composite in such a rapid-flow scenario validates its potential application in critical water treatment situations, including emergency response initiatives and small-scale community water systems. This innovative design not

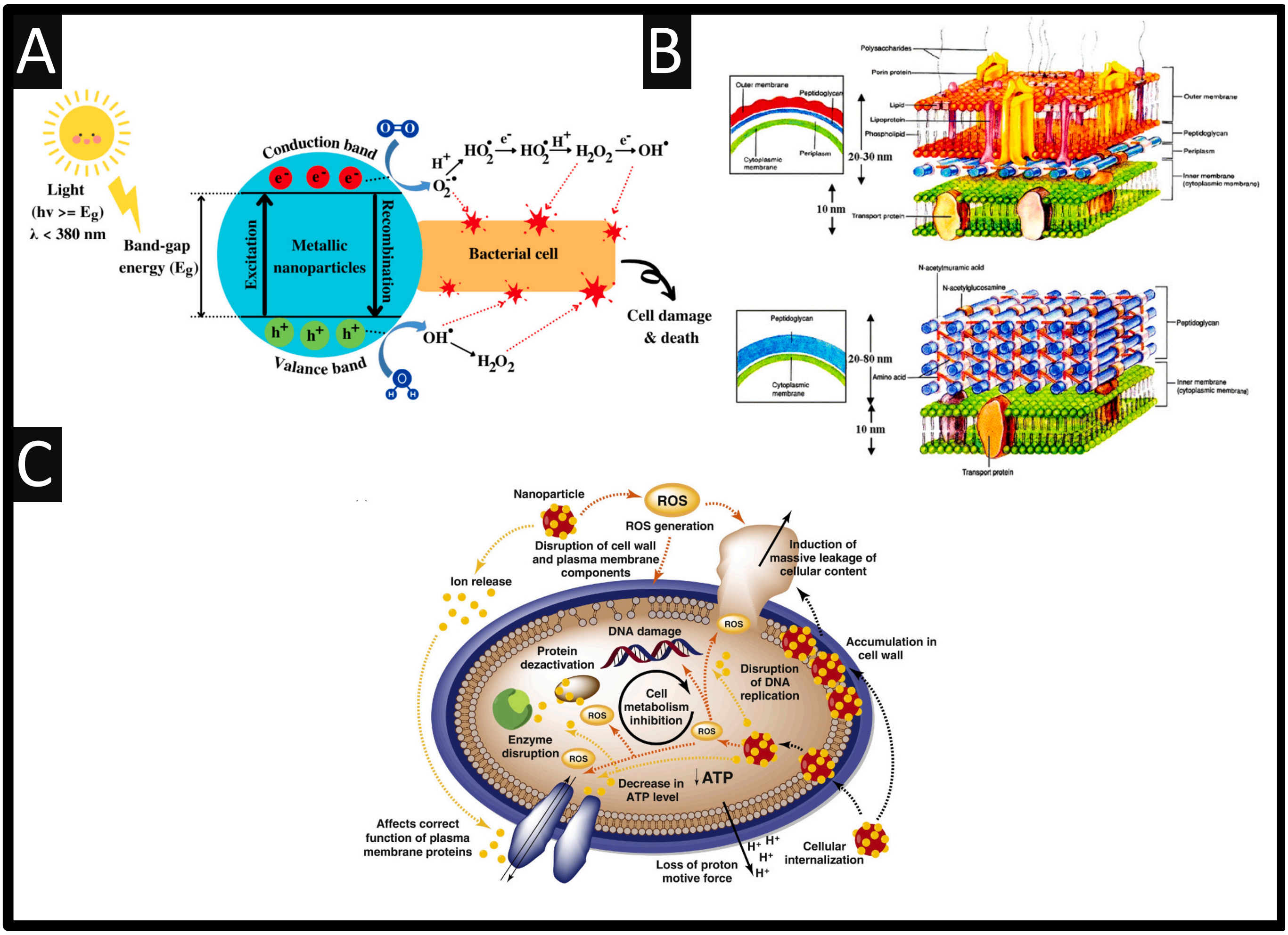

Fig. 18. A: Possible mechanism for the formation of ROS by NPs. Reproduced with permission from [272]. Copyright 2023 Elsevier, B: Contrast between Gram-negative and Gram-positive cell wall structures. Reproduced with permission from [273]. Copyright 2008 Royal Society of Chemistry; C: Possible mechanism of antimicrobial activities of metal ions. Reproduced with permission from [274]. Copyright 2016. Elsevier.

only offers a viable solution for addressing microbial contamination in water but also represents a forward step in the development of sustainable and effective water purification technologies.

4.7.2. Ag–Cu–Geopolymer filters manufactured by 3D printing

Another recent study [275], focused on the development of highly porous geopolymer filters specifically designed for water treatment applications. These innovative filters were manufactured using advanced techniques such as 3D printing, direct foaming, and granulation, which allowed for precise control over their structural properties. By impregnating the filters with Ag and Cu NPs, the researchers significantly enhanced the filters' disinfecting and catalytic capabilities. The presence of Ag NPs is known for its strong antibacterial properties, which can effectively eliminate a wide range of pathogens present in contaminated water. Meanwhile, Cu NPs contributed not only to antibacterial action but also facilitated chemical reactions that promoted the breakdown of organic pollutants. This dual action makes the geopolymer filters particularly effective in removing a variety of contaminants, including bacteria, viruses, and harmful chemical substances (see Fig. 19(A-B)).

4.7.3. Gravity-driven Cu—C disinfection system

Das and team members [276], developed a gravity-fed water disinfection device utilizing acid-functionalized activated carbon that is impregnated with copper nanoparticles (Cu–NP/AC). This system operates without an external power source, making it particularly advantageous for settings with limited access to electricity. Throughout an extensive operational period of 8 days, with a Cu loading of 0.8 wt%, the device consistently demonstrated its long-term disinfection efficacy by effectively treating water contaminated with *E. coli*. Remarkably, it maintained a zero bacterial count at the outlet during this time while processing a total of 22.11 L of contaminated water. The hybrid material, Cu–NP/AC, not only facilitates the removal of pathogens but also showcases the potential for enhanced water purification capabilities. This setup is particularly significant for decentralized, low-energy water treatment solutions, especially in off-grid or rural areas where traditional water purification systems may not be feasible (see Fig. 19 (C-D)).

4.7.4. CuO-modified activated carbon for virus inactivation

A research study by Shimabuku et al. [346], investigated the application of granular activated carbon (GAC) modified with Ag and CuO NPs for the removal and/or inactivation of the T4 bacteriophage, a model virus. Continuous flow experiments were conducted using household filters, and the findings revealed that GAC modified with Ag and CuO NPs demonstrated significant inactivation capabilities, achieving reductions reaching 5.53 log reduction at GAC/Ag0.5 %Cu1.0 %. The levels of Ag and Cu released in filtered water were below the recommended limits in drinking water.

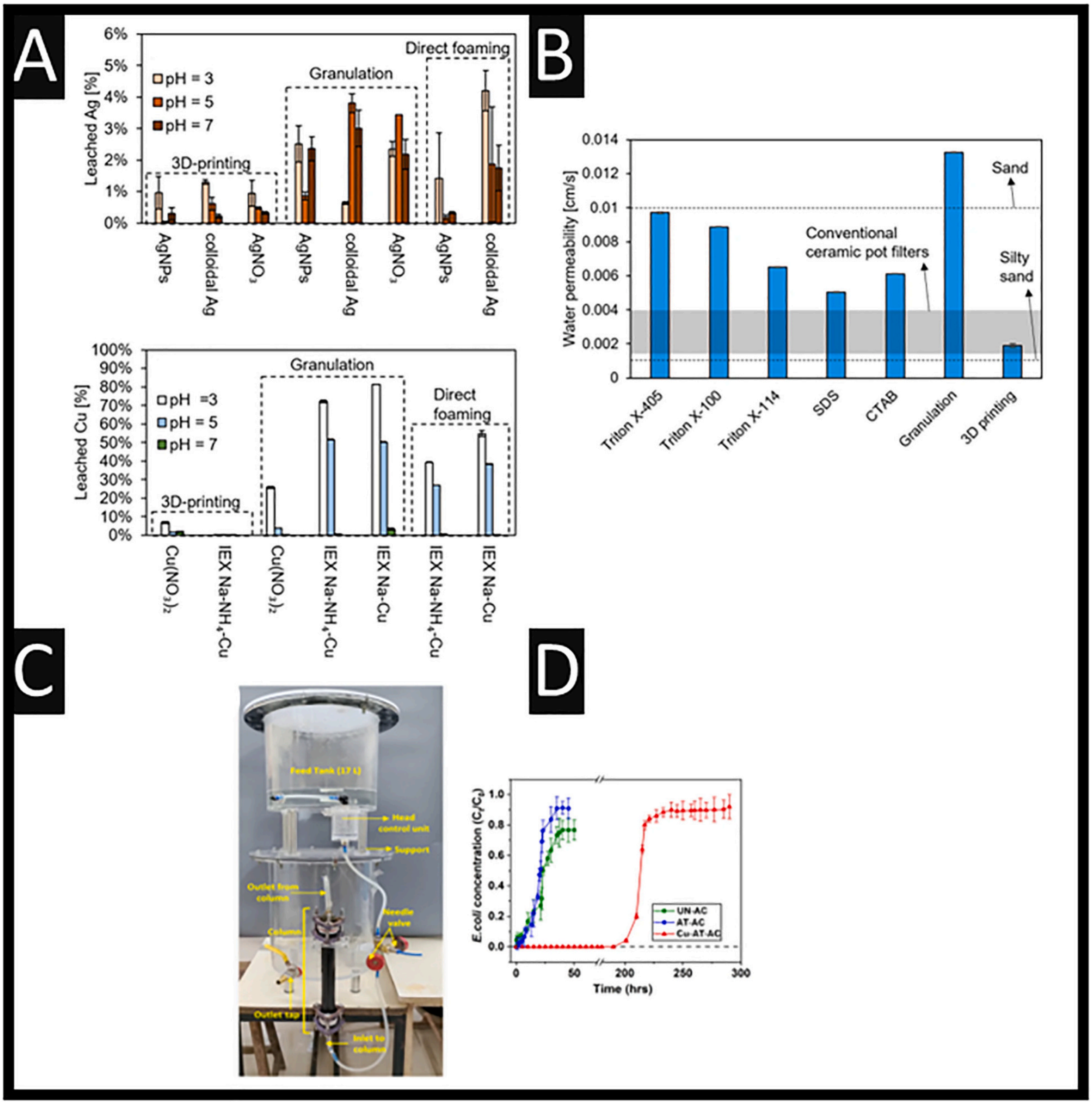

Fig. 19. (A) Batch leaching results for Ag and Cu at an initial pH of 3, 5, or 7 with differently prepared and modified geopolymer filters. (B) Ag- or Cu-modified geopolymer filters for water treatment manufactured by 3D printing, direct foaming, or granulation. Figures reproduced from reference [275]. **(C)** Continuous mode experiments for *E. coli* killing: **a** gravity-driven device designed for continuous water disinfection. **(D)** bacterial death comparison for Cu-48-AT-AC, 48-AT-AC and UN-AC (48-AT: acid treated for 48 h; UN-AC: untreated-AC). Figures reproduced from reference [276].

Table 3
Summary of Pilot Studies on Cu—C Nanohybrids.

Study	Cu–C Material	System Type	Contaminants Targeted	Performance	Duration	Reference
Continuous flow column	Ag–Cu on activated carbon	Packed-bed column	*E. coli*	4-log reduction in 7 min; 5.32 L/h flow	5 days	[345]
Gravity-driven disinfection	Cu–NP on acid-functionalized activated carbon	Gravity-fed unit (no power)	*E. coli*	0 CFU/mL at outlet; 22.11 L treated	8 days	[276]
Ag–Cu–Geopolymer Filters	Ag–Cu nanoparticles in geopolymer	Additively manufactured (3D printed)/granulated filters	Bacteria, organic contaminants	To enhanced disinfection and catalytic properties	–	[275]
CuO-Modified GAC	CuO nanoparticles on GAC	Household filter	T4 bacteriophage (virus)	>3 log reduction in virus count	Continuous flow	[346]
CuAc/NiCl$_2$–PVDF Membrane	CuAc/NiCl$_2$ nanoparticles in PVDF membrane	Ultrafiltration system	Humic substances in peat water	Improved flux, rejection, and fouling resistance	–	[347]

4.7.5. Copper acetate monohydrate/nickel chloride impregnated PVDF ultrafiltration membrane

This study by Anwar and co-workers [347], developed an antifouling ultrafiltration membrane by impregnating polyvinylidene fluoride (PVDF) with the copper acetate monohydrate/nickel chloride/thiourea (CuNit) NPs (The CuNit composite composition: 16 wt% PVDF, 42 wt% N-Methyl-2-pyrrolidone (solvent), and 1–5 wt% CuNit particles). The modified membrane demonstrated improved performance in peat water treatment, with enhanced pure water flux, humic rejection, and fouling recovery rates compared to pristine PVDF membranes.

These findings (see summary in Table 3), highlight the promising application of Cu—C nanohybrids in improving access to safe drinking water in resource-limited environments. The studies highlight the promising potential of incorporating Cu—C nanohybrids into scalable manufacturing processes. Such innovations in water purification technology could address global water quality challenges, making clean and safe drinking water more accessible through efficient and cost-effective means.

5. Challenges and future perspectives of Cu—C heterojunctions in water treatment

While —Cu-C heterojunctions show great promise for water treatment applications, their successful implementation offers an opportunity to address several important challenges. By focusing on optimizing the stability, safety, and efficiency of these materials under various environmental conditions, we can enhance their performance and durability over time.

5.1. Scalability and cost considerations

One of the primary challenges in implementing Cu—C heterojunctions at an industrial scale is the development of cost-effective and environmentally friendly synthesis methods. Current laboratory-scale fabrication techniques, such as hydrothermal synthesis, electrodeposition, and chemical vapor deposition, often involve high energy consumption, expensive precursors, and complex processing steps.

5.1.1. Scalable synthesis approaches

Future research should focus on scalable, green synthesis methods, such as biomass-derived carbon supports, solution-based methods, and electrochemical deposition techniques that allow for large-scale production at reduced costs.

5.1.2. Sustainable and low-cost precursors

Using earth-abundant carbon sources (e.g., biochar, graphene oxide from waste materials) and alternative copper precursors can lower costs while minimizing environmental impact.

5.1.3. Manufacturing integration

Evaluating the compatibility of Cu—C heterojunctions with existing water treatment systems, such as sand filtration units, activated carbon beds, and membrane bioreactors, is crucial for promoting their industrial adoption. A thorough analysis of how these composites interact with various filtration technologies can reveal potential enhancements in efficiency and effectiveness in contaminant removal, offering a promising outlook for water treatment systems. Modular designs should be developed to incorporate Cu—C composites into replaceable cartridges or serve as advanced coatings on filtration membranes to optimize integration. This approach not only facilitates easy maintenance and replacement but also assures the adaptability of the treatment process based on water quality needs, enhancing the flexibility of water treatment systems.

Pilot-scale demonstrations should be conducted alongside comprehensive techno-economic analyses to substantiate these composites' feasibility and operational effectiveness. These studies will validate the performance metrics, evaluate scalability, and assess the costs of integrating Cu—C heterojunctions into existing systems. Furthermore, it is essential to emphasize that these initiatives will thrive only through collaborative efforts. Engaging researchers, water treatment companies, and engineering firms throughout the development and implementation phases is not just important, it's crucial. This inclusive approach ensures a multidisciplinary perspective, yielding innovative solutions that address technical challenges and economic viability in water treatment applications.

5.1.4. Practical scale-up challenge

Despite promising lab-scale performance, translating Cu—C heterojunction systems to full-scale water treatment faces several hurdles. Pilot studies, a rarity in this field, are crucial for understanding the challenges and potential solutions. Batch-to-batch material reproducibility remains a significant concern. Engineering challenges include the integration of these nanomaterials into existing flow-through systems and ensuring consistent catalytic activity in real, variable water matrices. Cost–benefit analysis is also essential. While Cu is abundant and carbon can be derived from waste biomass, the overall economic process must account for catalyst regeneration, infrastructure adaptation, and lifecycle impacts. Collaborations between materials scientists, process engineers, and water utilities are critical for bridging the lab-to-field gap.

5.2. Stability and reusability for continuous operation

Long-term operational stability is essential for any material used in water purification, as degradation over time can reduce efficiency and increase maintenance costs. The repeated exposure of Cu—C heterojunctions to harsh environmental conditions, including fluctuating pH, temperature variations, and prolonged catalytic reactions, can lead to structural degradation and loss of catalytic activity.

5.2.1. Enhancing structural stability

Strategies such as encapsulating Cu NPs with protective shells (e.g., metal oxides like NiO or TiO_2) or embedding them within porous carbon matrices can prevent oxidation and agglomeration.

5.2.2. Improving catalyst reusability

Developing regeneration techniques, such as electrochemical self-cleaning [348], or chemical reactivation [349], can extend the functional lifespan of Cu—C catalysts in continuous flow systems [350].

5.2.3. Durability in real-world conditions

More studies are needed to evaluate how Cu—C heterojunctions perform under real wastewater conditions, including competing ions, organic matter, and industrial pollutants.

5.3. Addressing toxicity and environmental impact

A significant concern in using Cu-based nanomaterials is the potential release of copper ions or NPs into treated water, which could pose environmental and health risks. Even trace amounts of copper can be toxic to aquatic life and must be carefully managed to prevent secondary contamination.

5.3.1. Minimizing copper leaching and enhancing catalyst stability in electrocatalytic CCNH systems

In the electrocatalytic filtration system utilizing CCNHs [95], the application of a mild negative potential (e.g., −0.5 V vs. Ag/AgCl) played a dual role in enhancing both catalytic efficiency and structural stability. Electrochemical bias accelerated interfacial electron transfer at the Cu–carbon junction, thereby promoting the formation of ROS such as $O_2\bullet^-$ and •OH. Simultaneously, the reductive environment helps maintain copper in its metallic or lower oxidation state, limiting oxidative dissolution and enhancing catalyst longevity. To complement this electrochemical stabilization, advanced materials engineering strategies are essential to mitigate the release of copper ions during operation. Key approaches include:

1. Core-shell Architectures: This approach involves the encapsulation of Cu NPs within stable, porous TiO_2 or SiO_2. By creating a core-shell structure, direct contact between the Cu NPs and water is minimized, significantly limiting the dissolution of copper ions into the aquatic environment. The choice of oxide can enhance the stability and reactivity of the nanostructures, providing additional advantages for various environmental applications.
2. Covalent Anchoring: Another effective strategy is the covalent anchoring of copper onto functionalized carbon surfaces, specifically N- or S-doped graphene. This method utilizes the chemical modification of graphene to create stronger Cu—C bonding interactions, thereby enhancing the bonding strength between the copper and the carbon matrix. Improved bonding reduces the likelihood of copper dissolution into water, ensuring that the beneficial properties of the copper are retained while mitigating environmental risks.
3. Post-Synthesis Surface Passivation: After synthesizing these materials, it is crucial to implement surface passivation techniques using biocompatible coatings or stabilizers. These protective layers can be designed to suppress copper ion release during operation, thereby enhancing the overall safety and performance of the treated materials. Common coatings include polymeric films or inorganic stabilizers that effectively shield copper from leaching in aqueous environments, ultimately contributing to long-term stability and efficacy in water treatment applications [351–353].

By integrating these advanced strategies, we can significantly reduce the release of toxic copper species into treated water, ensuring improved environmental safety and efficacy in water purification processes. Once again, environmental engineers, researchers, and professionals in water treatment and material science play a crucial role in implementing these strategies and ensuring a safer environment.

5.3.2. *Regulatory compliance and safety testing*

The environmental and human health risks associated with Cu—C heterojunctions must be critically assessed, particularly the potential release of copper ions (Cu^{2+}) or nanoparticles into treated water. Studies have shown that Cu^{2+} concentrations above 1300 μg/L violate EPA drinking water standards, while chronic exposure at even lower concentrations can disrupt aquatic ecosystems, underscoring the urgent need for this assessment [354]. Therefore, leaching studies under realistic pH, ionic strength, and organic matter conditions are essential. Recent tests on Cu—C catalysts indicate leaching levels between 2 μg/L and 15 μg/L under neutral conditions, which fall below regulatory thresholds but may vary under acidic or oxidative conditions [270]. Toxicological assays using *Daphnia magna* and zebrafish embryos have further supported the need for immobilization strategies such as encapsulation or surface passivation to prevent uncontrolled copper release [355–357].

5.3.3. *Smart filtration and recovery systems*

Innovative filtration systems can be meticulously designed to effectively capture and recover copper ions or NPs that may leach during various industrial processes. For instance, combining Cu—C composites with advanced ion-exchange membranes enables selective absorption of copper ions, thereby enhancing recovery efficiency. Additionally, integrating magnetic separation techniques allows for the extraction of magnetic NPs from effluents. Selective adsorbents, which are designed to have a high affinity for copper ions due to their unique chemical properties, can sequester free copper ions based on these affinities. These hybrid systems are pivotal in mitigating environmental risks associated with copper pollution and play a crucial role in copper's recyclability. These technologies significantly enhance material sustainability by facilitating the separation and recovery of valuable copper materials from waste streams. This reduces the reliance on virgin copper sources and minimizes the ecological footprint of mining and refining processes, contributing to a circular economy.

5.4. *Future research directions*

To overcome these challenges and enable the commercialization of Cu—C heterojunctions, future research should focus on several key areas such as:

5.4.1. *Development of hybrid nanomaterials with enhanced durability*

Exploring composite materials by combining Cu—C heterojunctions with other functional materials such as TiO_2, ZnO, or MXenes to improve stability and catalytic performance. Utilizing defect engineering and doping strategies to tailor electronic structures for higher efficiency in pollutant degradation.

5.4.2. *Advanced functionalization strategies*

Functionalizing carbon supports with oxygen, nitrogen, or sulfur groups enhances catalytic activity. Designing hierarchical porous structures to maximize active surface area and improve mass transport during catalytic reactions.

5.4.3. *Integration into commercial water treatment systems*

Future work should focus on several key areas to enhance the development of scalable, modular Cu-C-based units that can be retrofitted into existing treatment systems. One crucial aspect is testing Cu—C heterojunctions in pilot-scale continuous flow systems, ensuring they perform effectively under real wastewater conditions. So far, most pilot-scale studies are on microbial disinfection or deactivation and not on catalytic degradation.

Additionally, it is essential to conduct life cycle assessments (LCA) and cost-benefit analyses, allowing for a thorough comparison of their performance against conventional catalysts. Equally important is the collaboration with industry stakeholders and regulatory agencies, as their input will be critical in streamlining pathways for certification and deployment. Lastly, addressing compliance with environmental standards, such as the limits set by the WHO and the EPA for copper in water, will be crucial for the practical use of these innovative systems.

6. Conclusions

Copper-carbon nanohybrid heterojunctions (CCNHs) offer a promising solution for advanced water treatment technologies due to their distinctive properties. However, for these materials to be effectively integrated into practical applications, it is crucial to address several key challenges, particularly scalability, stability, and environmental safety. Scalability involves the capacity to produce CCNHs in substantial quantities without compromising their quality. Current synthesis methods may limit their industrial applicability, necessitating future research aimed at developing more efficient and cost-effective fabrication techniques. This could involve exploring alternative precursor materials and optimizing reaction conditions to enhance production yields. Stability is also a significant concern, as the performance of heterojunctions can deteriorate over time due to environmental factors such as pH fluctuations and exposure to light. It is essential to investigate the long-term durability of these materials under realistic operating conditions. Future studies should focus on modifying the chemical composition of CCNHs to improve their resistance to degradation and extend their lifecycle.

Lastly, addressing environmental concerns is vital. The potential toxicity of the materials used in CCNHs raises significant questions about their sustainability and safety. Implementing rigorous regulatory measures and safety protocols will be essential to ensure that these materials do not pose risks to human health or ecosystems. By overcoming these challenges through focused research and development efforts, CCNHs can play a transformative role in advancing sustainable and efficient water purification technologies, ultimately supporting global initiatives to ensure clean water access for all.

CRediT authorship contribution statement

Enyioma C. Okpara: Conceptualization, Formal analysis, Writing – review & editing. **Taiwo W. Quadri:** Writing – review & editing. **Eno E. Ebenso:** Supervision. **Samuel J. Rowley-Neale:** Formal analysis, Resources, Writing – review & editing. **Craig E. Banks:** Conceptualization, Formal analysis, Resources, Writing – review & editing.

Declaration of competing interest

The authors declare that they have no known competing financial interests or personal relationships that could have appeared to influence the work reported in this paper.

Data availability

No data was used for the research described in the article.

References

[1] M. Letchinger, Pollution and water quality, neighbourhood water quality assessment, Proj. Oceanogr 3 (1) (2000) 247–249.
[2] D.H. Pink, Investing in tomorrow's liquid gold, Yahoo. Archived from the original on April 23 (2006) 2006.
[3] W. Larry, World Water Day, A billion people worldwide lack safe drinking, 2006.
[4] F.N. Chaudhry, M. Malik, Factors affecting water pollution: a review, J. Ecosyst. Ecography 7 (1) (2017) 225–231.
[5] S. Afshin, et al., Removal of basic blue-41 dye from water by stabilized magnetic iron nanoparticles on clinoptilolite zeolite, Rev. Chim. 71 (2) (2020) 218–229.
[6] C.M. Roșu, et al., Performances of Pichia kudriavzevii in decolorization, biodegradation, and detoxification of CI basic blue 41 under optimized cultural conditions, Environ. Sci. Pollut. Res. 26 (2019) 431–445.
[7] M. Sadiqa, et al., Preparation and characterization of catalysts and its application in microwave-assisted degradation of acid orange-8, Desalin. Water Treat. 231 (2021) 407–414.
[8] H. Zangeneh, et al., Photocatalytic oxidation of organic dyes and pollutants in wastewater using different modified titanium dioxides: a comparative review, J. Ind. Eng. Chem. 26 (2015) 1–36.
[9] H. Zangeneh, M. Farhadian, A.A. Zinatizadeh, N (urea) and CN (L-asparagine) doped TiO2-CuO nanocomposites: fabrication, characterization and photodegradation of direct red 16, J. Environ. Chem. Eng. 8 (1) (2020) 103639.
[10] B. Krishnakumar, M. Swaminathan, Influence of operational parameters on photocatalytic degradation of a genotoxic azo dye acid violet 7 in aqueous ZnO suspensions, Spectrochim. Acta A Mol. Biomol. Spectrosc. 81 (1) (2011) 739–744.
[11] H. Ben Mansour, et al., Acid violet 7 and its biodegradation products induce chromosome aberrations, lipid peroxidation, and cholinesterase inhibition in mouse bone marrow, Environ. Sci. Pollut. Res. 17 (2010) 1371–1378.
[12] T.M. Eldeeb, et al., Biosorption of acid brown 14 dye to mandarin-CO-TETA derived from mandarin peels, Biomass Convers. Biorefinery (2022) 1–21.
[13] https://www.cncolorchem.com/upLoad/file/20170315/14895669257183897.pdf.
[14] M.R. Samarghandi, et al., Degradation of azo dye acid red 14 (AR14) from aqueous solution using H2O2/nZVI and S2O82–/nZVI processes in the presence of UV irradiation, Water Environ. Res. 92 (8) (2020) 1173–1183.
[15] S. Naveenraj, et al., Interaction between toxic azo dye CI acid red 88 and serum albumins, JOL 143 (2013) 715–722.
[16] T.J. Ashaolu, et al., Phycocyanin, a super functional ingredient from algae; properties, purification characterization, and applications, Int. J. Biol. Macromol. 193 (2021) 2320–2331.
[17] G. Cheng, et al., Degradation of reactive brilliant red X-3B by photo-Fenton-like process: effects of water chemistry factors and degradation mechanism, Water 14 (3) (2022) 380.
[18] A. Maleki, A.H. Mahvi, B. Shahmoradi, Hydroxyl radical-based processes for decolourization of direct blue 71: a comparative study, Asian J. Chem. 23 (10) (2011) 4411–4415.
[19] M. Allmark, W. Mannell, H. Grice, Chronic toxicity studies on food colours: Part III. Observations on the toxicity of malachite green, new Coccine and nigrosine in rats, J. Pharm. Pharmacol. 9 (1) (1957) 622–628.
[20] J.P. Srivastava, Pathophysiologic mechanism of erythrocyte morphological alteration in freshwater fish Channa punctata under exposure of nigrosine black (acid Black-2 a tanning industry dye), Int. J. Environ., Agricul. Biotechnol. 7 (1) (2022) 162–167.
[21] R.G. Saratale, et al., Bacterial decolorization and degradation of azo dyes: a review, J. Taiwan Inst. Chem. Eng. 42 (1) (2011) 138–157.
[22] S. Rezaei, et al., Laccase-catalyzed decolorization and detoxification of acid blue 92: statistical optimization, microtoxicity, kinetics, and energetics, J. Environ. Health Sci. Eng. 13 (2015) 1–9.
[23] M.R. Jalali Sarvestani, Z. Doroudi, Removal of reactive black 5 from waste waters by adsorption: a comprehensive review, J. Water Environ. Nanotechnol. 5 (2) (2020) 180–190.
[24] M.A. Ali, S.A. Bashier, Effect of fast green dye on some biophysical properties of thymocytes and splenocytes of albino mice, Food Addit. Contam. 23 (5) (2006) 452–461.
[25] Y. Tanaka, et al., Effects of synthetic food colors on [3H] serotonin release from rat basophilic leukemia cells (RBL-2H3), Eisei kagaku 41 (3) (1995) 206–211.
[26] H. AsHIDA, et al., Synergistic effects of food colors on the toxicity of 3-amino-1, 4-dimethyl-5H-pyrido [4, 3-b] indole (Trp-P-1) in primary cultured rat hepatocytes, J. Nutr. Sci. Vitaminol. 46 (3) (2000) 130–136.
[27] J.A. van Hooft, Fast green FCF (food green 3) inhibits synaptic activity in rat hippocampal interneurons, Neurosci. Lett. 318 (3) (2002) 163–165.
[28] M. Vinuth, et al., Rapid removal of hazardous rose Bengal dye using Fe (III)–montmorillonite as an effective adsorbent in aqueous solution, J. Environ. Anal. Toxicol. 6 (2) (2016) 1000355.
[29] Z. Wei, et al., Cu3–x Ni x Al-layered double hydroxide-reduced graphene oxide nanosheet array for the reduction of 4-nitrophenol, ACS Appl. Nano Mater. 2 (4) (2019) 2383–2396.
[30] R. Fatima, et al., Photocatalytic degradation performance of various types of modified TiO2 against nitrophenols in aqueous systems, J. Clean. Prod. 231 (2019) 899–912.
[31] S.R. Subashchandrabose, et al., P-Nitrophenol toxicity to and its removal by three select soil isolates of microalgae: the role of antioxidants, Environ. Toxicol. Chem. 31 (9) (2012) 1980–1988.
[32] M. Megharaj, H. Pearson, K. Venkateswarlu, Toxicity of phenol and three nitrophenols towards growth and metabolic activities of Nostoc linckia, isolated from soil, Arch. Environ. Contam. Toxicol. 21 (1991) 578–584.
[33] T. Ruan, et al., Evaluation of the in vitro estrogenicity of emerging bisphenol analogs and their respective estrogenic contributions in municipal sewage sludge in China, Chemosphere 124 (2015) 150–155.
[34] A. Li, et al., Serum concentration of bisphenol analogues in pregnant women in China, Sci. Total Environ. 707 (2020) 136100.
[35] A. Tarafdar, et al., The hazardous threat of bisphenol a: toxicity, detection and remediation, J. Hazard. Mater. 423 (2022) 127097.
[36] H. Zhou, N. Yin, F. Faiola, Tetrabromobisphenol A (TBBPA): A controversial environmental pollutant, J. Environ. Sci. 97 (2020) 54–66.
[37] A. Abd Gami, et al., Phenol and its toxicity, J. Environ. Microbiol. Toxicol. 2 (1) (2014) 11–23.
[38] S. Bull, *HPA Compendium of chemical hazards phenol.* CRCE HQ, HPA (Version 4), 2007.
[39] S. Chakraborty, et al., Biodegradation of phenol by native microorganisms isolated from coke processing wastewater, J. Environ. Biol. 31 (3) (2010) 293.
[40] A. Nuhoglu, B. Yalcin, Modelling of phenol removal in a batch reactor, Process Biochem. 40 (3–4) (2005) 1233–1239.
[41] J. Michałowicz, W. Duda, Phenols–Sources and Toxicity, Pol. J. Environ. Stud. 16 (3) (2007).
[42] Z.I. Bhatti, H. Toda, K. Furukawa, P-Nitrophenol degradation by activated sludge attached on nonwovens, Water Res. 36 (5) (2002) 1135–1142.
[43] N. Wang, et al., New insight into photodegradation mechanisms, kinetics and health effects of p-nitrophenol by ozonation in polluted water, J. Hazard. Mater. 403 (2021) 123805.
[44] W.-J. Yang, et al., Exposure to 2, 4-dichlorophenol, 2, 4, 6-trichlorophenol, pentachlorophenol and risk of thyroid cancer: a case-control study in China, Environ. Sci. Pollut. Res. 28 (43) (2021) 61329–61343.
[45] E. Jerschow, et al., Dichlorophenol-containing pesticides and allergies: results from the US National Health and nutrition examination survey 2005-2006, Ann. Allergy Asthma Immunol. 109 (6) (2012) 420–425.
[46] E. Jerschow, et al., Relationship between urine dichlorophenol levels and asthma morbidity, Ann. Allergy Asthma Immunol. 112 (6) (2014) 511–518 (e1).
[47] B.E. Benson, et al., Amlodipine toxicity in children less than 6 years of age: a dose-response analysis using National Poison Data System Data, J. Emerg. Med. 39 (2) (2010) 186–193.
[48] M. Parolini, Toxicity of the non-steroidal anti-inflammatory drugs (NSAIDs) acetylsalicylic acid, paracetamol, diclofenac, ibuprofen and naproxen towards freshwater invertebrates: a review, Sci. Total Environ. 740 (2020) 140043.
[49] G.-M.A. Lucero, et al., Naproxen-enriched artificial sediment induces oxidative stress and genotoxicity in Hyalella azteca, Water Air Soil Pollut. 226 (2015) 1–10.
[50] R.K. Madan, J. Levitt, A review of toxicity from topical salicylic acid preparations, J. Am. Acad. Dermatol. 70 (4) (2014) 788–792.
[51] E. Prášková, et al., Acute toxicity of acetylsalicylic acid to juvenile and embryonic stages of Danio rerio, Neuroendocrinol. Lett. 33 (2012) 72–76.
[52] Y.-C. Lo, C.-C. Yang, J.-F. Deng, Acute alachlor and butachlor herbicide poisoning, Clin. Toxicol. 46 (8) (2008) 716–721.
[53] S.-J. Seok, et al., Acute oral poisoning due to chloracetanilide herbicides, J. Korean Med. Sci. 27 (2) (2012) 111–114.
[54] A. Al-Turki, Microbial polycyclic aromatic hydrocarbons degradation in soil, Res. J. Environ. Toxicol. 3 (1) (2009) 1–8.
[55] K. Hayakawa, et al., Polycyclic aromatic hydrocarbons in surface water of the southeastern Japan Sea, Chem. Pharm. Bull. 64 (6) (2016) 625–631.

[56] A. Mojiri, et al., Comprehensive review of polycyclic aromatic hydrocarbons in water sources, their effects and treatments, Sci. Total Environ. 696 (2019) 133971.

[57] J.F. Acar, A comparison of side effects of levofloxacin to other agents concerning the ecological and microbiological effects on normal human flora, Chemotherapy 47 (Suppl. 3) (2001) 15–23.

[58] H.H. Liu, Safety profile of the fluoroquinolones, Drug Saf. 33 (5) (2010) 353–369.

[59] E.S. Fisher, S.C. Curry, Chapter ten - evaluation and treatment of acetaminophen toxicity, in: A. Ramachandran, H. Jaeschke (Eds.), Advances in Pharmacology, Academic Press, 2019, pp. 263–272.

[60] H.N.P. Vo, et al., Acetaminophen micropollutant: historical and current occurrences, toxicity, removal strategies and transformation pathways in different environments, Chemosphere 236 (2019) 124391.

[61] D. Xu, Y. Xie, J. Li, Toxic effects and molecular mechanisms of sulfamethoxazole on Scenedesmus obliquus, Ecotoxicol. Environ. Saf. 232 (2022) 113258.

[62] E.B. Samrén, et al., Antiepileptic drug regimens and major congenital abnormalities in the offspring, Annals of Neurology: Official Journal of the American Neurological Association and the Child Neurology Society 46 (5) (1999) 739–746.

[63] J.W. Olney, et al., Environmental agents that have the potential to trigger massive apoptotic neurodegeneration in the developing brain, Environ. Health Perspect. 108 (Suppl. 3) (2000) 383–388.

[64] R. Andreozzi, et al., Carbamazepine in water: persistence in the environment, ozonation treatment and preliminary assessment on algal toxicity, Water Res. 36 (11) (2002) 2869–2877.

[65] A. Alok, N. Chaudhury, Tetracycline hydrochloride: a potential clinical drug for radioprotection, Chem. Biol. Interact. 245 (2016) 90–99.

[66] R. Daghrir, P. Drogui, Tetracycline antibiotics in the environment: a review, Environ. Chem. Lett. 11 (2013) 209–227.

[67] Y. Qiu, et al., Long-term low-dose oxytetracycline potentially leads to neurobehavioural changes, Ecotoxicol. Environ. Saf. 223 (2021) 112546.

[68] A.R. Sánchez, R.S. Rogers III, P.J. Sheridan, Tetracycline and other tetracycline-derivative staining of the teeth and oral cavity, Int. J. Dermatol. 43 (10) (2004) 709–715.

[69] A. Wright, G. Colver, Tetracyclines—how safe are they? Clin. Exp. Dermatol. 13 (2) (1988) 57–61.

[70] C.M. Bowman, et al., Hepes may stimulate cultured endothelial cells to make growth-retarding oxygen metabolites, In Vitro Cell. Dev. Biol. 21 (3) (1985) 140–142.

[71] N. Zargar Baboldashti, et al., Platelet-rich plasma protects tenocytes from adverse side effects of dexamethasone and ciprofloxacin, Am. J. Sports Med. 39 (9) (2011) 1929–1935.

[72] T. Lu, et al., Evaluation of the taxonomic and functional variation of freshwater plankton communities induced by trace amounts of the antibiotic ciprofloxacin, Environ. Int. 126 (2019) 268–278.

[73] A.R. Sapkota, et al., What do we feed to food-production animals? A review of animal feed ingredients and their potential impacts on human health, Environ. Health Perspect. 115 (5) (2007) 663–670.

[74] P. Wang, et al., Highly efficient removal of p-arsanilic acid with Fe(II)/peroxydisulfate under near-neutral conditions, Water Res. 177 (2020) 115752.

[75] E. Wołejko, et al., Chlorpyrifos occurrence and toxicological risk assessment: a review, Int. J. Environ. Res. Public Health 19 (19) (2022) 12209.

[76] A.M. Olejnik, et al., In vitro studies on atrazine effects on human intestinal cells, Water Air Soil Pollut. 213 (2010) 401–411.

[77] S. Antunes-Kenyon, G. Kennedy, A review of the toxicity and environmental fate of triclopyr, Massachusetts department of Agricultural Resources (2004).

[78] M. Bartels, et al., Review of the pharmacokinetics and metabolism of triclopyr herbicide in mammals: impact on safety assessments, Regul. Toxicol. Pharmacol. 116 (2020) 104714.

[79] D. Das, D. Charumathi, N. Das, Bioaccumulation of the synthetic dye basic violet 3 and heavy metals in single and binary systems by Candida tropicalis grown in a sugarcane bagasse extract medium: modelling optimal conditions using response surface methodology (RSM) and inhibition kinetics, J. Hazard. Mater. 186 (2–3) (2011) 1541–1552.

[80] S. Singh, et al., Toxicity and detoxification of monocrotophos from ecosystem using different approaches: a review, Chemosphere 275 (2021) 130051.

[81] R. Pamanji, et al., Developmental toxic effects of monocrotophos, an organophosphorous pesticide, on zebrafish (Danio rerio) embryos, Environ. Sci. Pollut. Res. 22 (2015) 7744–7753.

[82] S.K. Abbiramy, et al., Monocrotophos, its toxic effect (dermal) on Eisenia fetida (Savigny), Toxicol. Environ. Heal. Sci. 10 (2018) 330–335.

[83] G. Burdock, D. Pence, R. Ford, Safety evaluation of benzophenone, Food Chem. Toxicol. 29 (11) (1991) 741–750.

[84] R.O. Beauchamp, et al., A critical review of the literature on nitrobenzene toxicity, CRC Crit. Rev. Toxicol. 11 (1) (1982) 33–84.

[85] N.T. Program, *Nitrobenzene.* Report on carcinogens: carcinogen profiles 12 (2011) 294–296.

[86] H. Choudhury, et al., Health and environmental effects profile for pentachloronitrobenzene, Toxicol. Ind. Health 3 (1) (1987) 5–69.

[87] A. Dorsey, F. Llados, Toxicological profile for 1, 3-dinitrobenzene and 1, 3, 5-trinitrobenzene, 1995.

[88] M. Matsumoto, et al., Thirteen-week oral toxicity of Para-and ortho-chloronitrobenzene in rats and mice, J. Toxicol. Sci. 31 (1) (2006) 9–22.

[89] Y. Morita, et al., Allergic contact dermatitis caused by N, N-diethyl-p-phenylenediamine used in water quality analysis, Contact Derm. 69 (2) (2013) 118–119.

[90] Z.-Q. Shi, et al., Occurrence, toxicity and transformation of six typical benzotriazoles in the environment: a review, Sci. Total Environ. 661 (2019) 407–421.

[91] K.J.G. Pollitt, et al., 1, 4-Dioxane as an emerging water contaminant: state of the science and evaluation of research needs, Sci. Total Environ. 690 (2019) 853–866.

[92] E. Devlin, J. Brammer, R. Puyear, Effect of toluene on fathead minnow (Pimephales promelas Rafinesque) development, Arch. Environ. Contam. Toxicol. 14 (1985) 595–603.

[93] Y. Wang, H. Qian, Phthalates and their impacts on human health, Healthcare (Basel) 9 (5) (2021).

[94] D. Toloman, et al., Visible-light-driven photocatalytic degradation of different organic pollutants using cu doped ZnO-MWCNT nanocomposites, J. Alloys Compd. 866 (2021) 159010.

[95] W. Zheng, et al., A novel electrocatalytic filtration system with carbon nanotube supported nanoscale zerovalent copper toward ultrafast oxidation of organic pollutants, Water Res. 194 (2021) 116961.

[96] Y. Wang, H. Zhao, G. Zhao, Iron-copper bimetallic nanoparticles embedded within ordered mesoporous carbon as effective and stable heterogeneous Fenton catalyst for the degradation of organic contaminants, Appl. Catal. B Environ. 164 (2015) 396–406.

[97] X. Li, et al., Novel N-doped CNTs stabilized Cu2O nanoparticles as adsorbent for enhancing removal of malachite green and tetrabromobisphenol a, Chem. Eng. J. 292 (2016) 326–339.

[98] S. Kang, et al., Facile synthesis of copper-substituted Prussian blue analog immobilized ion exchange resins for high-performance ammonium recovery from wastewater: adsorption kinetics, isotherms, and regeneration, Chem. Eng. J. 457 (2023) 141128.

[99] E.C. Okpara, et al., Electrochemical detection of selected heavy metals in water: a case study of African experiences, RSC Adv. 12 (40) (2022) 26319–26361.

[100] M. Yateh, et al., Energy consumption and carbon emissions management in drinking water treatment plants: a systematic review, J. Clean. Prod. 437 (2024) 140688.

[101] M. Ramírez-Melgarejo, T. Stringer, Wastewater treatment, energy consumption, and greenhouse gas emissions: An operational approach to comparing Barcelona and Mexico City, J. Environ. Manag. 353 (2024) 120175.

[102] W. Liao, et al., Graphitized cu-β-cyclodextrin polymer driving an efficient dual-reaction-center Fenton-like process by utilizing electrons of pollutants for water purification, J. Environ. Sci. 126 (2023) 565–574.

[103] S. Deng, et al., The utilization of reclaimed water: possible risks arising from waterborne contaminants, Environ. Pollut. 254 (2019) 113020.

[104] C. Yang, et al., Determining the radiation enhancement effects of gold nanoparticles in cells in a combined treatment with cisplatin and radiation at therapeutic megavoltage energies, Cancers 10 (5) (2018) 150.

[105] I. Fratoddi, et al., Gold nanoparticles functionalized by rhodamine B isothiocyanate: a new tool to control plasmonic effects, J. Colloid Interface Sci. 513 (2018) 10–19.

[106] V. Neuschmelting, et al., Dual-modality surface-enhanced resonance Raman scattering and multispectral optoacoustic tomography nanoparticle approach for brain tumor delineation, Small 14 (23) (2018) 1800740.

[107] F. Zaera, Nanostructured materials for applications in heterogeneous catalysis, Chem. Soc. Rev. 42 (7) (2013) 2746–2762.

[108] E. Herrfahrdt-Pähle, et al., *Empowering global water governance: taking the* 2023 UN water conference outcomes forward to address the current water crises, Water Int. (2025) 1–7.

[109] A. Boretti, L. Rosa, Reassessing the projections of the world water development report, NPJ Clean Water 2 (1) (2019) 15.

[110] N. Jiang, et al., A dual-reaction-center Fenton-like process on–C [triple bond, length as m-dash] N–Cu linkage between copper oxides and defect-containing gC 3 N 4 for efficient removal of organic pollutants, J. Mater. Chem. A 6 (36) (2018) 17819–17828.

[111] F.L. Lam, A.C. Yip, X. Hu, Copper/MCM-41 as a highly stable and pH-insensitive heterogeneous photo-Fenton-like catalytic material for the abatement of organic wastewater, Ind. Eng. Chem. Res. 46 (10) (2007) 3328–3333.

[112] X. Chen, et al., High-performance wearable sensor inspired by the neuron conduction mechanism through gold-induced sulfur vacancies, ACS sensors 7 (3) (2022) 816–826.

[113] C. Fan, et al., Fast and recoverable NO 2 detection achieved by assembling ZnO on Ti 3 C 2 T x MXene nanosheets under UV illumination at room temperature, Nanoscale 14 (9) (2022) 3441–3451.

[114] C. Liu, et al., Highly sensitive and recoverable room-temperature NO2 gas detection realized by 2D/0D MoS2/ZnS heterostructures with synergistic effects, Sensors Actuators B Chem. 347 (2021) 130608.

[115] M.E. Lamm, et al., Recent advances in functional materials through cellulose nanofiber templating, Adv. Mater. 33 (12) (2021) 2005538.

[116] J. Li, et al., Mesoporous WS2-decorated cellulose nanofiber-templated CuO heterostructures for high-performance chemiresistive hydrogen sulfide sensors, Anal. Chem. 94 (46) (2022) 16160–16170.

[117] S. Luo, et al., Nanozyme-mediated signal amplification for ultrasensitive photoelectrochemical sensing of Staphylococcus aureus based on cu–C3N4–TiO2 heterostructure, Biosens. Bioelectron. 216 (2022) 114593.

[118] S. Bonthula, et al., Recent Advances in Copper-Based Materials for Environmental Remediation, 2023.

[119] Z. Wan, et al., A sustainable biochar catalyst synergized with copper heteroatoms and CO 2 for singlet oxygenation and electron transfer routes, Green Chem. 21 (17) (2019) 4800–4814.

[120] D. Gasper, A. Shah, S. Tankha, The framing of sustainable consumption and production in SDG 12, Global Pol. 10 (2019) 83–95.
[121] S. Küfeoğlu, SDG-6 clean water and sanitation, in: Emerging Technologies: Value Creation for Sustainable Development, Springer, 2022, pp. 289–304.
[122] X. Ren, Y. Chang, C. Ge, State-of-the-art carbon-nanotubes-reinforced copper-based composites: the Interface design of CNTs and cu matrix, Int. J. Mol. Sci. 25 (23) (2024) 12957.
[123] J. Tyczkowski, H. Kierzkowska-Pawlak, Classical concept of semiconductor heterojunctions in the approach to Nanohybrid catalysts, ACS Appl. Mater. Interfaces 16 (29) (2024) 37339–37345.
[124] S. Yang, et al., Dual-functional Cu2O/g-C3N4 heterojunctions: a high-performance SERS sensor and photocatalytic self-cleaning system for water pollution detection and remediation, Microsyst. Nanoeng. 10 (1) (2024) 198.
[125] O.C. Olatunde, et al., Visible light driven CuBi2O4 heterostructures and their enhanced photocatalytic activity for pollutant degradation: a review, Journal of Water Process Engineering 66 (2024) 105890.
[126] F. Lin, et al., CuCo and sulfur doped carbon nitride composite as an effective Fenton-like catalyst in a wide pH range, Front. Chem. 10 (2022) 982818.
[127] Y. Zhang, et al., Hard-breakable Ohmic contact in 2D CrSi2N4-metal heterostructures: a DFT study, AIP Adv. 13 (3) (2023).
[128] H. Na, et al., High-quality schottky and ohmic contacts in planar 4H-SiC metal semiconductor field-effect transistors and device performance, J. Electron. Mater. 33 (2004) 89–93.
[129] A. Allain, et al., Electrical contacts to two-dimensional semiconductors, Nat. Mater. 14 (12) (2015) 1195–1205.
[130] M. Chhowalla, D. Jena, H. Zhang, Two-dimensional semiconductors for transistors, Nat. Rev. Mater. 1 (11) (2016) 1–15.
[131] Mitta, S.B., et al., Electrical characterization of 2D materials-based field-effect transistors. 2D Materials, 2020. 8(1): p. 012002.
[132] R. Du, et al., Cu□ C (O) interfaces deliver remarkable selectivity and stability for CO2 reduction to C2+ products at industrial current density of 500 mA cm− 2, Small 19 (28) (2023) 2301289.
[133] J. Wang, et al., Cu-MOF derived cu–C nanocomposites towards high performance electrochemical supercapacitors, RSC Adv. 10 (8) (2020) 4621–4629.
[134] Y. Jiang, et al., Dynamic Cu0/cu+ interface promotes acidic CO2 electroreduction, ACS Catal. 14 (11) (2024) 8310–8316.
[135] M. Lu, et al., Enhanced electron transfer and ion transport by binary and multidimensional CuCo2S4/Fe2O3 on carbon cloth for water oxidation, Chem.–a Eur. J. 27 (1) (2021) 238–241.
[136] E.C. Okpara, et al., Green wastes mediated zinc oxide nanoparticles: synthesis, characterization and electrochemical studies, Materials 13 (19) (2020) 4241.
[137] I. Sameera, R. Bhatia, V. Prasad, Preparation, characterization and electrical conductivity studies of MWCNT/ZnO nanoparticles hybrid, Phys. B Condens. Matter 405 (7) (2010) 1709–1714.
[138] C. Shang, et al., Electric field-dependent conductivity achieved for carbon nanotube-introduced ZnO matrix, RSC Adv. 5 (22) (2015) 16993–16999.
[139] Z. Ma, et al., Cu-doped ZnO electronic structure and optical properties studied by first-principles calculations and experiments, Materials 12 (1) (2019) 196.
[140] Y. Kashiwaba, et al., Fabrication of Schottky barrier diodes using H2O2-treated non-polar ZnO 101¯ 0 substrates, Appl. Surf. Sci. 286 (2013) 126–130.
[141] A. Nakamura, J. Temmyo, Schottky contact on ZnO nano-columnar film with H2O2 treatment, J. Appl. Phys. 109 (9) (2011).
[142] J.-C. Xu, et al., Doping metal ions only onto the catalyst surface, J. Mol. Catal. A Chem. 219 (2) (2004) 351–355.
[143] Q. Ye, et al., Enhancement of peroxymonosulfate activation for antibiotics removal by nano zero valent tungsten induced cu (II)/cu (I) redox cycles, Chem. Eng. J. 382 (2020) 123054.
[144] H.R. Kim, et al., Origin of antibacterial activity of ZnO nanoparticles: the roles of protonic and electronic conductions, Part. Part. Syst. Charact. 36 (9) (2019) 1900141.
[145] K.H. Lee, et al., Optimized cu-doping in ZnO electro-spun nanofibers for enhanced photovoltaic performance in perovskite solar cells and photocatalytic dye degradation, RSC Adv. 14 (22) (2024) 15391–15407.
[146] F. Yu, et al., The photocatalytic properties of Al-doped ZnO nanotubes decorated with Cu2O nanoparticles, Phys. Status Solidi A 216 (18) (2019) 1900386.
[147] P. Zhang, H. Liu, X. Li, Plasmonic CuCo/carbon dots: an unconventional photocatalyst used for photocatalytic overall water splitting, ACS Sustain. Chem. Eng. 8 (49) (2020) 17979–17987.
[148] W. BELAY, Synthesis of Silver-Copper Reduced Graphene Oxide Nanocomposite and its Catalytic Dye Degradation Activit, 2022.
[149] Q. Chen, et al., Fabrication of two novel amino-functionalized and starch-coated CuFe2O4-modified magnetic biochar composites and their application in removing Pb2+ and Cd2+ from wastewater, Int. J. Biol. Macromol. 258 (2024) 128973.
[150] A. Mehtab, et al., Type-II CuFe2O4/graphitic carbon nitride heterojunctions for high-efficiency photocatalytic and electrocatalytic hydrogen generation, ACS Appl. Mater. Interfaces 14 (39) (2022) 44317–44329.
[151] L. Lyu, et al., Efficient destruction of pollutants in water by a dual-reaction-center Fenton-like process over carbon nitride compounds-complexed cu (II)-CuAlO2, Environ. Sci. Technol. 52 (7) (2018) 4294–4304.
[152] G. Kumar, et al., Flexible rGO/cu/Ni/ZnO nanocomposites with enhanced optoelectronic, anticorrosive, photocatalytic, and magnetic properties, Inorg. Chem. Commun. 176 (2025) 114202.
[153] M. Liu, et al., Preparation of Fe/CuFe 2 O 4 embedded in porous carbon composites for removal of tetracycline from aqueous solution, New J. Chem. 48 (18) (2024) 8277–8289.
[154] E.C. Okpara, et al., An overview of advanced oxidation processes using copper-based catalytic degradation of organic pollutants in water, Appl. Mater. Today 36 (2024) 102053.
[155] Y. Gao, et al., A review on N-doped biochar for oxidative degradation of organic contaminants in wastewater by persulfate activation, Int. J. Environ. Res. Public Health 19 (22) (2022) 14805.
[156] M. Tang, Y. Zhang, Enhancing the activation of persulfate using nitrogen-doped carbon materials in the electric field for the effective removal of p-nitrophenol, RSC Adv. 11 (60) (2021) 38003–38015.
[157] S. Noh, et al., Cobalt–copper-embedded nitrogen-doped carbon nanostructures derived from zeolite Imidazolate frameworks as Electrocatalysts for the oxygen reduction reaction, ACS omega 9 (27) (2024) 29431–29441.
[158] S. Zhou, et al., Accelerating Electron-transfer and tuning product selectivity through surficial vacancy engineering on CZTS/CdS for Photoelectrochemical CO2 reduction, Small 17 (31) (2021) 2100496.
[159] C. Chen, et al., Structure and band alignment engineering of CdS/TiO2/Bi2WO6 trilayer nanoflake array for efficient photoelectrochemical water splitting, ChemElectroChem 6 (20) (2019) 5248–5254.
[160] Y. Wen Teh, et al., Fabrication of Bi2WO6/cu/WO3 all-solid-state Z-scheme composite photocatalyst to improve CO2 photoreduction under visible light irradiation, ChemCatChem 11 (24) (2019) 6431–6438.
[161] Y. Wang, et al., The effects of doping copper and mesoporous structure on photocatalytic properties of TiO2, J. Nanomater. 2014 (1) (2014) 178152.
[162] P. Kasirajan, et al., Fabrication of copper molybdate nanoflower combined polymeric graphitic carbon nitride heterojunction for water depollution: synergistic photocatalytic performance and mechanism insight, Environ. Res. 233 (2023) 116428.
[163] X. Li, et al., Progress of copper-based Nanocatalysts in advanced oxidation degraded organic pollutants, ChemCatChem 16 (6) (2024) e202301108.
[164] M. Elias, et al., A highly efficient and stable photocatalyst; N-doped ZnO/CNT composite thin film synthesized via simple sol-gel drop coating method, Molecules 26 (5) (2021) 1470.
[165] P. Zhu, et al., Enhanced visible photocatalytic activity of Fe-cu-ZnO/graphene oxide photocatalysts for the degradation of organic dyes, Can. J. Chem. Eng. 96 (7) (2018) 1479–1488.
[166] W. Jia, et al., Nitrogen-doped porous carbon-encapsulated copper composite for efficient reduction of 4-nitrophenol, J. Colloid Interface Sci. 594 (2021) 254–264.
[167] T. Zhang, et al., Synthesis of CuO/GO-DE catalyst and its catalytic properties and mechanism on ciprofloxacin degradation, Nanomaterials 12 (23) (2022) 4305.
[168] A. Singh, et al., Highly selective and efficient electrochemical sensing of ascorbic acid via CuO/rGO nanocomposites deposited on conductive fabric, Appl. Phys. A 128 (4) (2022) 262.
[169] D.F. Katowah, et al., Network structure-based decorated CPA@ CuO hybrid nanocomposite for methyl orange environmental remediation, Sci. Rep. 11 (1) (2021) 5056.
[170] M.A. Malik, et al., Oxidation of alcohols into carbonyl compounds using a CuO@ GO Nano catalyst in oxygen atmospheres, Catalysts 13 (1) (2022) 55.
[171] P. Hajipour, et al., Chemical bath synthesis of CuO-GO-ag nanocomposites with enhanced antibacterial properties, J. Alloys Compd. 821 (2020) 153456.
[172] M. Gijare, et al., A facile synthesis of GO/CuO-blended nanofiber sensor electrode for efficient enzyme-free amperometric determination of glucose, Journal of Analytical Science and Technology 12 (1) (2021) 1–10.
[173] Z. Zhang, et al., Facile hydrothermal synthesis of CuO–cu 2 O/GO nanocomposites for the photocatalytic degradation of organic dye and tetracycline pollutants, New J. Chem. 44 (16) (2020) 6420–6427.
[174] H.W. Haso, et al., High performance copper based metal organic framework for removal of heavy metals from wastewater, Frontiers in Mater. 9 (2022) 840806.
[175] A.G. Bekru, et al., Microwave-assisted synthesis of rGO-ZnO/CuO nanocomposites for photocatalytic degradation of organic pollutants, Crystals 13 (1) (2023) 133.
[176] I.K. Muritala, et al., High temperature production of hydrogen: assessment of non-renewable resources technologies and emerging trends, Int. J. Hydrog. Energy 45 (49) (2020) 26022–26035.
[177] A. Hermawan, et al., CuO nanoparticles/Ti3C2T x MXene hybrid nanocomposites for detection of toluene gas, ACS Appl. Nano Mater. 3 (5) (2020) 4755–4766.
[178] X. Feng, et al., Removal of uranyl ion from wastewater by magnetic adsorption material of polyaniline combined with CuFe2O4, Adsorpt. Sci. Technol. 2021 (2021) 1–16.
[179] W. Fan, et al., Hollow carbon Nanopillar arrays encapsulated with Pd–cu alloy nanoparticles for the oxygen evolution reaction, ACS Appl. Mater. Interfaces 15 (10) (2023) 13600–13608.
[180] S. Bonthula, et al., Recent advances in copper-based materials for sustainable environmental applications, Sustainable Chem. 4 (3) (2023) 246–271.
[181] S. Sonia, et al., Hydrothermal synthesis of highly stable CuO nanostructures for efficient photocatalytic degradation of organic dyes, Mater. Sci. Semicond. Process. 30 (2015) 585–591.
[182] P. Zhang, et al., Effective charge carrier utilization in photocatalytic conversions, Acc. Chem. Res. 49 (5) (2016) 911–921.
[183] J.C. Yu, L. Zhang, J. Yu, Direct sonochemical preparation and characterization of highly active mesoporous TiO2 with a bicrystalline framework, Chem. Mater. 14 (11) (2002) 4647–4653.
[184] H. Wang, et al., Isomerism: minor changes in the bromine substituent positioning lead to notable differences in photovoltaic performance, CCS Chemistry 3 (9) (2021) 2591–2601.
[185] H. Lv, et al., Single-crystalline mesoporous palladium and palladium-copper nanocubes for highly efficient electrochemical CO2 reduction, CCS Chemistry 4 (4) (2022) 1376–1385.

[186] A. Clastin Indira, et al., Photocatalytic efficacy and degradation kinetics of chitosan-loaded Ce-TiO2 nanocomposite towards for rhodamine B dye, Catalysts 13 (12) (2023) 1506.

[187] E.C. Okpara, et al., Applications of transition metal oxides and chalcogenides and their composites in water treatment: a review, Environmental Advances 11 (2023) 100341.

[188] Z. Zhang, et al., An organic–inorganic hybrid material based on benzo [ghi] perylenetri-imide and cyclic titanium-oxo cluster for efficient perovskite and organic solar cells, CCS Chemistry 4 (3) (2022) 880–888.

[189] A. Hajjiah, A. Hajiah, Study of heat generation via trap-assisted tunneling recombination in Cu2ZnSn (S, se) 2 thin-film solar cells, J. Electron. Mater. 52 (9) (2023) 5987–5995.

[190] M.Z. Rahman, C.B. Mullins, Understanding charge transport in carbon nitride for enhanced photocatalytic solar fuel production, Acc. Chem. Res. 52 (1) (2018) 248–257.

[191] F. Adnan, S. Phattarapattamawong, Enhancing photocatalytic degradation of methyl orange by crystallinity transformation of titanium dioxide: a kinetic study, Water Environ. Res. 91 (8) (2019) 722–730.

[192] X. Bai, et al., High crystallinity and conjugation promote the polarization degree in O-doped gC 3 N 4 for removing organic pollutants, CrystEngComm 23 (6) (2021) 1366–1376.

[193] S. Baruah, et al., Enhanced visible light photocatalysis through fast crystallization of zinc oxide nanorods, Beilstein J. Nanotechnol. 1 (1) (2010) 14–20.

[194] J. Di, et al., Porous membranes with special wettabilities: designed fabrication and emerging application, CCS Chemistry 3 (3) (2021) 2280–2297.

[195] E. Masolo, et al., Evaluation of the anatase/rutile phase composition influence on the photocatalytic performances of mesoporous TiO2 powders, Int. J. Hydrog. Energy 40 (42) (2015) 14483–14491.

[196] A. Rani, et al., A review on the progress of nanostructure materials for energy harnessing and environmental remediation, J. Nanostructure Chem. 8 (2018) 255–291.

[197] L.-B. Zhong, et al., Facile one-pot synthesis of urchin-like Fe–Mn binary oxide nanoparticles for effective adsorption of cd (II) from water, RSC Adv. 6 (105) (2016) 103438–103445.

[198] K.S. Ibrahim Khan, I. Khan, Nanoparticles: properties, applications and toxicities, Arab. J. Chem. 12 (7) (2017) 908–931.

[199] Y. Wang, N. Herron, Nanometer-sized semiconductor clusters: materials synthesis, quantum size effects, and photophysical properties, J. Phys. Chem. 95 (2) (1991) 525–532.

[200] R.A. Gonçalves, et al., Green synthesis and applications of ZnO and TiO2 nanostructures, Molecules 26 (8) (2021) 2236.

[201] Q. Li, F.-T. Li, Recent advances in surface and interface design of photocatalysts for the degradation of volatile organic compounds, Adv. Colloid Interf. Sci. 284 (2020) 102275.

[202] G. Li, et al., Effect of the agglomeration of TiO2 nanoparticles on their photocatalytic performance in the aqueous phase, J. Colloid Interface Sci. 348 (2) (2010) 342–347.

[203] M. Azmina, et al., Enhanced photocatalytic activity of ZnO nanoparticles grown on porous silica microparticles, Appl. Nanosci. 7 (2017) 885–892.

[204] X. Kang, et al., Ultrafine copper nanoparticles anchored on reduced graphene oxide present excellent catalytic performance toward 4-nitrophenol reduction, J. Colloid Interface Sci. 566 (2020) 265–270.

[205] W. Wu, et al., Cu–N dopants boost electron transfer and photooxidation reactions of carbon dots, Angew. Chem. Int. Ed. 54 (22) (2015) 6540–6544.

[206] C. Bittencourt, et al., Study of the interaction between copper and carbon nanotubes, Chem. Phys. Lett. 535 (2012) 80–83.

[207] T.P. Maher, H.N. Schafer, Determination of acidic functional groups in low-rank coals: comparison of ion-exchange and non-aqueous titration methods, Fuel 55 (2) (1976) 138–140.

[208] W. Xing, et al., Oxygen-containing functional group-facilitated CO 2 capture by carbide-derived carbons, Nanoscale Res. Lett. 9 (2014) 1–8.

[209] M. Jerigová, M. Odziomek, N. López-Salas, "We are Here!" oxygen functional groups in carbons for electrochemical applications, ACS omega 7 (14) (2022) 11544–11554.

[210] X. Yang, et al., Surface functional groups of carbon-based adsorbents and their roles in the removal of heavy metals from aqueous solutions: a critical review, Chem. Eng. J. 366 (2019) 608–621.

[211] X. Li, et al., In-situ synthesis of highly dispersed cu-CuxO nanoparticles on porous carbon for the enhanced persulfate activation for phenol degradation, Sep. Purif. Technol. 276 (2021) 119260.

[212] Y. Wang, Y. Xue, C. Zhang, Copper embedded in nitrogen-doped carbon matrix derived from metal-organic frameworks for boosting peroxide production and electro-Fenton catalysis, Electrochim. Acta 368 (2021) 137643.

[213] K. Deng, et al., Carbonized MOF-coated zero-valent cu driving an efficient dual-reaction-center Fenton-like water treatment process through utilizing pollutants and natural dissolved oxygen, Acs Es&T Water 2 (1) (2021) 174–183.

[214] A. Muthukrishnaraj, et al., Enhanced photocatalytic activity of Cu2O Cabbage/RGO nanocomposites under visible light irradiation, Polymers. 13 (11) (2021) 1712.

[215] C. Wang, et al., Ultrasound assisted Fenton-like degradation of dyes using copper doped graphitic carbon nitride, Water Sci. Technol. 84 (5) (2021) 1146–1158.

[216] S. Chen, et al., CuCo2O4 supported on activated carbon as a novel heterogeneous catalyst with enhanced peroxymonosulfate activity for efficient removal of organic pollutants, Environ. Res. 183 (2020) 109245.

[217] W. Wang, H. Yao, L. Yue, Supported-catalyst CuO/AC with reduced cost and enhanced activity for the degradation of heavy oil refinery wastewater by catalytic ozonation process, Environ. Sci. Pollut. Res. 27 (7) (2020) 7199–7210.

[218] A. Rehman, M. Park, S.-J. Park, Current progress on the surface chemical modification of carbonaceous materials, Coatings 9 (2) (2019) 103.

[219] C. Huang, et al., Influence of surface functionalities of pyrogenic carbonaceous materials on the generation of reactive species towards organic contaminants: a review, Chem. Eng. J. 404 (2021) 127066.

[220] N. Karousis, N. Tagmatarchis, D. Tasis, Current progress on the chemical modification of carbon nanotubes, Chem. Rev. 110 (9) (2010) 5366–5397.

[221] Zhu Pei, et al., Fabrication of N, S co-doped carbon immobilized high-density Co single atoms toward electro-oxidation of organic sulfides with water as feedstock, Nano Research 16 (2023) 6593–6600.

[222] J. Son, et al., Hydrogenated monolayer graphene with reversible and tunable wide band gap and its field-effect transistor, Nat. Commun. 7 (1) (2016) 13261.

[223] I. Panorel, et al., Oxidation of aqueous pharmaceuticals by pulsed corona discharge, Environ. Technol. 34 (7) (2013) 923–930.

[224] D. ChangMing, et al., Adsorption of acid orange II from aqueous solution by plasma modified activated carbon fibers, Plasma Chem. Plasma Process. 33 (2013) 65–82.

[225] W. Zhang, et al., Enhancement of dibenzothiophene adsorption on activated carbons by surface modification using low temperature oxygen plasma, Chem. Eng. J. 209 (2012) 597–600.

[226] K.N. Pandiyaraj, et al., Dye wastewater degradation by the synergetic effect of an atmospheric pressure plasma treatment and the photocatalytic activity of plasma-functionalized cu–TiO2 nanoparticles, J. Hazard. Mater. 405 (2021) 124264.

[227] M. Russo, et al., Non-thermal plasma coupled with catalyst for the degradation of water pollutants: a review, Catalysts 10 (12) (2020) 1438.

[228] M. Skiba, O. Pivovarov, Plasma-assisted advanced oxidation process and novel materials for water and wastewater treatment. Water and Water Purification Technologies, Scientific and Technical News 28 (3) (2020) 37–47.

[229] M.K. Jha, et al., Surface modified activated carbons: sustainable bio-based materials for environmental remediation, Nanomaterials 11 (11) (2021) 3140.

[230] L. Nayak, M. Rahaman, R. Giri, Surface modification/functionalization of carbon materials by different techniques: An overview, Carbon-containing polymer composites (2018) 65–98.

[231] Z. Tang, et al., Effect of surfactant on the pore structure of mesoporous carbon, Microporous Mesoporous Mater. 111 (1–3) (2008) 48–54.

[232] F. Xi, et al., Amphiphilic graphene quantum dots as a new class of surfactants, Carbon 153 (2019) 127–135.

[233] D. Zabiegaj, et al., Carbon soot–ionic surfactant mixed layers at water/air interfaces, J. Nanosci. Nanotechnol. 15 (5) (2015) 3618–3625.

[234] C. Sanchís, et al., Switchable surfactant-assisted carbon nanotube coatings: innovation through pH shift, Frontiers in Mater. 2 (2015) 1.

[235] J. García-Martín, et al., Ligand adsorption on an activated carbon for the removal of chromate ions from aqueous solutions, Langmuir 21 (15) (2005) 6908–6914.

[236] L. Liang, et al., Selective adsorption of high ionization potential value organic pollutants in wastewater, Proc. Natl. Acad. Sci. 121 (29) (2024) e2403766121.

[237] J.E. Lee, Y.-K. Park, Applications of modified biochar-based materials for the removal of environment pollutants: a mini review, Sustainability 12 (15) (2020) 6112.

[238] F. Wang, D. Zhu, W. Chen, Effect of copper ion on adsorption of chlorinated phenols and 1-naphthylamine to surface-modified carbon nanotubes, Environ. Toxicol. Chem. 31 (1) (2012) 100–107.

[239] J. Cai, et al., Accurate removal of toxic organic pollutants from complex water matrices, Environ. Sci. Technol. 56 (5) (2022) 2917–2935.

[240] L. Lyu, et al., Efficient Fenton-like process for organic pollutant degradation on Cu-doped mesoporous polyimide nanocomposites, Environ. Sci. Nano 6 (3) (2019) 798–808.

[241] Q. Zou, et al., Roles and mechanisms of carbonaceous materials in advanced oxidation coupling processes for degradation organic pollutants in wastewater: a review, Biochar 5 (1) (2023) 86.

[242] S.G. Babu, et al., Synergistic effect of sono-photocatalytic process for the degradation of organic pollutants using CuO-TiO2/rGO, Ultrason. Sonochem. 50 (2019) 218–223.

[243] H. Safajou, et al., Green synthesis and characterization of RGO/cu nanocomposites as photocatalytic degradation of organic pollutants in waste-water, Int. J. Hydrog. Energy 46 (39) (2021) 20534–20546.

[244] P. Nagababu, et al., Graphene oxide-copper nanocomposite: An efficient material for rapid degradation of organic dyes, Environ. Nanotechnol., Monitoring & Manage. 16 (2021) 100545.

[245] S. Sagadevan, et al., Enhanced photocatalytic activity of rGO-CuO nanocomposites for the degradation of organic pollutants, Catalysts 11 (8) (2021) 1008.

[246] B.A. Aragaw, A. Dagnaw, Copper/reduced graphene oxide nanocomposite for high performance photocatalytic methylene blue dye degradation, Ethiopian J. Sci. Technol. 12 (2) (2019) 125–137.

[247] R. Krishna, et al., Novel synthesis of highly catalytic active cu@ Ni/RGO nanocomposite for efficient hydrogenation of 4-nitrophenol organic pollutant, Int. J. Hydrog. Energy 41 (27) (2016) 11608–11615.

[248] M. Wang, et al., Reduced graphene oxide–cuprous oxide composite via facial deposition for photocatalytic dye-degradation, J. Alloys Compd. 568 (2013) 26–35.

[249] S. Jabeen, et al., Fabrication of B–CuO nanostructure and B-CuO/rGO binary nanocomposite: A comparative study in the context of photodegradation and antimicrobial activity assessment, Mater. Today Chem. 33 (2023) 101712.

[250] W. Zhang, et al., In situ preparation of cubic Cu2O-RGO nanocomposites for enhanced visible-light degradation of methyl orange, Nanotechnology 27 (26) (2016) 265703.
[251] Z. Jin, et al., Copper-doped carbon dots with enhanced Fenton reaction activity for rhodamine B degradation, Nanoscale Adv. 4 (14) (2022) 3073–3082.
[252] W. Guo, et al., Recent advances in mechanistic understanding of metal-free carbon Thermocatalysis and Electrocatalysis with model molecules, Nano-Micro Lett. 16 (1) (2024) 125.
[253] W. Qi, et al., Oxidative dehydrogenation on nanocarbon: identification and quantification of active sites by chemical titration, Angew. Chem. Int. Ed. 52 (52) (2013).
[254] Y. Jia, et al., Defect graphene as a trifunctional catalyst for electrochemical reactions, Adv. Mater. 28 (43) (2016) 9532–9538.
[255] X. Luo, et al., Defect engineering of carbons for energy conversion and storage applications, Energy Environ. Mater. 6 (3) (2023) e12402.
[256] J. Oh, et al., Negative Effects of Dopants on Copper–Ceria Catalysts for CO Preferential Oxidation Under the Presence of CO 2 and H 2 O, Catal. Lett. 147 (2017) 2987–3003.
[257] J. Zhang, et al., Cu2O/Ti3C2MXene heterojunction photocatalysts for improved CO2 photocatalytic reduction performance, Appl. Surf. Sci. 542 (2021) 148685.
[258] B.-X. Zhou, et al., Type-II/type-II band alignment to boost spatial charge separation: a case study of gC 3 N 4 quantum dots/a-TiO 2/r-TiO 2 for highly efficient photocatalytic hydrogen and oxygen evolution, Nanoscale 12 (10) (2020) 6037–6046.
[259] N.A.A. Samad, et al., *Recent Advances of Heterogeneous Nanosized Hybrid Catalysts for Water Treatment Application.* Advanced Heterogeneous Catalysts Volume 2: Applications at the Single-Atom Scale, 2020, pp. 227–240.
[260] K. Kaur, et al., Photodegradation of organic pollutants using heterojunctions: a review, J. Environ. Chem. Eng. 8 (2) (2020) 103666.
[261] R.-P. Ye, et al., Recent progress in improving the stability of copper-based catalysts for hydrogenation of carbon–oxygen bonds, Cat. Sci. Technol. 8 (14) (2018) 3428–3449.
[262] N. Jalali, et al., Photocatalytic activity and pH-induced morphological changes of ZnO/CuO nanocomposites prepared by chemical bath precipitation, Energy Adv. 2 (7) (2023) 1051–1063.
[263] R. Zhang, et al., Vital role of synthesis temperature in co–cu layered hydroxides and their Fenton-like activity for RhB degradation, Catalysts 12 (6) (2022) 646.
[264] E. Rahimi, et al., Insights into galvanic corrosion behavior of Ti-cu dissimilar joint: effect of microstructure and Volta potential, Materials 11 (10) (2018) 1820.
[265] Z. An, et al., Mechanically strengthened graphene-cu composite with reduced thermal expansion towards interconnect applications, Microsyst. Nanoeng. 5 (1) (2019) 20.
[266] C.D.S. Tuck, C.A. Powell, J. Nuttall, 3.07 - corrosion of copper and its alloys, in: B. Cottis, et al. (Eds.), Shreir's Corrosion, Elsevier, Oxford, 2010, pp. 1937–1973.
[267] E. Sarver, et al., Copper pitting in chlorinated, high-pH potable water, J. Am. Water Works Assoc. 103 (3) (2011) 86–98.
[268] D.A. Bulushev, et al., Copper on carbon materials: stabilization by nitrogen doping, J. Mater. Chem. A 5 (21) (2017) 10574–10583.
[269] S. Wang, et al., N-doped carbon-coated Cu2O nanowire arrays on copper foam for rapid and stable water disinfection, J. Colloid Interface Sci. 625 (2022) 761–773.
[270] X. Zhang, et al., Carbon nitride nanotubes anchored with high-density CuNx sites for efficient degradation of antibiotic contaminants under photo-Fenton process: performance and mechanism, Appl. Catal. B Environ. 306 (2022) 121119.
[271] L. Zhu, Y.-B. Zhang, Crystallization of covalent organic frameworks for gas storage applications, Molecules 22 (7) (2017) 1149.
[272] D.T.C. Nguyen, et al., New frontiers of invasive plants for biosynthesis of nanoparticles towards biomedical applications: A review, Sci. Total Environ. 857 (2023) 159278.
[273] S. Josset, et al., Numeration methods for targeting photoactive materials in the UV-A photocatalytic removal of microorganisms, Chem. Soc. Rev. 37 (4) (2008) 744–755.
[274] G. Wyszogrodzka, et al., Metal-organic frameworks: mechanisms of antibacterial action and potential applications, Drug Discov. Today 21 (6) (2016) 1009–1018.
[275] T. Luukkonen, et al., Ag- or cu-modified geopolymer filters for water treatment manufactured by 3D printing, direct foaming, or granulation, Sci. Rep. 10 (1) (2020) 7233.
[276] A. Das, A. Patil, R. Bandyopadhyaya, Metallic copper nanoparticle impregnated activated carbon for the development of a continuous, gravity-driven, water disinfection device, Trans. Indian Inst. Metals 77 (12) (2024) 4443–4451.
[277] C. Arnaud, et al., High strength–high conductivity double-walled carbon nanotube–copper composite wires, Carbon 96 (2016) 212–215.
[278] P.-M. Hannula, et al., Corrosion behaviour of cast and deformed copper-carbon nanotube composite wires in chloride media, J. Alloys Compd. 746 (2018) 218–226.
[279] S.M. Uddin, et al., Effect of size and shape of metal particles to improve hardness and electrical properties of carbon nanotube reinforced copper and copper alloy composites, Compos. Sci. Technol. 70 (16) (2010) 2253–2257.
[280] X. Wei, et al., Enhancement of mechanical properties and conductivity in carbon nanotubes (CNTs)/cu matrix composite by surface and intratube decoration of CNTs, Mater. Sci. Eng. A 816 (2021) 141248.
[281] K. Li, et al., Copper–carbon nanotube composites enabled by electrospinning for advanced conductors, ACS Appl. Nano Mater. 3 (7) (2020) 6863–6875.
[282] H. Jiang, et al., Copper–Carbon Nanotube Composites Enabled by Brush Coating for Advanced Conductors, ACS Appl. Nano Mater. 7 (10) (2024) 11176–11183.
[283] M. Akbarpour, et al., Enhanced tensile properties and electrical conductivity of cu-CNT nanocomposites processed via the combination of flake powder metallurgy and high pressure torsion methods, Mater. Sci. Eng. A 773 (2020) 138888.
[284] G. Yang, et al., Nano-silver modified carbon nanotubes to reinforce the copper matrix composites and their mechanical properties, Adv. Powder Technol. 33 (8) (2022) 103672.
[285] J. Xu, et al., Organic wastewater treatment by a single-atom catalyst and electrolytically produced H2O2, Nat. Sustain. 4 (3) (2021) 233–241.
[286] X. Zhang, et al., High-density dispersion of CuNx sites for H2O2 activation toward enhanced photo-Fenton performance in antibiotic contaminant degradation, J. Hazard. Mater. 423 (2022) 127039.
[287] W. Wang, et al., Sulfur doped carbon quantum dots loaded hollow tubular g-C3N4 as novel photocatalyst for destruction of Escherichia coli and tetracycline degradation under visible light, Chem. Eng. J. 378 (2019) 122132.
[288] X. Zhang, et al., Efficiently enhanced visible-light photocatalytic activity by in situ deposition of ag@ AgBr on g-C3N4/Fe3O4 magnetic heterogeneous materials, Sep. Purif. Technol. 254 (2021) 117596.
[289] S. An, et al., High-density ultra-small clusters and single-atom Fe sites embedded in graphitic carbon nitride (g-C3N4) for highly efficient catalytic advanced oxidation processes, ACS Nano 12 (9) (2018) 9441–9450.
[290] X. Zhang, et al., Tetracycline degradation by peroxymonosulfate activated with CoNx active sites: performance and activation mechanism, Chem. Eng. J. 431 (2022) 133477.
[291] X. Qiu, et al., Applications of nanomaterials in asymmetric photocatalysis: recent progress, challenges, and opportunities, Adv. Mater. 33 (6) (2021) 2001731.
[292] X. Wang, et al., Direct and indirect exciton dynamics in few-layered ReS2 revealed by photoluminescence and pump-probe spectroscopy, Adv. Funct. Mater. 29 (6) (2019) 1806169.
[293] X. Wang, et al., Synthesis, properties, and applications of hollow micro−/ nanostructures, Chem. Rev. 116 (18) (2016) 10983–11060.
[294] Z. Mo, et al., Self-assembled synthesis of defect-engineered graphitic carbon nitride nanotubes for efficient conversion of solar energy, Appl. Catal. B Environ. 225 (2018) 154–161.
[295] M. Wu, et al., Constructed palladium-anchored hollow-rod-like graphitic carbon nitride created rapid visible-light-driven debromination of hexabromocyclododecane, Appl. Catal. B Environ. 297 (2021) 120409.
[296] Z. Tong, et al., Tubular g-C3N4 isotype heterojunction: enhanced visible-light photocatalytic activity through cooperative manipulation of oriented electron and hole transfer, Small 12 (30) (2016) 4093–4101.
[297] Q. Gao, et al., The origin of the enhanced photocatalytic activity of carbon nitride nanotubes: a first-principles study, J. Mater. Chem. A 5 (10) (2017) 4827–4834.
[298] J. Fu, et al., Hierarchical porous O-doped g-C3N4 with enhanced photocatalytic CO2 reduction activity, small 13 (15) (2017) 1603938.
[299] L. Yu, et al., Complex hollow nanostructures: synthesis and energy-related applications, Adv. Mater. 29 (15) (2017) 1604563.
[300] L. Nyarko, et al., Tracking changes in organic-copper speciation during wastewater treatment using LC-ICPMS-ESIMS, ACS Environ. Au 5 (2) (2025) 230–240.
[301] J. Timoshenko, B. Roldan Cuenya, In situ/operando Electrocatalyst characterization by X-ray absorption spectroscopy, Chem. Rev. 121 (2) (2021) 882–961.
[302] T. Lais, et al., Elucidation of copper environment in a cu–Cr–Fe oxide catalyst through in situ high-resolution XANES investigation, Phys. Chem. Chem. Phys. 23 (10) (2021) 5888–5896.
[303] Q. Su, et al., A review on Cu2O-based composites in Photocatalysis: synthesis, modification, and applications, Molecules 28 (14) (2023) 5576.
[304] S.K. Saraswat, D.D. Rodene, R.B. Gupta, Recent advancements in semiconductor materials for photoelectrochemical water splitting for hydrogen production using visible light, Renew. Sust. Energ. Rev. 89 (2018) 228–248.
[305] M. Tahir, et al., Selective photocatalytic reduction of CO2 by H2O/H2 to CH4 and CH3OH over cu-promoted In2O3/TiO2 nanocatalyst, Appl. Surf. Sci. 389 (2016) 46–55.
[306] L. Yan, et al., Highly efficient and stable Cu2O–TiO2 intermediate photocatalytic water splitting, Ceram. Int. 46 (7) (2020) 9455–9463.
[307] P. Isherwood, Copper zinc oxide: investigation into a p-type mixed metal oxide system, Vacuum 139 (2017) 173–177.
[308] J. Zhao, et al., Enhanced CO2 photoreduction activity of black TiO2− coated cu nanoparticles under visible light irradiation: role of metallic cu, Appl. Catal. A Gen. 510 (2016) 34–41.
[309] M.R.D. Khaki, et al., Evaluating the efficiency of nano-sized cu doped TiO2/ZnO photocatalyst under visible light irradiation, J. Mol. Liq. 258 (2018) 354–365.
[310] W.S. Koe, Nitrogen and Sulphur co-Doped Carbon Quantum Dots/Titanium Dioxide Photocatalytic Membrane for Photodegradation of Diclofenac in Water, UTAR, 2019.
[311] R. Leary, A. Westwood, Carbonaceous nanomaterials for the enhancement of TiO2 photocatalysis, Carbon 49 (3) (2011) 741–772.
[312] S.M. Klein, G. Cohen, A.I. Cederbaum, Production of formaldehyde during metabolism of dimethyl sulfoxide by hydroxyl radical-generating systems, Biochemistry 20 (21) (1981) 6006–6012.
[313] C.E. Diaz-Uribe, et al., Visible light superoxide radical anion generation by tetra (4-carboxyphenyl) porphyrin/TiO2: EPR characterization, J. Photochem. Photobiol. A Chem. 215 (2–3) (2010) 172–178.
[314] S.J. Alyani, et al., Growing co-doped TiO2 nanosheets on reduced graphene oxide for efficient photocatalytic removal of tetracycline antibiotic from aqueous solution and modeling the process by artificial neural network, J. Alloys Compd. 799 (2019) 169–182.

[315] Y. Haldorai, et al., Sol-gel synthesized CuO nanoparticles supported on reduced graphene oxide nanocomposite for sunlight-catalytic methylene blue degradation and nanofluid applications, J. Sol-Gel Sci. Technol. 111 (3) (2024) 689–702.

[316] P. Nethravathi, et al., Ag-Cu2O decorated reduced graphene oxide nanocomposite for photocatalytic water splitting, methylene blue dye degradation, electrochemical nitrite sensing, photoluminescence and selected biological applications, Biomass Convers. Biorefinery 14 (4) (2024) 5711–5734.

[317] S. Tao, D. Jiang, Covalent organic frameworks for energy conversions: current status, challenges, and perspectives, CCS Chemistry 3 (1) (2021) 2003–2024.

[318] Y. Ji, et al., Non-activated peroxymonosulfate oxidation of sulfonamide antibiotics in water: kinetics, mechanisms, and implications for water treatment, Water Res. 147 (2018) 82–90.

[319] C. Lyu, et al., Cobalt oxyhydroxide as an efficient heterogeneous catalyst of peroxymonosulfate activation for oil-contaminated soil remediation, Sci. Total Environ. 680 (2019) 61–69.

[320] F. Chen, et al., Catalytic degradation of ciprofloxacin by a visible-light-assisted peroxymonosulfate activation system: performance and mechanism, Water Res. 173 (2020) 115559.

[321] X. Cheng, et al., Insights into the mechanism of nonradical reactions of persulfate activated by carbon nanotubes: activation performance and structure-function relationship, Water Res. 157 (2019) 406–414.

[322] Z. Liu, et al., Electrochemical activation of peroxymonosulfate with ACF cathode: kinetics, influencing factors, mechanism, and application potential, Water Res. 159 (2019) 111–121.

[323] Z. Wang, et al., Resolving the kinetic and intrinsic constraints of heat-activated peroxydisulfate oxidation of iopromide in aqueous solution, J. Hazard. Mater. 384 (2020) 121281.

[324] J. Qin, et al., Rational design of efficient metal-free catalysts for peroxymonosulfate activation: selective degradation of organic contaminants via a dual nonradical reaction pathway, J. Hazard. Mater. 398 (2020) 122808.

[325] Y. Liu, et al., Electroactive modified carbon nanotube filter for simultaneous detoxification and sequestration of Sb (III), Environ. Sci. Technol. 53 (3) (2019) 1527–1535.

[326] Y. Xu, J. Ai, H. Zhang, The mechanism of degradation of bisphenol a using the magnetically separable CuFe2O4/peroxymonosulfate heterogeneous oxidation process, J. Hazard. Mater. 309 (2016) 87–96.

[327] K. Deng, et al., Vanadium tetrasulfide cross-linking graphene-like carbon driving a sustainable electron supply chain from pollutants through the activation of dissolved oxygen and hydrogen peroxide, Environ. Sci. Nano 8 (1) (2021) 86–96.

[328] M. Han, et al., In situ generation and efficient activation of H2O2 for pollutant degradation over CoMoS2 nanosphere-embedded rGO nanosheets and its interfacial reaction mechanism, J. Colloid Interface Sci. 543 (2019) 214–224.

[329] N. Jiang, et al., A dual-reaction-center Fenton-like process on –C□N–cu linkage between copper oxides and defect-containing g-C3N4 for efficient removal of organic pollutants, J. Mater. Chem. A 6 (36) (2018) 17819–17828.

[330] L. Li, et al., Framework cu-doped boron nitride nanobelts with enhanced internal electric field for effective Fenton-like removal of organic pollutants, J. Mater. Chem. A 7 (12) (2019) 6946–6956.

[331] J. Wang, J. Tang, Fe-based Fenton-like catalysts for water treatment: preparation, characterization and modification, Chemosphere 276 (2021) 130177.

[332] L. Wang, et al., Notable light-free catalytic activity for pollutant destruction over flower-like BiOI microspheres by a dual-reaction-center Fenton-like process, J. Colloid Interface Sci. 527 (2018) 251–259.

[333] Y. Wang, et al., Magnetic ordered mesoporous copper ferrite as a heterogeneous Fenton catalyst for the degradation of imidacloprid, Appl. Catal. B Environ. 147 (2014) 534–545.

[334] W. Cao, et al., Efficient Fenton-like process induced by fortified Electron-rich O microcenter on the reduction state cu-doped CNO polymer, ACS Appl. Mater. Interfaces 11 (18) (2019) 16496–16505.

[335] Y. Yao, et al., Equilibrium and kinetic studies of methyl orange adsorption on multiwalled carbon nanotubes, Chem. Eng. J. 170 (1) (2011) 82–89.

[336] Y.-H. Li, et al., Competitive adsorption of Pb2+, Cu2+ and Cd2+ ions from aqueous solutions by multiwalled carbon nanotubes, Carbon 41 (14) (2003) 2787–2792.

[337] Y. Yao, et al., Adsorption behavior of methylene blue on carbon nanotubes, Bioresour. Technol. 101 (9) (2010) 3040–3046.

[338] R.Q. Long, R.T. Yang, Carbon nanotubes as superior sorbent for dioxin removal, J. Am. Chem. Soc. 123 (9) (2001) 2058–2059.

[339] Y. Ren, et al., Adsorption of Pb (II) and cu (II) from aqueous solution on magnetic porous ferrospinel MnFe2O4, J. Colloid Interface Sci. 367 (1) (2012) 415–421.

[340] N. Kansara, et al., Wastewater treatment by ion exchange method: a review of past and recent researches, ESAIJ (Environmental Science, An Indian Journal) 12 (4) (2016) 143–150.

[341] S.-Y. Kang, et al., Competitive adsorption characteristics of Co2+, Ni2+, and Cr3+ by IRN-77 cation exchange resin in synthesized wastewater, Chemosphere 56 (2) (2004) 141–147.

[342] Q. Li, et al., Antimicrobial nanomaterials for water disinfection and microbial control: potential applications and implications, Water Res. 42 (18) (2008) 4591–4602.

[343] J. Li, et al., Antibacterial activity of large-area monolayer graphene film manipulated by charge transfer, Sci. Rep. 4 (1) (2014) 4359.

[344] X. Zeng, et al., Graphene-based antimicrobial nanomaterials: rational design and applications for water disinfection and microbial control, Environ. Sci. Nano 4 (12) (2017) 2248–2266.

[345] P. Biswas, R. Bandyopadhyaya, Synergistic antibacterial activity of a combination of silver and copper nanoparticle impregnated activated carbon for water disinfection, Environ. Sci. Nano 4 (12) (2017) 2405–2417.

[346] Q.L. Shimabuku, et al., Water treatment with exceptional virus inactivation using activated carbon modified with silver (ag) and copper oxide (CuO) nanoparticles, Environ. Technol. 38 (16) (2017) 2058–2069.

[347] K.A. Mohamad Said, et al., Copper acetate monohydrate/nickel chloride impregnated PVDF ultrafiltration membrane: An antifouling membrane for peat water treatment, ChemistrySelect 9 (41) (2024) e202402599.

[348] C.A. Obasanjo, et al., In situ regeneration of copper catalysts for long-term electrochemical CO2 reduction to multiple carbon products, J. Mater. Chem. A 10 (37) (2022) 20059–20070.

[349] T.N. Nguyen, et al., Catalyst regeneration via chemical oxidation enables Long-term electrochemical carbon dioxide reduction, J. Am. Chem. Soc. 144 (29) (2022) 13254–13265.

[350] Q. Song, et al., Deactivation mechanism and regeneration of the CuCl/activated carbon catalyst for gas-solid acetylene dimerization, ACS Omega 7 (47) (2022) 43265–43272.

[351] W. Yang, et al., Enhancement of copper catalyst stability for catalytic ozonation in water treatment using ALD Overcoating, ACS Appl. Mater. Interfaces 10 (50) (2018) 43323–43326.

[352] F. Grillo, et al., Passivation of copper: Benzotriazole films on cu(111), J. Phys. Chem. C 118 (16) (2014) 8667–8675.

[353] H.T. Nguyen, et al., Polymeric molecular coating for oxidation resistance property of copper surface, Polym. Bull. 76 (5) (2019) 2311–2319.

[354] EPA, E.P.A, National primary drinking water regulations: long term 1 enhanced surface water treatment rule. Final rule, Fed. Regist. 67 (9) (2002) 1811–1844.

[355] Z. Gajda-Meissner, et al., Importance of surface coating to accumulation dynamics and acute toxicity of copper nanomaterials and dissolved copper in Daphnia magna, Environ. Toxicol. Chem. 39 (2) (2020) 287–299.

[356] W.H. Fan, et al., Enhanced oxidative stress and physiological damage in Daphnia magna by copper in the presence of Nano-TiO2, J. Nanomater. 2012 (1) (2012) 398720.

[357] Y. Sun, et al., Effects of copper oxide nanoparticles on developing zebrafish embryos and larvae, Int. J. Nanomedicine 11 (2016) 905–918.

Further reading

[358] T. Gan, et al., Highly sensitive determination of Orange II based on the dual amplified electrochemical signal of graphene and mesoporous TiO 2, Anal. Methods 5 (12) (2013) 2964–2970.

[359] M. Irfan, et al., Electrochemical sensing platform based on functionalized multi-walled carbon nanotubes and metal oxide for the detection and degradation studies of orange II dye, ACS Omega 7 (36) (2022) 32302–32312.

[360] S. Srivastava, R. Sinha, D. Roy, Toxicological effects of malachite green, Aquat. Toxicol. 66 (3) (2004) 319–329.

[361] S. Seshadri, P.L. Bishop, A.M. Agha, Anaerobic/aerobic treatment of selected azo dyes in wastewater, Waste Manag. 14 (2) (1994) 127–137.

[362] J. Barot, A. Bahadur, Toxic impacts of CI acid Orange 7 on behavioural, haematological and some biochemical parameters of Labeo rohita fingerlings, IJSRES 3 (8) (2015) 0284–0290.

[363] G. Parshetti, et al., Decolorization and detoxification of sulfonated azo dye methyl orange by Kocuria rosea MTCC 1532, J. Hazard. Mater. 176 (1–3) (2010) 503–509.

[364] E. Haque, J.W. Jun, S.H. Jhung, Adsorptive removal of methyl orange and methylene blue from aqueous solution with a metal-organic framework material, iron terephthalate (MOF-235), J. Hazard. Mater. 185 (1) (2011) 507–511.

[365] I. Khan, et al., Review on methylene blue: its properties, uses, toxicity and photodegradation, Water 14 (2) (2022) 242.

[366] R.C. Cutlip, W.S. Monlux, Experimental crystal violet and methyl violet poisoning in dogs and cattle, Can. J. Comp. Med. Vet. Sci. 31 (3) (1967) 80.

[367] S.I. Siddiqui, et al., Investigation of Congo red toxicity towards different living organisms: a review, Processes 11 (3) (2023) 807.

[368] F.H. Hussein, A.N. Alkhateeb, J.K. Ismail, Solar photolysis and photocatalytic decolorization of thymol blue, E-J. Chem. 5 (2) (2008) 243–250.

[369] D.C. Khandekar, A.R. Bhattacharyya, R. Bandyopadhyaya, Role of impregnated nano-photocatalyst (SnxTi (1-x) O2) inside mesoporous silica (SBA-15) for degradation of organic pollutant (rhodamine B) under UV light, J. Environ. Chem. Eng. 7 (5) (2019) 103433.

[370] A. Inyinbor, F. Adekola, G.A. Olatunji, Kinetics, isotherms and thermodynamic modeling of liquid phase adsorption of rhodamine B dye onto Raphia hookerie fruit epicarp, Water Resources and Industry 15 (2016) 14–27.

[371] R.O. Beauchamp, et al., A critical review of the literature on nitrobenzene toxicity, CRC Crit. Rev. Toxicol. 11 (1) (1982) 33–84.